The effect of acute phase proteins on hepatic insulin signalling

by

Tammy Speelman

Thesis presented in fulfilment of the requirements for the degree of Master of Science in the Faculty of Science at Stellenbosch University

Supervisor: Dr Nicolette Verhoog
Co-supervisor: Prof. Ann Louw

March 2020

Declaration

By submitting this thesis electronically, I declare that the entirety of the work contained therein is my own, original work, that I am the sole author thereof (save to the extent explicitly otherwise stated), that reproduction and publication thereof by Stellenbosch University will not infringe any third party rights and that I have not previously in its entirety or in part submitted it for obtaining any qualification.

March 2020

ABSTRACT

Insulin resistance is the main risk factor for the development of type-2 diabetes (T2D). It is described as perturbed insulin signalling in the peripheral target tissues (which include the liver, skeletal muscle and adipose tissue), resulting in deficient insulin action. In the liver, this leads to the inability of insulin to regulate glucose metabolism by decreasing hepatic glucose production (HGP), and thus decrease blood glucose concentrations, aiding in the progression to T2D. Numerous factors contribute to the development of insulin resistance, such as stress and obesity, however inflammation is known to play a key role. An increased inflammatory state is associated with enhanced production of acute phase proteins (APPs). Increased serum levels of APPs, such as plasminogen activator inhibitor-1 (PAI-1), serum amyloid A (SAA), and C-reactive protein (CRP) have additionally been associated with T2D and are commonly used as biological markers for this disease state. However, whether these APPs are more than just biological markers for T2D and could contribute to the development of insulin resistance has not yet been established. Although some studies support the possibility that PAI-1, SAA, and CRP impair insulin signalling, their role in the development of hepatic insulin resistance requires investigation. The aim of this study was thus to investigate the effect of PAI-1, SAA, and CRP on hepatic insulin signalling by investigating key proteins in the insulin signalling pathway which, comprise the insulin receptor (IR), insulin receptor substrate-2 (IRS-2), and the central protein, Akt, in a murine hepatoma and human liver carcinoma cell line, BWTG3 and HepG2, respectively. Additionally, HGP was investigated as well as the transcriptional regulation of G6Pase and PEPCK, two key enzymes involved in gluconeogenesis, which is an important process contributing to HGP. The overall results in this study showed that all three APPs impair hepatic insulin signalling in both liver cell models although to different degrees depending on the dose and length of exposure. Specifically, CRP was most effective in modulating the activation of key proteins (the IR and Akt) in the insulin signalling pathway, which subsequently correlated to its ability to increase G6Pase and PEPCK mRNA levels as well as HGP. The length of exposure played an integral role in this study as pro-longed exposure to PAI-1 and CRP enhanced their inhibitory effect on insulin signalling. This was not shown for SAA, which rather displayed dose-dependent effects. As far as could be determined, the results in this study is the first to support the role of PAI-1, SAA, and CRP in the development of hepatic insulin resistance as well as to directly compare the effects of these three APPs in the same experimental model. Although the molecular mechanism of these observed effects require further investigations, the findings in this study cement a foundation in the research linking APPs to hepatic insulin resistance.

OPSOMMING

Insulienweerstandigheid is die hoof-risikofaktor vir die ontwikkeling van tipe-2 diabetes (T2D). Dit word beskryf as versteurde insulien-seintransduksie in die perifere teikenweefsel (waaronder die lewer, skeletale spiere en adipose weefsel), wat tot ’n tekort aan insulien-aksie lei. In die lewer lei dit tot die onvermoë van insulien om glukose-metabolisme te reguleer deur die hepatiese glukose-produksie (HGP) te verminder, en gevolglik bloedglukosekonsentrasie verminder, wat die progressie van T2D aanhelp. Talle faktore dra by tot die ontwikkeling van insulienweerstandigheid, soos stres en vetsug, maar dit is bekend dat inflammasie ’n sleutelrol speel. ’n Verhoogde inflammatoriese staat word verbind met versterkte produksie van akute fase-proteïene (APP’s). Verhoogde serumvlakke van APP’s, soos plasminogeenaktivator-remmer-1 (PAI-1), serum amiloïed A (SAA), en C-reaktiewe proteïene (CRP) is bykomend ook geassosieer met T2D en meer algemeen gebruik as biologiese merkers vir hierdie siektetoestand. Maar of hierdie APP’s meer is as slegs biologiese merkers vir T2D en kan bydra tot die ontwikkeling van insulienweerstandigheid is nog nie bevind nie. Al het sommige studies die moontlikheid ondersteun dat PAI-1, SAA en CRP insulien-seintransduksie benadeel, vereis hul rol in die ontwikkeling van hepatiese insulienweerstandigheid verdere ondersoek. Die doel van hierdie studie was dus om die effek van PAI-1, SAA en CRP op hepatiese insulien-seintransduksie te ondersoek deur ondersoek in te stel na die sleutelproteïene in die insulien-seintransduksie-weg, wat bestaan uit die insulienreseptor (IR), insulienreseptor subtraat-2 (IRS-2), en die sentrale proteïen, Akt, in ’n muriene hepatoom en menslik lewer karsinoom-sellyn, onderskeidelik BWTG3 en HepG2. Daarby is HGP ondersoek, asook die transkripsionele regulering van G6Pase en PEPCK, twee sleutel-ensieme betrokke in glukoneogenese, wat ’n belangrike proses is wat bydra tot HGP. Die algehele resultate in hierdie studie wys dat al drie APP’s benadeel hepatiese insulien-seintransduksie in albei lewerselmodelle, maar tot ’n ander graad afhangend van die dosis en lengte van blootstelling. Spesifiek CRP was die mees effektiewe in die modulering van die aktivering van sleutelproteïene (die IR en Akt) in die insulien-seintransduksie-weg, wat gevolglik gekorreleer het met sy vermoë om G6Pase en PEPCK mRNA-vlakke te verhoog, asook HGP. Die lengte van blootstelling speel ’n integrale rol in hierdie studie omdat langdurige blootstelling aan PAI-1 en CRP hul inhiberende effek van insulien-seintransduksie te vergroot. Dit is nie vir SAA getoon nie, wat aan die ander kant dosis-afhanklike effekte getoon het. So ver vasgestel kon word, is die resultate in hierdie studie die eerste om die rol van PAI-1, SAA en CRP te ondersteun in die ontwikkeling van hepatiese insulienweerstandigheid, asook om direk die effekte van hierdie drie APP’s te vergelyk in dieselfde eksperimentele model. Al verg die molekulêre meganismes van hierdie waargeneemde effekte verdere ondersoek, bied die bevindings in hierdie studie ’n basis in die navorsing oor wat APP’s aan hepatiese insulienweerstandigheid verbind.

ACKNOWLEDGEMENTS

I would like to express my sincere gratitude to the following people who made this thesis possible:

Firstly, I'd like to thank my amazing supervisor, Dr Nicolette Verhoog, without whom I could not have progressed this far in my project as well as my academic career. Thank you so much for your immense support, encouragement, patience, laughter and belief in me as a scientist. You kept me grounded when I was anxious, without knowing it, and you were always my rock. Thank you for your kind and caring nature and always pushing me to do better. Your passion and love for science is an inspiration, and I know that the Verhoog Research Group will achieve so much. Thank you for allowing me to be apart of this journey in establishing your research group, which has granted me so many opportunities that I will forever be grateful for. Also, thank you for your financial support in my two years of completing my Master's project under your guidance. Your support in more ways than one, really has influence me greatly, and any successes I achieve in my future are yours too because you helped me to reach them. You have influenced my life greatly and I truly am grateful. You are an inspiration for many women in science and it was an honour to be mentored by you.

To my co-supervisor, Prof Ann Louw, who was also my supervisor for my honours project. Thank you for your meaningful feedback, guidance and support.

Thank you to my parents, Mary and Stephen Speelman, without whom this could not have been possible. You have always worked hard to provide an education for me and supported me in more ways than I can imagine. Thank you for encouraging me to work hard by setting great examples for me to follow and thank you for supporting my education and academic career, even when you didn't fully understand the journey. Thank you for always trusting and believing in me and for doing everything in your capacity to help and support me throughout this journey and my entire life. I am very grateful and proud to have parents like you.

To my lab partner (in crime), colleague, and friend, Nicole Green – Thank you. These past two years have been challenging and I couldn't imagine doing it without you. Your friendship means a lot to me and I am forever grateful. Thank you for supporting and helping me always, in every avenue of my life, and always lending an ear during rough times. You were my rock throughout this journey, and I could not have not done it without you.

To my close friends: Anika Wyngaard, Fabian Meiring and Bernadette Madell. Thank you for always being there for me, helping me, supporting me and always caring about my well-being. Your friendship has helped me a lot and I truly appreciate it.

Thank you to Rozanne Adams, who assisted me during my honours project and has been a dear friend ever since. Thank you for always helping me in times of need and guiding me through rough times during my Master's write-up. I appreciate your kind and caring nature.

I'd like to thank the members of the Louw-Verhoog lab, Lee-Maine, Lieke and Ankia, for the laughter and support throughout the two years of my Master's and for making the lab environment fun and great to work in. Thank you helping me in times of need and for all the great memories. It truly has been a pleasure. Also, to the members of the Africander lab, thank you for helping me throughout this journey and providing guidance. And to Dr Renate Louw-du Toit, thank you for being the person that we can run to in our labs, who was always willing to help and provide insight.

To my lab manger for 2018 and half of 2019, Bradley Khoza. Thank you for being such a dear friend, and for all the laughter and adventures. Even with all the headaches, you have assisted me always and made my time in the biochemistry department great. I am grateful for your friendship.

To Vishaal Patel, thank you for assisting me in the lab in 2018, my first year of Master's. Also thank you for being a friend and lifting my spirit in tough times. Thank you also to my flatmate, Anina Rademeyer, who always gave me pep talks through the rough times. We have had an adventure living together, and I am grateful for those memories.

Finally, I'd like to thank the National Research Foundation (NRF) and Stellenbosch University for their financial assistance.

ALPHABETICAL LIST OF ABBREVIATIONS

ANOVA	Analysis of Variance
APP	Acute phase proteins
APR	Acute phase response
bp	Base pair
cDNA	Complementary DNA
CRP	C-Reactive protein
Dex	Dexamethasone
DM	Diabetes Mellitus
DMEM	Dulbecco's Modified Eagle's Medium
EF-1α1	Elongation factor-1 alpha 1
ERK	Extracellular signal regulated kinase
FBS	Fetal bovine serum
FoxO1	Forkhead box protein O1
G6Pase	Glucose 6-phosphatase
GAPDH	Glyceraldehyde 3-phosphate dehydrogenase
GC	Glucocorticoid
GLUT	Glucose transporter
GOD	Glucose oxidase
GSK3	Glycogen synthase kinase-3
HGP	Hepatic glucose production
HRP	Horse radish peroxidase
Hsp90	Heat shock protein 90
IKKβ	Inhibitor of nuclear factor kappa B subunit beta
IL-1	Interleukin-1

IL-6	Interleukin-6
IR	Insulin Receptor
IRS	Insulin receptor substrate
JNK	c-Jun N-terminal kinase
kb	Kilobases
kDa	Kilodalton
MAPK	Mitogen-activated protein kinase
mRNA	Messenger RNA
mTOR	Mammalian target of rapamycin
NFκB	Nuclear factor kappa B
PAI-1	Plasminogen activator inhibitor-1
PAGE	Polyacrylamide gel electrophoresis
PBS	Phosphate buffered saline
PCR	Polymerase chain reaction
PDK1	Phosphoinositide-dependent kinase 1
PI3K	Phosphoinositide 3-kinase
p-IR	Phosphorylated insulin receptor
p-IRS2	Phosphorylated insulin receptor substrate-2
p-Akt	Phosphorylated Akt
POD	Peroxidase
qPCR	Quantitative PCR
RLU	Relative light units
RNA	Ribonucleic acid
SAA	Serum Amyloid A
T2D	Type-2 diabetes
TBS	Tris-buffered saline

TNF-α	Tumour necrosis factor-α

TABLE OF CONTENTS

CHAPTER 1:

LITERATURE REVIEW

1.1 Introduction

Diabetes Mellitus (DM), a common disease in western society, is described as a metabolic disorder, characterized by a dysfunction in glucose metabolism, which is normally regulated by insulin secreted from pancreatic β-cells (1). DM can be classified into two categories, namely type-I (T1D) and type-II diabetes (T2D). T1D, also referred to as "insulin-dependent DM", occurs when the pancreas fails to produce sufficient insulin leading to insulin deficiency (2). This type accounts for 5-10% of individuals with DM (3). Type-II diabetes (T2D), however, which is also known as "non-insulin dependent DM", is the most common type accounting for more than 90% of patients with DM (2, 4), with resistance to the effects of insulin the main causative factor, which sets the stage for the development of the disease. Insulin resistance is defined as the inability of peripheral target tissues (which includes the liver, skeletal muscle, and adipose tissue) to respond normally to insulin, resulting in chronic increases in blood glucose levels (hyperglycaemia), a key characteristic of T2D (4, 5). Despite increasing knowledge concerning the risk factors for T2D, the incidence and prevalence of the disease continues to rise globally (2, 4, 6). In 2017, it was estimated by the International Diabetes Federation that 451 million people live with DM worldwide (2, 4) and this number is expected to increase to 693 million by the year 2045 (7). Additionally, the burden of non-communicable diseases, which include T2D and cardiovascular disease, continues to rise in South Africa (SA), in addition to being one of the leading causes of death in SA adults (8, 9). Therefore, a better understanding of the pathophysiology of the disease is of great importance. Although current treatments for T2D, including drugs such as metformin and thiazolidinediones (TZDs), which aim to decrease blood glucose levels and increase insulin sensitivity, are often effective, these drugs are linked to gastrointestinal side effects and increased cardiovascular complications, respectively (10, 11). Therefore, novel therapeutic approaches are warranted.

As insulin resistance is the main risk factor for T2D, an understanding of the pathophysiology of an insulin-resistant state would be beneficial. The molecular mechanism of insulin resistance is not well understood, but involves the insulin signalling pathway, an integrated network of signalling proteins and secondary messengers. A defect or disruption to any of the signalling proteins or production of secondary messengers results in deficient insulin action, which sets the scene for the development of T2D (12, 13). Insulin mainly targets the liver, adipose tissue, and skeletal muscle, all of which can become resistant to insulin. The liver especially is of interest as not only is it the first organ reached by secreted insulin, it is also a major contributor to hyperglycaemia observed in T2D (10). Furthermore, it has been reported that insulin resistance is initiated firstly in the liver before the skeletal muscle and adipose tissue is affected (14, 15), establishing the liver as an important gate-keeper to the onset of insulin resistance and T2D (16). Several factors are known to contribute to insulin resistance and affect the insulin signalling pathway. These include, obesity, stress (resulting in increased levels of

glucocorticoids), and chronic inflammation (17–19). Approximately 60% of patients with T2D are obese (2) and one of the possible mechanisms linking obesity to the development of T2D, is increased inflammation, amongst other factors (19–21). Additionally, it has been shown that pro-inflammatory cytokines such as tumour necrosis-alpha (TNF-α) and interleukin-6 (IL-6), which are increased in response to obesity, induce insulin resistance at a molecular level by modulating the insulin signalling pathway (22–25). These pro-inflammatory cytokines together with glucocorticoids (GCs) induce the expression of several acute phase proteins (APPs), including plasminogen activator inhibitor-1 (PAI-1), serum amyloid A (SAA), and C-reactive protein (CRP) (26–33). These APPs are used routinely as biological markers for T2D as their levels are significantly increased in the serum of T2D patients (34–41). However, whether these APPs could lead to the development of T2D remains to be elucidated. Some studies have shown an association between PAI-1, SAA, and CRP in the development of insulin resistance, therefore it is possible that these APPs may be the correlative link between inflammation and insulin resistance, however, evidence supporting this hypothesis is limited and requires more attention.

The aim of this review is to highlight the importance of the insulin signalling pathway and insulin action in the liver, which regulates glucose metabolism. In addition, the molecular mechanism of insulin resistance and the development thereof will be discussed, as well as the important role inflammation plays in this process. Finally, the association of APPs with insulin resistance will be reviewed as a novel approach to understanding the development of T2D.

1.2 The liver: a key role player in glucose homeostasis

"*The dynamic regulation of glucose metabolism is essential for systemic carbohydrate homeostasis and organism survival." – Titchenell, P et al., 2015* (42).

The liver is widely described as an essential metabolic organ that governs whole-body energy metabolism. It specifically plays a key role in glucose metabolism by maintaining a balance between glucose production and glucose storage in the form of glycogen (10, 11, 43). After a meal, there is an increase in blood glucose, free fatty acids (FFAs), and amino acids, which are transported to the liver where they are metabolized. Blood glucose enters the liver *via* a plasma glucose transporter (GLUT), which exists as four isoforms (GLUT1-4). GLUT2, a bi-directional glucose transporter, is mainly expressed in hepatocytes (the main cell type in the liver (~80%)) (43). Once glucose enters the liver, *via* GLUT2, various processes regulating the breakdown and storage of glucose in the form of glycogen occurs to facilitate decreasing blood glucose concentrations (11, 43). These processes include glycolysis (which involves the breakdown of glucose to produce energy in the form of ATP) and glycogen synthesis (the production of glycogen using glucose as a substrate) (43) (Table 1.1). Upon entrance to the liver, glucose is phosphorylated to glucose-6 phosphate (G6P) by a liver specific hexokinase, known as glucokinase (10, 43). G6P can no longer be exported and is thus retained in hepatocytes (10, 44), where it can either be catabolised *via* the glycolytic pathway, or alternatively converted to glycogen. Under fasting conditions, when nutrients are scarce, the opposite occurs and the liver releases glucose in to the blood by increasing the metabolic pathways involved in hepatic glucose production (HGP), which will be discussed later in this section (43, 45). These processes are tightly regulated by hormones such as insulin and dysregulation of this process can cause hyperglycaemia, leading to the progression of T2D (11).

HGP involves two metabolic reactions: the breakdown of glycogen to form glucose (known as glycogenolysis) and *de novo* glucose synthesis (gluconeogenesis) (43). Both of these processes are suppressed by insulin in the fed state (11, 46, 47) (Table 1.1). However, under fasting conditions, when the plasma glucose levels are relatively low, the liver produces glucose to meet energy demands. The contribution of glycogenolysis and gluconeogenesis to the supply of glucose is approximately equivalent, however, over time the glycogen content in the liver becomes limited and gluconeogenesis becomes the principal source of glucose (10, 45, 48).

The process of gluconeogenesis involves the formation of glucose from substrates such as pyruvate, lactate, glycerol, and amino acids like alanine and glutamine (43, 44, 46, 49), which together account for approximately 90% of gluconeogenic substrates (44). This process involves a biochemical pathway, which is essentially the inverse of the glycolytic pathway, but requires four additional enzymes (45, 46). Two of these enzymes, phosphoenolpyruvate carboxykinase (PEPCK), which catalyses one of the rate-limiting steps; the conversion of oxaloacetate to phosphoenolpyruvate, and glucose-6 phosphatase

(G6Pase) that catalyses the hydrolysis of G6P to free glucose, the final step of gluconeogenesis, are considered key enzymes of gluconeogenesis (46). The first step in the breakdown of glycogen is catalyzed by the enzyme glycogen phosphorylase, which is responsible for the production of G6P (10, 43). The final step in glycogen synthesis, which is catalyzed by glycogen synthase, can be regulated by glycogen synthase kinase 3 (GSK3), which phosphorylates and thereby inactivates glycogen synthase (10, 43, 50). As previously mentioned, all these enzymatic processes can be regulated by insulin, which is secreted from the pancreatic β-cells in response to increasing blood glucose concentrations. The ability of insulin to regulate HGP is imperative to maintain glucose homeostasis, as a defect in this process can result in the hyperglycaemia observed in T2D. Therefore, the molecular mechanisms through which insulin regulates glucose metabolism in the liver will be discussed in the following section.

1.2.1 Insulin action in the liver

As mentioned previously, one of the main aims of insulin is to decrease blood glucose concentrations. In addition, it also prevents blood glucose from increasing by directly inhibiting HGP, by suppressing gluconeogenesis and glycogenolysis, amongst other processes. Insulin rather promotes the utilization and storage of glucose in the liver, by upregulating glycolysis and glycogen synthesis (11, 43) (Table 1.1). It acts directly on HGP by two mechanisms: acute changes to metabolic pathways, which is controlled by modifications to proteins or allosteric effectors, and long-term alterations in gene expression of the key enzymes involved (10, 42). The effect of insulin on glycogen synthesis is acute, involving post-translational modifications of GSK3, the main regulatory enzyme of glycogen synthase, that entails an inhibitory phosphorylation that essentially results in the activation of glycogen synthase (Table 1.1) (43). Additionally, insulin mediates a more long-term effect on the direct regulation of hepatic gluconeogenesis. Unlike most metabolic enzymes, the two key gluconeogenic enzymes, PEPCK and G6Pase, are not regulated allosterically or *via* posttranslational modifications, but instead at a transcriptional level (46, 49), which is supported by the presence of multiple binding sites for hormonally responsive transcription factors in the promoter of the genes encoding for these enzymes (46). Specifically, insulin suppresses the transcription of the *G6Pase* and *PEPCK* genes, by influencing their regulatory transcription factors *via* its signalling cascade (44, 46, 51, 52).

In addition to directly affecting gluconeogenesis through the transcriptional regulation of key gluconeogenic enzymes, as described above, insulin also indirectly affects gluconeogenesis *via* extrahepatic tissues (42) (Table 1.1). Insulin can decrease lipolysis and proteolysis in adipose tissue and skeletal muscle, respectively, thus reducing the levels of FFAs, glycerol, and amino acids made available as substrates for gluconeogenesis (43, 44, 47, 53). Additionally, an increase in circulating insulin levels results in a decrease in glucagon secretion from pancreatic α-cells, which is known to upregulate gluconeogenesis (44). It was recently shown that the indirect effects of insulin on the

regulation of gluconeogenesis is sufficient to maintain normal glucose metabolism (54). The direct effect of insulin was demonstrated *in vivo*, in canines, where portal plasma insulin suppressed HGP without changes observed in glucagon levels or gluconeogenic substrates (55, 56). In a mouse model, however, insulin was shown to be more effective in decreasing HGP *via* extrahepatic tissues i.e. indirectly (57), thus suggesting that both of these processes are needed to observe suppression of HGP.

Gluconeogenesis is much less sensitive to acute changes in plasma insulin concentrations than glycogenolysis both *in vitro* and *in vivo* (58), with higher insulin concentrations over a longer period of time required to effect gluconeogenesis, which involves the transcriptional regulation of *G6Pase* and *PEPCK* genes (47, 59). In support of this phenomenon, excess insulin levels were demonstrated to suppress gluconeogenesis by 20%, while glycogenolysis was completely suppressed in healthy individuals (60). Nevertheless, since gluconeogenesis is a primary source of HGP in patients with T2D (11, 61), and its rate is increased in this disease (61, 62), it is important to better understand how insulin regulates this process, as individuals with insulin resistance fail to suppress HGP (11, 53). This might provide insight into the inability of the liver to respond to insulin, which will help to understand the pathophysiology of T2D (44).

Table 1.1. Effects of insulin on the regulation of glucose metabolism in the liver under normal conditions.

Metabolic reaction	Effect of insulin	Direct or indirect	Mechanism of regulation	Reference
Glycolysis	Increases	Direct	Upregulation of glucokinase	Liangyou, R 2014 (43)
Glycogen synthesis	Increases	Direct	Inhibition of GSK3 Activation of glycogen synthase	Liangyou, R 2014 (43)
Gluconeogenesis	Suppresses	Both	Transcriptional regulation of gluconeogenic enzymes Decreased gluconeogenic precursors from skeletal muscle and adipose tissue Decrease in glucagon secretion from pancreatic α-cells	Liangyou, R 2014 (43) Lin & Acilli 2011 (47) Titchenell *et al.* 2017 (53) Hatting *et al.* 2018 (44)
Glycogenolysis	Suppresses	Direct	Posttranslational modification of glycogen phosphorylase	Liangyou, R 2014 (43)

1.3 Insulin & the insulin signalling network

Discovered in 1921 by Banting *et al.*, (63), insulin is an endocrine anabolic peptide hormone that consists of 51 amino acids that controls whole-body metabolism, cell growth and differentiation (64). Insulin is active as a monomer, which consists of two polypeptide chains: a 21 amino acid residue (the "A"-chain) and 30 amino acid residue (the "B"-chain) bound by disulphide linkages (65). The conformational state of insulin is dependent on the insulin concentration and surrounding pH. The monomer tends to form dimers as the insulin concentration rises and forms hexamers at pH 6.0, which is consequently the storage form of insulin (66).

Insulin is produced in the β-cells of the Islets of Langerhans in the pancreas. Initially, insulin is synthesized as prepoinsulin, then processed to the precursor – proinsulin – which is then converted to insulin and a C-peptide and stored in secretory "granules" awaiting to be secreted in response to nutrient availability (66). Insulin secretion is triggered by a series of events which include an increase in circulating plasma glucose levels and involves the fusion of the granules with the β-cell membrane and subsequent exocytosis. The concentration of insulin stored in the β-granules is roughly 40 nM (66). Insulin secretion consists of two phases – a transient first phase, which in humans peak at 1.4 nM/min when glucose levels are ~7 mM and lasts for ~10 minutes (66). The sustained second phase displays a secretion rate of 0.4 nM/min. This biphasic pattern is less prominent in mice than in rats and humans, due to the relatively higher plasma insulin levels in mice (8-9 nM in mice vs 4-5 nM in rats and humans) (66). After secretion, insulin travels *via* the bloodstream to its peripheral target tissues (liver, adipose tissue, and skeletal muscle) to regulate cell metabolism through the activation of the insulin signalling pathway.

1.3.1 Insulin signalling pathway

The insulin signalling pathway is a large multicomplex network, which can be branched into three major pathways that are activated by insulin. The phosphatidylinositol-3-kinase (PI3K)/Akt pathway mediates the metabolic effects of insulin such as the regulation of glucose, lipid, and protein metabolism in peripheral target tissues. The mitogen-activated protein kinase (MAPK) pathway controls the mitogenic, growth, and cell differentiation effects and the CAP/Cb1/Tc10 (Cb1-associated protein/cannabinoid receptor type-1/G-binding protein TC-10) pathway mediates the membrane translocation of glucose transporter 4 (GLUT4) in muscle and adipose tissue, which aids in glucose uptake in these cells (67–71). For the purpose of investigating the metabolic signal of the insulin signalling pathway, this study will focus on the PI3K/Akt pathway (depicted in Fig.1.3). This signalling cascade differs between the three peripheral target tissues, resulting in different metabolic outcomes. For instance, regulation of glucose metabolism is the most important outcome of insulin signalling in the liver, thus HGP is regulated. In contrast, insulin-stimulated glucose uptake is more important in

adipose tissue and skeletal muscle, which account for ~70% of glucose uptake (71–73). Additionally, lipid and protein metabolism are mainly regulated in adipose tissue and skeletal muscle, respectively (68, 74).

In the following section, the PI3K/Akt pathway will be reviewed according to three of its main components: the insulin receptor, insulin receptor substrates, and the central protein Akt. Additionally, the downstream effects as a result of this pathway as well as its regulation will be discussed.

1.3.1.1 Insulin Receptor

The insulin receptor as a mediator for the biological effects of insulin was first reported by Freychet and colleagues in 1971 (75). Subsequently, throughout the 1980's, the structural and functional properties of the insulin receptor was characterized (76–79). The insulin receptor is a member of a superfamily of receptor tyrosine kinases (RTK), which are single transmembrane polypeptide chains that exert their signalling effect through tyrosine kinase activity (80, 81). Within the superfamily of RTK, the insulin receptor subfamily exists, which consists of the insulin receptor (IR), the insulin-like growth factor receptor (IGF-R), and the orphan insulin related receptor (IRR) (80, 82). All three receptors are expressed in most mammalian tissues, especially in the peripheral target tissues (67, 82). The insulin receptor is tetrameric and consists of two extracellular α-subunits (135 kDa) and two intracellular β-subunits (95 kDa) that are covalently linked by disulphide bonds, as depicted in Fig.1.1. The IR, IGF-R and IRR are unique from the other members of the RTK superfamily in that they are maintained as a covalent dimer in the absence of ligand (80, 83). The extracellular α-subunits contain the insulin binding site and the β-subunits possess three compartmentalized regions - the extracellular, transmembrane, and cytosolic domains (Fig.1.1) (80, 84, 85). The cytosolic tyrosine kinase domain contains the ATP binding consensus sequence and three clusters of tyrosine residues that can be phosphorylated in response to insulin, as first described in 1982 (76–78, 80, 84). The IR exists as two isoforms, IR-A and IR-B, which is formed when the IR mRNA undergoes alternative splicing at exon 11 and only differs by the absence (IR-A) or presence (IR-B) of 12 amino acids at the carboxy terminal of the α-subunit (84, 86, 87). These isoforms are differentially expressed in tissue, with IR-B expressed in abundance in peripheral target tissues. Nonetheless, insulin binds both isoforms with similar affinity (87).

Prior to insulin binding, the α-subunits exhibit an inhibitory effect on the β-subunits (88). Upon binding of insulin, the IR undergoes a conformational change that relieves the inhibitory effect. The mechanism of relief has been extensively investigated and a number of models have been proposed (89–92), all resulting in the autophosphorylation of at least five distinct sites in the β-subunits (93). Phosphorylation of a cluster of residues (Tyr1158, Tyr1162, Tyr1163) within the kinase domain has been shown to be necessary for activation of the kinase allowing it to recognise other substrates (85, 94, 95) (Fig.1.1). Additionally, Tyr1146, Tyr1150, and Tyr1151 in the kinase regulatory domain (Fig.1.1) are considered

major sites of phosphorylation (80, 96–98). Finally, phosphorylation of Tyr960 in the juxtamembrane region is required for receptor internalization and binding of the phosphotyrosine-binding (PTB) domain of insulin receptor substrate (IRS) proteins for subsequent phosphorylation on tyrosine residues (98, 99), which will be discussed later (Section 1.3.1.2).

The importance of the IR in insulin signalling in peripheral target tissues was demonstrated with tissue-specific knockout studies (100). IR knockout of the pancreatic β cell resulted in dysfunction of insulin secretion and impaired glucose tolerance (101). Additionally, liver-specific deletion of the IR led to severe insulin resistance and dysregulation of glucose metabolism (102), however when Okamoto and colleagues (103) partially restored hepatic IR expression in IR knockout mice, insulin signalling in the liver was restored, but hepatic insulin action *in vivo* i.e. the ability of insulin to decrease HGP, was not. Interestingly, muscle-specific deletion of the IR did not alter glucose tolerance, although insulin signalling in the muscle was abolished (104). Muscle-specific deletion of both the IR and IGF1-R displayed enhanced basal glucose uptake, suggesting that other tyrosine kinases that activate the insulin signalling pathway may be enhanced in the absence of the IR and IGF-1R (105). Finally, adipocyte-specific IR knockout mice were protected from age-related obesity and its subsequent metabolic abnormalities (106). Together these studies suggest that the IR plays a significant role in insulin signalling and insulin action in the liver.

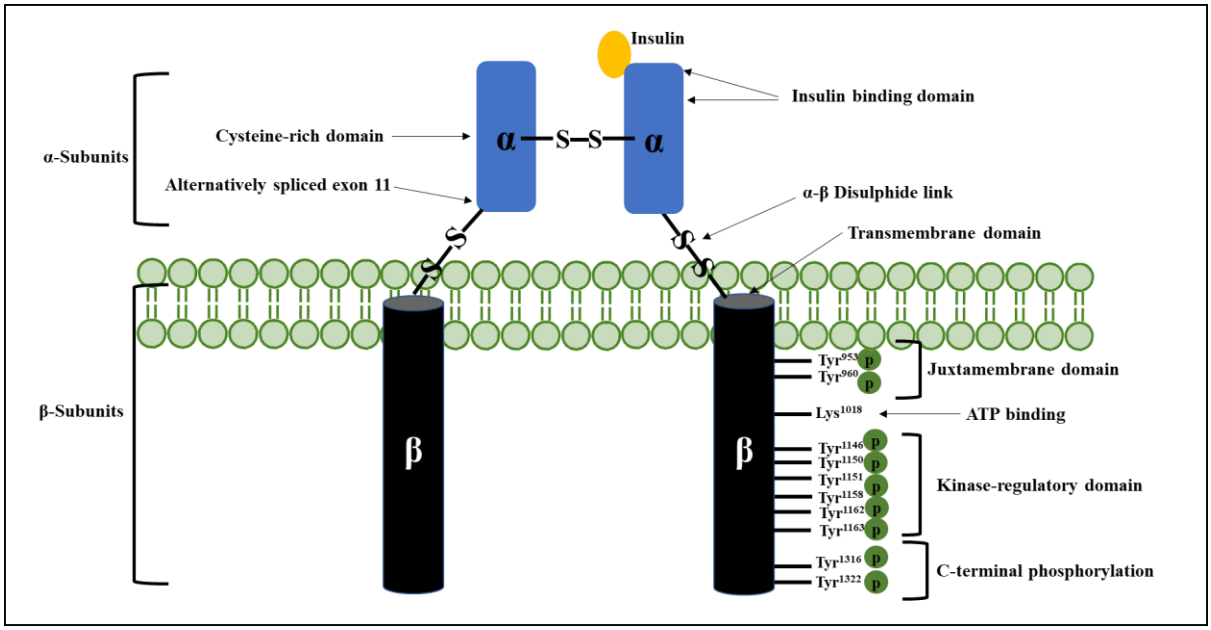

Figure 1.1. Schematic illustration of the structure of the insulin receptor. The insulin receptor, present in the plasma membrane as a dimer, consists of two extracellular α-subunits and two intracellular β-subunits that are covalently linked by disulphide bonds. The α-subunit contains the insulin binding domain and intracellular β-subunit contains tyrosine residues that regulate the kinase activity upon insulin binding. Image was redrawn and adapted from Patti & Kahn 1998 (84) and Cheatham *et al.* 1995 (85).

1.3.1.2 Insulin Receptor Substrates (IRS)

Activation of the insulin receptor results in the recruitment of intracellular substrates containing phosphotyrosine binding (PTB) domains, of which the best described is the insulin receptor substrate (IRS) family. These proteins act as scaffolds to mediate the binding of intracellular effectors (68, 82) that amplify the insulin signal. The main role of the IRS proteins in the insulin signalling pathway is to convert the tyrosine phosphorylation signal into a lipid kinase signal (64), of which the mechanism will be discussed later in this section (Section 1.3.1.3). The IRS family consists of six isoforms (IRS-1-6), of which IRS-1 and IRS-2 mediate the metabolic effects of the IR. IRS proteins have NH_2-terminal pleckstrin homology (PH) domains, allowing these proteins to bind to phosphoinositides with high affinity and specificity (107), and PTB domains (~100 residues) that target them to the activated IR (Fig.1.2A). Additionally, their COOH-terminal tail contains multiple tyrosine and serine/threonine phosphorylation sites that act as "on" and "off" switches, respectively (68). IRS-1 and 2 contain common functional domains, however there are some differences. A review by White (108) details that IRS-1 contains 21 putative tyrosine phosphorylation sites (not all are shown in Fig.1.2A), of which 14 of these sites are conserved in IRS-2, three sites from IRS-1 are not found in IRS-2 and four novel sites exist in IRS-2. Additionally, unique to IRS-2 is the existence of a kinase regulatory loop binding region (KRLB) (residues 591-733), which interacts with the tyrosine kinase domain of the IR (109) (Fig.1.2A). Detailed studies of IRS-1 phosphorylation upon insulin stimulation demonstrated that at least 8 tyrosine residues on IRS-1 that undergo phosphorylation including Tyr608, Tyr628, Tyr939, and Tyr987 (108). The proposed mechanism of IRS binding to the IR is shown in Fig.1.2B. The PTB domain of the IRS protein attracts and associates with the juxtamembrane region of the IR (residues Tyr972 (68) and Tyr960 (98, 108) has been described), resulting in the phosphorylation and further activation of multiple IRS tyrosine residues.

Results from different knockout studies, summarised in Table 1.2, have shown that different IRS proteins appear to have specific roles in different tissues (67, 110). IRS-1-deficient mice show growth retardation and mild insulin resistance, especially in the muscle, but did not develop T2D due to increased insulin secretion by pancreatic β-cells to compensate for the mild-resistance (111, 112). These mice also displayed normal glucose tolerance. Additionally, pre-adipocytes of IRS-1 deficient mice showed defects in adipocyte differentiation (113). In contrast, IRS-2 deficient mice displayed defective insulin signalling in the liver and inadequate compensatory insulin secretion resulting in hyperglycaemia and the development of T2D (111, 114–116) These studies illustrate that IRS-1 seems to be the key mediator of insulin signalling in skeletal muscle, adipose tissue and pancreatic β-cells whereas IRS-2 is important for liver metabolism (67, 110). The latter is supported by Rother and colleagues (117) who demonstrated in mice lacking the IR in hepatocytes, a reduction in IRS-2, and not IRS-1, phosphorylation. This was subsequently associated with a lack of insulin to regulate glucose

metabolism (117). Therefore, in summary the activation of IRS-1 or IRS-2 will result in different metabolic effects in peripheral target tissues, with IRS-2 showing importance in the regulation of HGP.

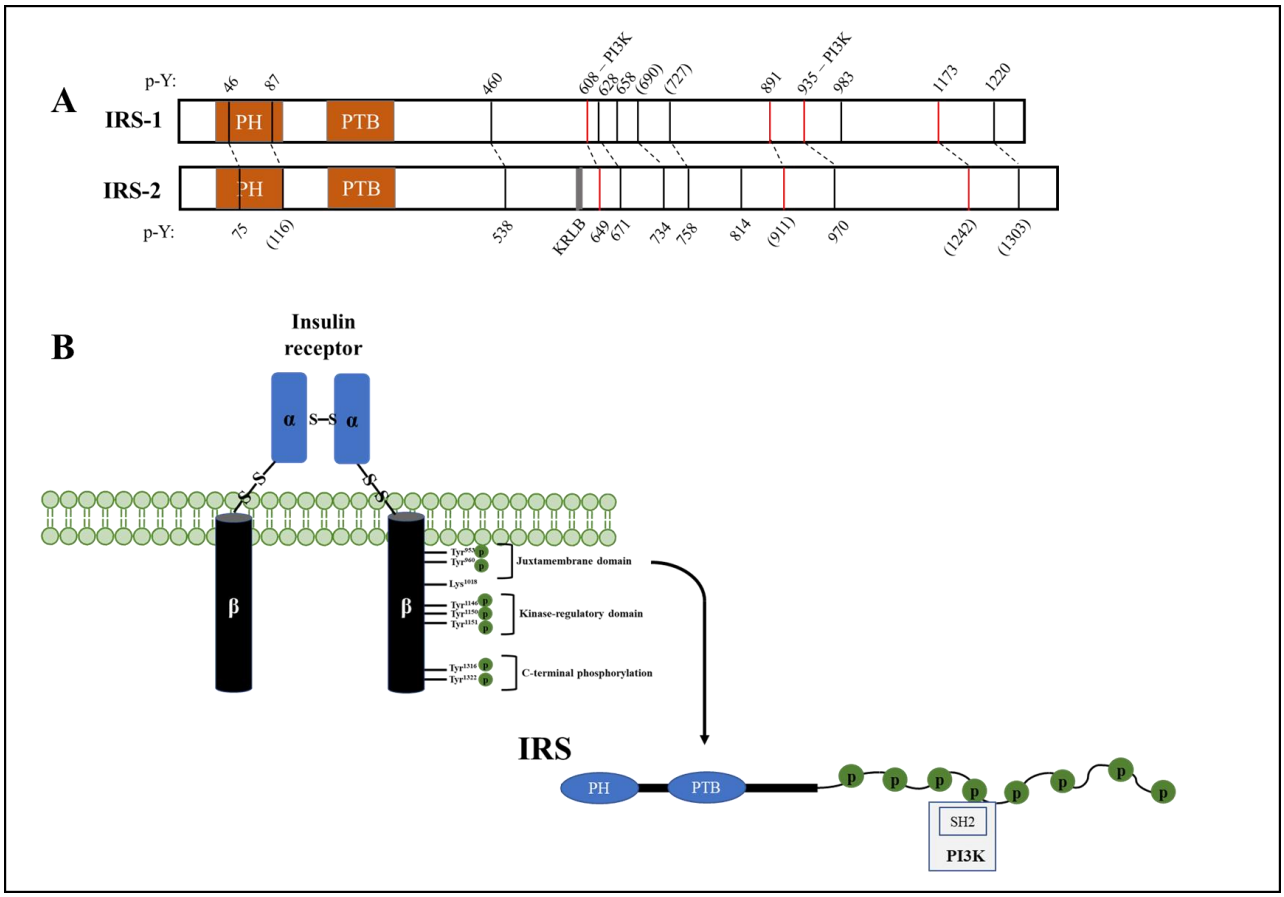

Figure 1.2. Schematic illustration of the structure of IRS-1 and 2 (A) and binding of the IRS protein to the activated IR (B). (A) The IRS-1 and IRS-2 proteins have structural similarity, pertaining to the NH_2-terminal PH and PTB domains (which consists of ~100 amino acids). On the right is shown the COOH-terminal with phosphorylated tyrosine residues (conserved residues lacking evidence of phosphorylation are shown in parentheses). Tyrosine residues that recruits intracellular effectors which include PI3K, are shown by red bars. The unique kinase regulatory loop binding region (KRLB), which modulates interaction with the IR, in IRS-2 is also shown. **(B)** It is proposed that the PTB domain of the IRS attracts and associates with the juxtamembrane region of the IR, resulting in the phosphorylation of multiple IRS tyrosine residues and thus further activation by the IR. Images redrawn and adapted from Copps & White 2012 (118) **(A)** and White 1997 (108) **(B)**.

Table 1.2. Mice knockout* studies of the IR and IRS proteins and their different phenotypes in peripheral target tissues.

Tissue	Deletion			
	IR	IRS-1	IRS-2	
Liver	Severe insulin resistance and glucose intolerance, and the inability of insulin to inhibit glucose production (102)	Hepatic insulin resistance under re-fed conditions (116)	Severe hepatic insulin resistance under fasting conditions (116) and increased gluconeogenesis. Hyperglycaemia and impaired glucose tolerance and development of T2D (115).	**Metabolic phenotype**
Skeletal muscle	Little to no change in glucose homeostasis or muscle mass (104, 105)	Growth retardation. Mild insulin resistance. Normal glucose tolerance (111, 112)	**Unknown**	
Adipose tissue	Reduced fat-mass and protection against metabolic abnormalities (106)	Defects in adipocyte differentiation (113)	No effect on adipocyte differentiation. Impaired insulin-stimulated glucose transport (113)	
Pancreatic β-cell	Loss of insulin secretion and impairment of glucose tolerance (101)	**Unknown**	β-cell failure (115)	

1.3.1.3 Protein Kinase B/Akt

Protein kinase B/Akt is the central protein in the insulin signalling pathway. The PI3K/Akt pathway is a critical link between IRS proteins and the metabolic actions of insulin. As mentioned in section 1.3.1.2, activated IRS proteins recruit phosphoinositides to the plasma membrane with high affinity and specificity through their PH domains. Phosphatidylinositol 3-kinase (PI3K) is a class of heterodimers that consist of a regulatory (p85α) and catalytic subunit (p110) (Fig.1.3). These proteins contain a sequence-specific phosphotyrosine binding module in their regulatory subunits, known as Src homology-2 (SH2) domains, that allows them to recognize and dock to phosphorylated tyrosine residues on other proteins. Consequently, activation of the catalytic subunit occurs, which rapidly phosphorylates phosphatidylinositol 4,5-bisphosphate (PIP_2), thus generating the lipid messenger, phosphatidylinositol (3,4,5)-triphosphate (PIP_3) (82, 119, 120). This results in the recruitment of 3-phosphoinositide-dependent protein kinase 1 (PDK1) that mediates the metabolic effects of PI3K through the recruitment and activation of Akt. PDK1 contains a PH domain that binds to the membrane-

* Refs 101, 102, 103-106 & 116 = tissue-specific knockouts. Refs 111, 112, 113 & 115 = systemic/whole body knockouts

bound PIP_3, triggering its own activation, and subsequently activates the central protein Akt by phosphorylating Thr308 residue in its activation loop as described by Alessi and colleagues in 1993 (121) and Stephens and colleagues in 1998 (122).

Akt is a serine/threonine kinase that contains both a Thr308 and Ser473 residue required for full activation of the protein (121, 123–125). The Ser473 residue is situated in the carboxyl-terminal hydrophobic motif of the protein and identity of the kinase responsible for its phosphorylation has been debated in literature (125–127). Several candidates were proposed, including PDK1, integrin-linked kinase (ILK) (127) and Akt itself (125). Finally, the identity of this mystery kinase, referred to as "PDK2", was solved by Sarbassov and colleagues in 2005 (123) when they demonstrated that Akt becomes phosphorylated at its Ser473 residue by a unique complex of the mammalian target of rapamycin (mTOR) kinase. mTOR is a large protein kinase that exists in two distinct forms: a raptor-containing complex that is sensitive to the drug rapamycin (mTORC1) and regulates cell growth in part by phosphorylating S6K1 (a negative regulator of the insulin signalling pathway), and a rictor-containing complex (mTORC2) that is not sensitive to rapamycin and its cellular function is not entirely understood (123). Once it was established that Akt phosphorylation at the Ser473 residue is not sensitive to acute rapamycin treatment, Sarbassov (123) demonstrated that mTORC2 is responsible for Akt Ser473 phosphorylation using RNA interference in cultured *Drosophila* cells.

Overall, Akt phosphorylation at Ser473 is the most commonly used marker of cellular insulin action (68, 128) as it indicates final activation of the protein, increasing its kinase activity and resulting in subsequent downstream signals.

1.3.1.4 Downstream of Akt

Akt phosphorylates various downstream targets of the insulin signalling pathway, which either activates or inhibits its substrates (Fig.1.3). As described in Table 1.1, this results in the regulation of carbohydrate metabolism in the liver. Insulin-stimulated Akt acts upon two downstream targets that inhibits HGP (44, 47, 129). The first target involves the transcription factors of the Forkhead box O (FoxO) family that control the expression of gluconeogenic and lipogenic genes (82). Active, nuclear FoxO1 binds the transcriptional co-activator peroxisome proliferative activated receptor-γ coactivator 1-α (PGC1-α) to coordinate the transcription of the gluconeogenic genes, *G6Pase* and *PEPCK* (68). Three residues of FoxO1: Thr24, Ser256, and Ser319, is phosphorylated by Akt, which provides docking sites for binding proteins leading to the nuclear exclusion of FoxO1, thus attenuating its transcriptional activity (46, 82, 130), resulting in insulin-induced downregulation of gluconeogenic genes. The second target of Akt is glycogen synthase kinase 3 (GSK3), a serine/threonine kinase that regulates glycogen synthesis by phosphorylating and inhibiting glycogen synthase (Section 1.2) (46, 68). GSK3 exists as two isoforms, GSK3α and GSK3β that are structurally and functionally similar (68). The activation of Akt results in the phosphorylation of an amino-terminal motif conserved in both

GSK3α (Ser21) and GSK3β (Ser9) (130). Phosphorylation at these sites results in the inhibition of the protein, which favours dephosphorylation of glycogen synthase, thereby contributing to insulin stimulation of glycogen synthase activity and an increase in glycogen synthesis (68, 130).

Additionally, Akt also targets and upregulates the lipogenic transcriptional regulator, sterol regulatory element binding protein 1c (SREBP-1c), which promotes *de novo* lipogenesis by enhancing the transcription of several lipogenic enzymes (44, 68). SREBP-1c upregulation occurs primarily through transcription, but also through cleavage and nuclear translocation (68).

Akt targets a vast array of proteins, with only some mentioned in this section, that forms part of the insulin signal transduction network and is responsible the for action of insulin in the cell. In addition, some targets are involved in the negative regulation of the insulin signalling pathway itself (64, 68, 82). Dysregulation of any of these Akt target proteins have the potential to play a significant role in the development of insulin resistance.

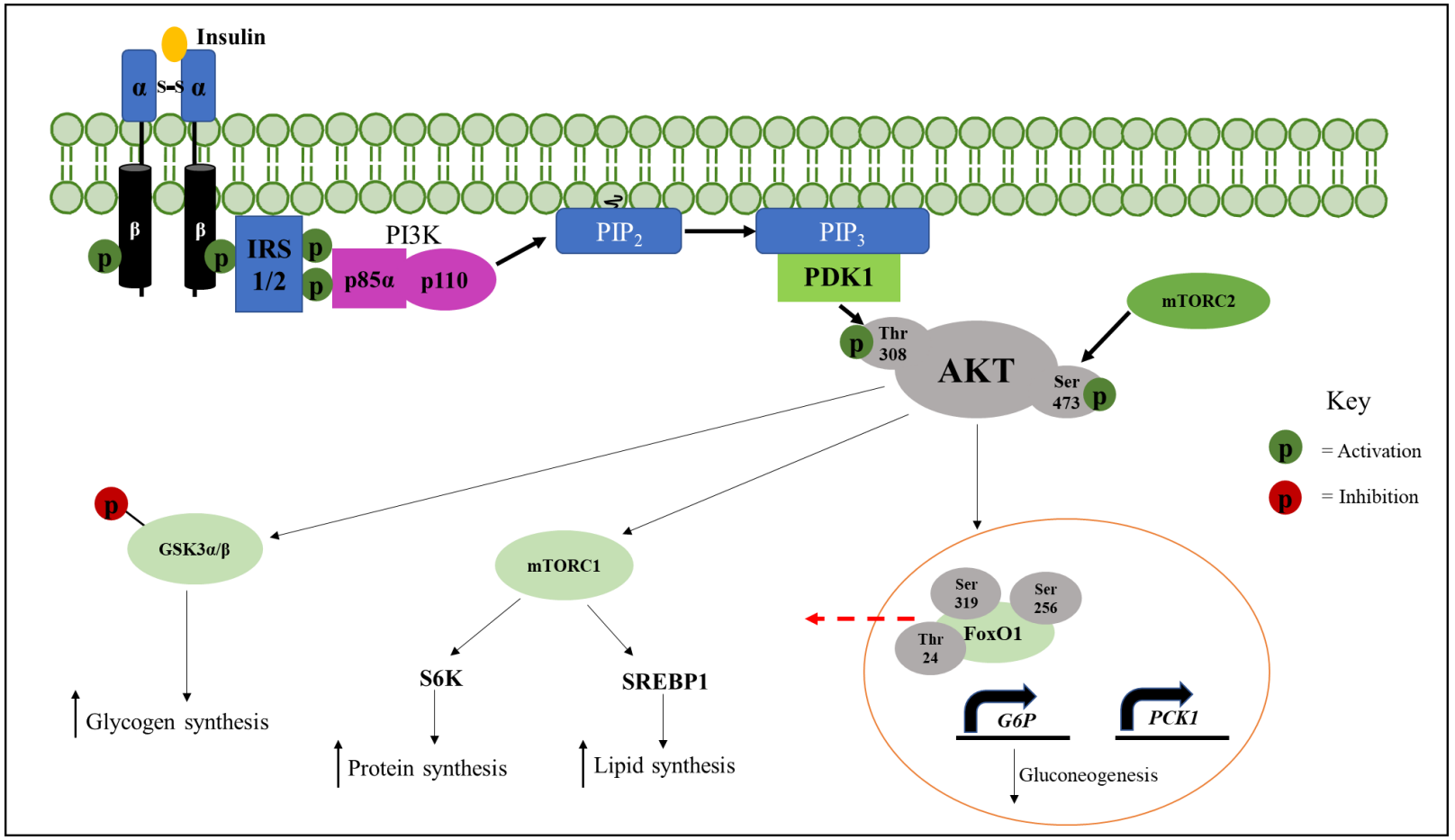

Figure 1.3. Schematic illustration of the PI3K/Akt pathway activated by insulin and the downstream targets of Akt in the liver. Insulin binding to the IR results in activation of the protein and subsequent recruitment and activation of IRS-1 and 2. Activated IRS-1 and 2 recruits the kinase PI3K, which catalyses the conversion of PIP_2 to the lipid messenger, PIP_3. This is followed by the recruitment of PDK1 that phosphorylates the central protein Akt, at its Thr308 residue. Additionally, mTORC2 phosphorylates Akt at Ser473 resulting in the full activation of the protein. Akt acts upon various downstream targets such as FoxO1, GSK3, mTORC1, S6K and SREBP1 that results in the regulation of glucose, lipid and protein metabolism. Image redrawn and adapted from Peterson, M *et al*., (68) and Boucher, J *et al*., (82)

1.3.1.5 Regulation of the insulin signalling pathway

The insulin signalling pathway is tightly controlled by various mechanisms of regulation as summarised in Fig.1.4. In this section, the regulation of the IR and IRS proteins and additionally Akt will be discussed. As mentioned above, the IR and IRS become activated *via* tyrosine phosphorylation, therefore tyrosine phosphatases can act as negative regulators of the insulin signalling pathway. Protein tyrosine phosphatase 1B (PTP1B), a very well-studied tyrosine phosphatase, acts by dephosphorylating the tyrosine residues on activated IR and IRS proteins (64, 82, 131). PTP1B is an essential protein that opposes insulin action (82, 131). The importance of PTP1B in regulating insulin sensitivity was demonstrated in PTP1B-knockout mice, which showed increased IR phosphorylation in muscle and liver tissues. Additionally, these mice were resistant to high fat diet-induced obesity and associated insulin resistance (131–133). The role of PTP1B in hepatic metabolism has also been extensively studied (134–138). Over-expression of PTP1B in Fao hepatoma cells, impaired insulin-stimulated glucose metabolism (137). Inversely, the reduction of PTP1B in these cells increased insulin signalling (134). Additionally, Gum *et al.*, (138) demonstrated an increase in IRS1/2 tyrosine phosphorylation and Akt activation in response to insulin in the liver of obese mice in which PTP1B expression was reduced by 60%. Another study, performed by Gonzalez-Rodriguez *et al.*, in 2007 (135), showed an increase in insulin sensitivity in hepatocytes from adult PTP1B-deficient mice, that specifically affected the insulin-mediated Akt/FoxO1 signalling pathway. Finally, a study from diabetic IRS-2 deficient mice show increased hepatic mRNA and protein levels of PTP1B, which resulted in impairment of the insulin-mediated Akt/FoxO1 pathway (136). These effects were reversed by PTP1B deletion in these mice, highlighting the important role of PTP1B in hepatic insulin signalling (136).

Furthermore, the IR and IRS proteins contains in their kinase domains, many serine/threonine residues, that when phosphorylated results in their inhibition, therefore reducing the activated insulin signal. Serine phosphorylation of the IRS proteins results in failure of these proteins to associate with the activated PI3K, thus decreasing the downstream effect of Akt (68, 139). Increased Ser/Thr phosphorylation of IR and IRS1/2 occurs in response to cytokines, FAs, hyperglycaemia, mitochondrial dysfunction, ER stress, and insulin itself *via* activation of multiple kinases, including p38 MAP kinase, c-Jun amino-terminal kinase (JNK), inhibitor κB kinase (IKK), protein kinase C (PKC), and also the mTORC1/S6K signalling pathway (64, 82, 118). Increased IR serine phosphorylation associated with decreased tyrosine phosphorylation has been observed in insulin-resistance states in mice and humans (82, 140, 141). Additionally, PKC was shown to inhibit IR autophosphorylation by phosphorylating the Thr1160 residue in the activation loop, a mechanism caused by lipotoxicity (142). Phosphorylation of IRS-1 at its serine residues has been well studied (143–147). Although IRS-1 has many serine residues (118), the best studied is Ser307 in rats and Ser312 in humans, which is located near the PTB domain (143) and is phosphorylated *via* several mechanisms including insulin-stimulated kinases such as MAPK and stress-activated kinases such as JNK (144, 148). The Ser307 residue of IRS-1 is a major

site of phosphorylation by JNK (144). Phosphorylation of IRS-1 at Ser307 by JNK disrupts the interaction between the PTB domain of IRS-1 and the catalytic domain of the IR (143). Aguirre *et al.*, (143) demonstrated that IRS-1 phosphorylation at Ser307 inhibited insulin-stimulation of PI3K and MAPK cascades, suggesting that phosphorylation at this site might be a general mechanism to regulate insulin signalling. Pederson *et al.*, (145) demonstrated that Ser/Thr phosphorylation of IRS-1 precedes through a rapamycin-dependent pathway (mTORC1 signalling), which is supported by Ueno and colleagues (146). Additionally, Ser307 (in rats, and Ser312 in humans) phosphorylation of IRS-1 is also induced by IKKβ, an enzyme which activates the transcription of NFκB (147). The serine phosphorylation of IRS-2 has not been as extensively studied (149, 150). Two serine residues of IRS-2 were investigated in 2011, Ser675 and Ser907 (150), both of which are situated adjacent to the PI3K and Grb2 binding domains. It was shown in insulin-stimulated hepatoma cells, that phosphorylation of IRS-2 at Ser675 was promoted by mTORC1 and Ser907 by ERK1/2, however these sites did not regulate downstream PI3K or Grb2 activity but might be implicated in the mTOR- and ERK-mediated negative feedback control (150).

Another site of regulation of the insulin signalling pathway is the recruitment and activation of Akt through PI3K *via* protein and lipid phosphatases. An example of a lipid phosphatase is phosphatase tensin homolog (PTEN), which is a 3'-phosphatase that converts PIP_3 into its precursor PIP_2, thus antagonizing PI3K signalling (64, 82). Deletion of PTEN in the liver of mice improved Akt signalling and enhanced insulin sensitivity (82, 151). A second lipid phosphatase, Src homology 2 (SH2)-containing inositol 5'-phosphatase-2 (SHIP2), has the same function as PTEN and has been shown to negatively regulate insulin-stimulated Akt phosphorylation in mice (82, 152, 153). Furthermore, there are two protein phosphatases that regulate Akt phosphorylation. Firstly, pleckstrin homology domain and leucine-rich repeat protein phosphatase 1 (PHLPP), is an Akt Ser473 phosphatase (64). Secondly, protein phosphatase 2A (PP2A) is another serine/threonine phosphatase that dephosphorylates Akt at both the Thr308 and Ser473 residue (64). Both of these phosphatases are involved in the negative feedback loop of the insulin signalling pathway (64).

In conclusion, multiple regulatory mechanisms as described in this section are in place to attenuate or terminate insulin signalling once activated. The ability to turn off the insulin signal is crucial for maintaining homeostasis, however dysfunction in the regulation of the insulin signalling pathway at its various nodes can lead to the development of insulin resistance.

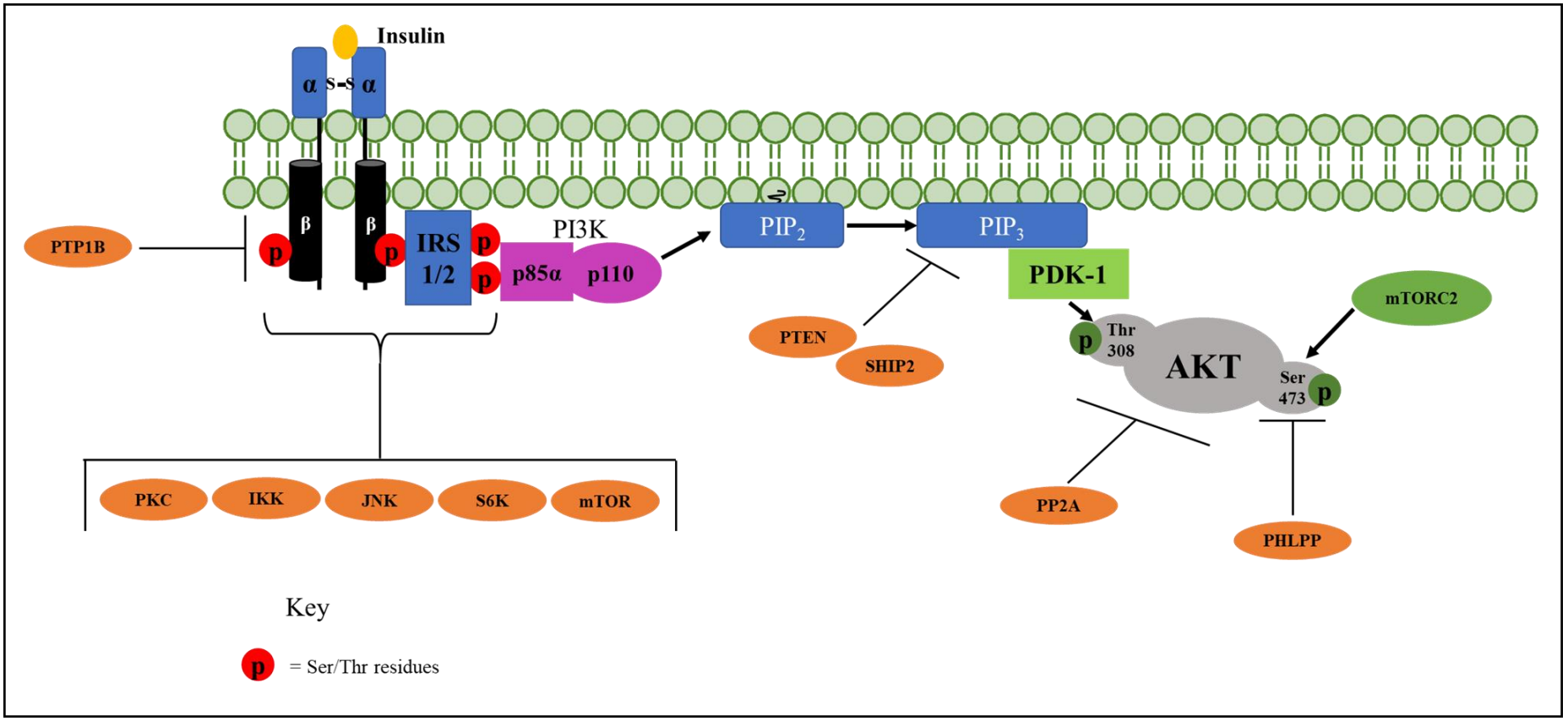

Figure 1.4. Negative regulation of the insulin signalling pathway. Overview of the various mechanisms that regulate the IR, IRS-1 and 2 proteins and Akt. The tyrosine phosphatase, PTP1B, dephosphorylates the tyrosine resides of the IR and IRS proteins. Phosphorylation of the IR and IRS at their Ser/Thr residues results in inhibition of the proteins. Protein kinase C (PKC) phosphorylates the IR at the Thr1160 residue. Inhibitor κB kinase (IKK), c-Jun amino-terminal kinase (JNK), S6K and mTOR phosphorylate IRS-1 and IRS-2 at their serine residues. Lipid phosphatases, PTEN and SHIP2, act by converting PIP_3 to the precursor PIP_2 thus antagonizing PI3K signalling. The protein phosphatases, PHLPP and PP2A act by dephosphorylating Akt at the Ser473 (PHLPP) or at both residues (PP2A). Image redrawn and adapted from Haeusler *et al.*, 2017 (64).

1.4 Insulin Resistance

Insulin resistance is defined as the inability of the peripheral target tissues (liver, adipose tissue, skeletal muscle) to respond normally to the physiological concentrations of insulin secreted by the pancreatic β-cells. The attenuated effect of insulin in these peripheral tissues precedes the development of hyperglycaemia. Defective insulin action manifests itself as reduced glucose uptake in skeletal muscle and adipose tissue and increased glucose production in the liver amongst other outcomes (67, 71). This leads to the inability of insulin to decrease blood glucose concentrations. In order to compensate for this effect, the pancreatic β-cells increases the secretion of insulin, which results in the characteristic hyperinsulinemia (excess plasma insulin levels) observed in insulin-resistant states and is a primary contributor to the development of T2D (154–156), in addition to hyperglycaemia (discussed in section 1.2) (11). Finally, when the β-cells fail to produce the excess amounts of insulin needed, due to β-cell dysfunction, T2D emerges (48, 157).

At the molecular level, two underlying mechanisms of insulin resistance have been proposed, which involves a defective insulin signalling pathway (17, 68, 154). The first mechanism describes decreased activation of key nodes in the insulin signalling pathway, which include the IR, IRS proteins, and Akt. This is described in Table 1.2, which shows that knockout of the IR as well as IRS proteins led to dramatic insulin resistance, specifically in the liver (102, 110, 114–116). For example, studies whereby IR and IRS were knocked out (Table 1.2), in rodent livers lead to hepatic insulin resistance, resulting in hyperglycaemia and glucose intolerance, which subsequently lead to the development of T2D (102, 115, 116) . Additionally, reduced tyrosine phosphorylation of the IR and IRS proteins have been observed in insulin-resistant states (24, 25, 158, 159), and hepatic inactivation of PI3K, PDK1, and mTORC2, which results in the inactivation of Akt, also induced hyperglycaemia and hyperinsulinemia in mice (160–162). A second mechanism involves an imbalance between two pathways mediating insulin action: the PI3K/Akt pathway and the MAPK pathway. Under normal conditions, there is a balance in the regulation of the PI3K/Akt pathway, to attenuate the metabolic signal, which is controlled by components of the MAPK pathway (including p38, ERK1/2 and JNK). However, dysregulation of the insulin signalling pathway, due to deficient IRS proteins shows an imbalance in this system (17, 154, 155, 163). Herein the PI3K/Akt pathway is inactivated, which disrupts nutrient homeostasis, while the activation of the MAPK pathway is sustained, promoting mitogenesis and overgrowth (17, 154). This results in increased Ser/Thr phosphorylation of the IRS proteins, leading to further inhibition of insulin signalling (67). This dysregulation can be caused by various additional factors, including the activation of inflammatory pathways, increased pro-inflammatory cytokines and FFAs as well as by stress and obesity (19, 23, 169–172, 24, 25, 159, 164–168).

Furthermore, insulin resistance in the different peripheral target tissues presents with different phenotypes: in the liver, HGP is increased due to inhibition of Akt-induced suppression of FoxO1 as

well as other transcription factors regulating glucose and lipid metabolism (section 1.3.1.4) (67, 68, 154). In adipose tissue, fat cell development is retarded and there is an increase in lipolysis (17, 154). The excessive FFAs travels to the liver and skeletal muscle, promoting gluconeogenesis and inhibiting glucose uptake, respectively, thus worsening hyperglycaemia (17). Additionally, hyperlipidemia (increased triglycerides levels in the blood), which is a key feature of insulin resistance, develops as a result of altered lipid metabolism, specifically in the liver, in which lipogenesis is increased (17, 67). Overall, insulin resistance is multifaceted and involves cross-talk between the peripheral target tissues (173) as well as various nodes in the insulin signalling pathway. Various factors such as stress, obesity and inflammation contribute to tissues becoming insulin resistant and will be discussed in the next section.

1.4.1 Factors that contribute to insulin resistance

1.4.1.1 Stress

In response to stress, glucocorticoids (GCs), are released from the cortex of the adrenal gland (10) to mediate important physiological effects on metabolism, specifically glucose metabolism (174, 175). These steroid hormones act *via* binding to the glucocorticoid receptor (GR) resulting in the transcriptional activation of the key gluconeogenic enzymes, G6Pase and PEPCK (10, 175, 176). Additionally, GCs also promote proteolysis in skeletal muscle and lipolysis in adipose tissue, leading to an increase in gluconeogenic substrates to be used in the liver (10, 177, 178). Therefore, a principal effect of GCs is to oppose insulin action in the liver (177).

GCs also exert immunosuppressive and anti-inflammatory actions, *via* the GR, by repressing the transcription of various pro-inflammatory genes (179). For this reason, synthetic GCs, such as prednisolone and dexamethasone (Dex) were developed to treat autoimmune and inflammatory diseases (175). However, it has been established that when present in excess, GCs, both synthetic and endogenous (cortisol, in humans, and corticosterone, in rodents) induce insulin resistance in the peripheral target tissues, due to their adverse metabolic effects (175, 176, 179, 180).

Patients with Cushing's syndrome, characterised by high circulating levels of endogenous GCs, are known to develop insulin resistance (178). This phenomenon stemming from this rare disease highlighted the role excess GCs play in insulin resistance. This is especially important since general chronic stress conditions will result in the activation of the hypothalamic-pituitary-adrenal (HPA) axis resulting in the increased production and secretion of endogenous GCs, which could affect insulin action similarly to what is observed in Cushing's syndrome patients. Furthermore, exogenous or synthetic GCs such as Dex and prednisolone, which are commonly prescribed to patients with inflammatory disease, also affect key components of the insulin signalling pathway (167-171, 181, 182). In the liver and skeletal muscle of rats, treatment with prednisolone decreased the

transcription of IRS-1, while increasing the transcription of PTP1B and p38 MAPK, two proteins that negatively affect insulin signalling (181, 182). Dex, on the other hand had a more pronounced effect on the insulin signalling pathway. For instance, Dex treatment decreased the insulin-stimulated phosphorylation status of the IR and IRS-1 in the liver and skeletal muscle as well as the association of IRS-1 with PI3K (167). Similarly, Sakoda *et al.*, (171) showed that in 3T3-L1 adipocytes, Dex decreased the tyrosine phosphorylation and protein expression of IRS-1. Furthermore, at the centre of the pathway, Dex is able to decrease the phosphorylation of Akt at both Thr308 and Ser473 in skeletal muscle (168, 170) and adipocytes (168) as well as the phosphorylation of GSK3-β (170), a downstream target of Akt. Finally, insulin-stimulated glucose uptake in adipose tissue (168, 169) and skeletal muscle, as well as glycogen synthesis (170) was decreased in the presence of Dex. It is evident that GCs, known for their anti-inflammatory action, also induce insulin resistance by affecting various nodes in insulin signalling.

1.4.1.2 Obesity

Obesity, which is an underlying cause of insulin resistance, is characterized by adipose tissue expansion owing to the increase in adipose tissue number (known as hyperplasia) and size (hypertrophy) (183). Obesity is also characterized by excessive accumulation of white adipose tissue (WAT), resulting from both hypertrophy of pre-existing adipocytes and increased adipocyte differentiation (183, 184). Studies in humans have shown that that weight loss/gain is associated with a decrease/increase in insulin sensitivity, respectively, therefore suggesting that obesity and insulin resistance present a cause-and-effect relationship (19, 185, 186). Mechanisms that associate the development of insulin resistance with obesity involve: FA metabolism and actions of adipokines (cytokines from adipose tissue).

Plasma FA concentrations increase in obese individuals mainly due to increased FA release associated with fat mass expansion (19, 187). As discussed previously in this section, these FAs in circulation serve as an energy source for gluconeogenesis in the liver, thus promoting hyperglycaemia. Additionally, FAs can serve as signalling molecules that activate protein kinases (these include PKC, JNK, NFκB, and IKKβ as previously discussed in section 1.3.1.5) which induce the Ser/Thr phosphorylation of IRS proteins (19, 188). Furthermore, increased plasma FAs can induce a defect in the insulin-stimulated tyrosine phosphorylation of IRS-1 as well as PI3K activation and glucose uptake in rats, as shown by Yu *et al.* (189).

In addition to increasing plasma FAs concentrations, obesity gives rise to a heightened state of inflammation (154, 165, 166). This was first shown by Hotamisligil *et al.*,(190) who showed a positive correlation between obesity and the mRNA levels of the pro-inflammatory cytokine, tumour necrosis factor (TNF-α), in mice. Subsequent experimental models of obesity also showed this effect along with an increase in TNF-α protein levels (159, 191–193). Furthermore, in the study performed by Hotamisligil *et al.*,(190) chronic exposure to TNF-α decreased the mRNA expression of Glut4, a

glucose transporter responsible for glucose uptake in adipocytes, thus affecting glucose metabolism. Moreover, *in vitro* studies have shown that in a variety of cell types including adipocytes (194), hepatoma cells (24), fibroblasts (172), and myeloid 32D cells (25), TNF-α caused a decrease in IR autophosphorylation and subsequent inhibition of IRS-1. Additionally, TNF-α also induced serine phosphorylation of IRS-1 in cultured adipocytes (25) and hepatoma cells (23), while mice lacking TNF-α were protected against the development of obesity-induced insulin resistance (159). Overall, these studies demonstrate how obesity-related inflammation can cause insulin resistance at a molecular level.

In addition to TNF-α, other adipokines such as interleukin-6 (IL-6), adiponectin, and resistin play a role in the development of insulin resistance (154). IL-6 and resistin, which can induce insulin resistance in mice (195–197), are markedly increased in obesity (198). At the cellular level, IL-6 decreased the tyrosine phosphorylation of IRS-1 as well as activation of Akt and glycogen synthesis in HepG2 cells and primary mouse hepatocytes (22), while *in vivo*, mice lacking resistin showed improved glucose homeostasis (in part due to decreased expression of gluconeogenic enzymes) (199). Levels of adiponectin, on the other hand, are decreased in obesity, unlike TNF-α, IL-6, and resistin. Adiponectin enhances insulin sensitivity in the liver, decreases influx of FAs, and reduces hepatic glucose output (200). Thus in an obese state with lower concentrations of adiponectin, the development of hepatic insulin resistance is promoted (154, 201).

Overall, obesity links inflammation to the development of insulin resistance, and causes biochemical abnormalities in adipose tissue, which can negatively affect the insulin signalling pathway, especially in the liver.

1.4.1.3 Inflammation (chronic inflammation)

As mentioned above inflammation as a result of obesity affects insulin resistance. Inflammation, more specific chronic inflammation of course does not only occur as a result of obesity. Thus a chronic inflammatory state as a result of various factors such as aging has the potential to induce insulin resistance (202). This was shown in mice, fed a high-fat diet, in which chronic inflammation was induced and essentially resulted in decreased insulin sensitivity in the liver, adipose tissue, and skeletal muscle (203). Indeed, protein expression of IRS-1, IRS-2, and Akt was decreased, as well as the phosphorylation of Akt at Thr308 (203). Subsequently, this resulted in hyperglycaemia and impaired β-cell function (203).

As already mentioned, an obese state results in the release of pro-inflammatory cytokines, TNF-α and IL-6. These pro-inflammatory mediators induce insulin resistance on a molecular level by affecting insulin signalling (22–25, 166, 172, 190, 194). In addition to TNF-α and IL-6, another pro-inflammatory cytokine, interleukin-1β (IL-1β) has been shown to affect the insulin signalling pathway. Chronic

treatment with IL-1β decreased insulin-stimulated glucose uptake in 3T3-L1 adipocytes by decreasing the protein expression of GLUT4 as well as its translocation to the plasma membrane (204). This decrease was accompanied by an inhibition of IRS-1 protein expression as well as a decrease in insulin-stimulated tyrosine phosphorylation of IRS-1 and Akt at Thr308 (204). In addition to affecting glucose uptake, IL-1β also decreased glycogen synthesis in primary cultured rat hepatocytes by inhibiting glycogen synthase activity (205). Furthermore, these pro-inflammatory cytokines exert their inhibitory effects, on IRS-1 specifically, *via* activation of MAPK pathway components such as JNK and ERK1/2 (21, 154, 164, 204), which could mediate the cross-talk between inflammatory signalling and insulin resistance (19).

Another factor linking chronic inflammation to insulin resistance, is the acute phase response (APR). A review by Pickup and Crooke (206) discussed how T2D can be considered a disease of the innate immune system. Herein, the authors proposed that T2D is an acute-phase disease, in which increased concentrations of pro-inflammatory cytokines and acute-phase proteins (APPs) are secreted, under the influence of various stimuli such as over nutrition (206, 207). This is supported by Rehman and Akash (202) who proposed that overnutrition is a major causative factor contributing to chronic inflammation in this disease state. APPs are evolutionary conserved proteins produced mainly in the liver in response to infection and inflammation (208) and their plasma levels have been associated with the complexities of T2D (39, 206, 207), leading to the question of whether they may play a role in development of the disease itself. Thus, in order to further understand this phenomenon, the importance of acute phase proteins in general biology needs to be discussed.

1.5 Acute phase proteins

1.5.1 The importance of the acute-phase response

The maintenance of homeostasis in mammals is ensured by a number of physiological mechanisms. When homeostasis is disturbed due to infection, trauma, tissue injury, surgery, or immunological disorders (206, 209, 210), the body responds by inducing a number of systemic and metabolic changes known as the acute phase response (APR) (211, 212).

The APR is a manifestation of the innate immune system (213) that comprises two reactions: the local and systemic reaction, as described by Heinrich *et al.*, (214) and shown in Fig.1.5. The local reaction is initiated at the site of invasion, which results in the release of pro-inflammatory cytokines, also known as early acute phase reactants (215). These include interleukin-6 (IL-6), interleukin-1 (IL-1), TNF-α, and interferon γ (IFNγ), of which IL-6 is considered the main regulator of the APR in the liver as shown in studies involving human hepatocytes (214, 216). The pro-inflammatory cytokines activate receptors on different target cells, which leads to intracellular signalling, resulting in the systemic reaction (Fig.1.5) characterized by a number of physiological responses in different tissues. These include fever, leucocytosis, increased levels of adrenocorticotrophic hormone (ACTH), and GCs, activation of complement, decrease in zinc and iron serum levels, changes in metabolism including increased gluconeogenesis, and finally synthesis of several plasma proteins, known as acute phase proteins (APPs), in the liver (209, 212, 214, 215). The concentrations of APPs can either be increased (known as positive APPs) or decreased (known as negative APPs) in response to inflammatory stimuli (209, 212). Positive APPs are further classified into three categories, dependent on the magnitude of their response (210). Major APPs increase 10-1000-fold in concentration within 48 hours, upon stimulation. This pronounced increase in concentration is followed by a rapid decline due to their short half-life (209, 210, 215). In contrast, the levels of moderate APPs increase by only 50% and minor APPs by 2-fold, and due to their longer half-life and depending on the stimuli have a prolonged duration (3-5 days) in circulation (209, 210, 215, 217). Thus, on average, the APR shows a rapid response that peaks within the first 48 hours but can last up to 3-5 days. The biological functions of the different positive APPs are vast (summarised in Table 1.3) and involve opsonization and trapping of microorganisms, activating the complement system, neutralizing enzymes, modulating the host's immune response as well as wound healing and tissue repair (209, 213).

Two major APPs, serum amyloid A (SAA) and C-reactive protein (CRP), have been extensively studied in literature due to their importance during the APR. This is reflected in their biological function, which involves processes in the host's immediate response to infection (Table 1.3). Indeed, Gruys *et al.*, (209) reports that their plasma concentrations become measurable within 4-5 hours after a single inflammatory stimulus, which can remain elevated up to 48 hours. However, in rat and mice studies, as

reported by Baumann (218) in 1989, peak levels of most APPs are observed at 24 hours, whereas SAA and CRP attain maximal levels at an earlier time point (8 to 12 hours). Importantly, SAA and CRP are sensitive markers of inflammation (215) and their plasma levels are routinely used to assess health in human patients and for diagnostic purposes (209, 219), because during situations of chronic inflammation (such as rheumatoid arthritis), their production is sustained (219). Their physiological concentrations reached during the APR have been investigated and will be discussed later (1.5.3 and 1.5.4).

The overall function of moderate and minor APPs involves processes important in healing, including antioxidant activity, the removal of enzymes released during tissue injury, and blood clotting, which is vital during tissue repair (Table 1.3). Unlike SAA and CRP, these proteins are not routinely used for clinical applications, yet they are still considered inflammatory markers in literature (210, 213, 217). Additionally, negative APPs, such as albumin and transferrin, decrease in concentration during the APR and for this reason is believed to not be as extensively studied (209). Their decrease allows for an increase in the unused pool of amino acids and hormones which can be used to generate positive APPs (210) and they are thus referred to as ”acute booster reactants” (209). Additionally, corticosteroid binding globulin (CBG), another negative APP, whose levels decrease during the APR, results in an increase in the concentration of free, biologically active GCs (220).

Overall the APR is important to restore homeostasis (212) and lack of resolution of the inflammatory stimulus results in chronic inflammation (215). A chronic APR has various disease implications: including T2D, metabolic syndrome X, atherosclerosis (an inflammatory process that results in lipid accumulation in the vascular wall), and cardiovascular disease (221). Pickup *et al.,* (206) in fact questioned whether or not T2D is an “acute phase disease”. In support of this, numerous studies have reported increased levels of APPs in diabetes (222, 223). The development of T2D as a result of a chronic APR is of special interest to this study, and therefore an overview of the significant APPs implicated in T2D, which include plasminogen activator inhibitor-1 (PAI-1), SAA, and CRP will be discussed in the following sections.

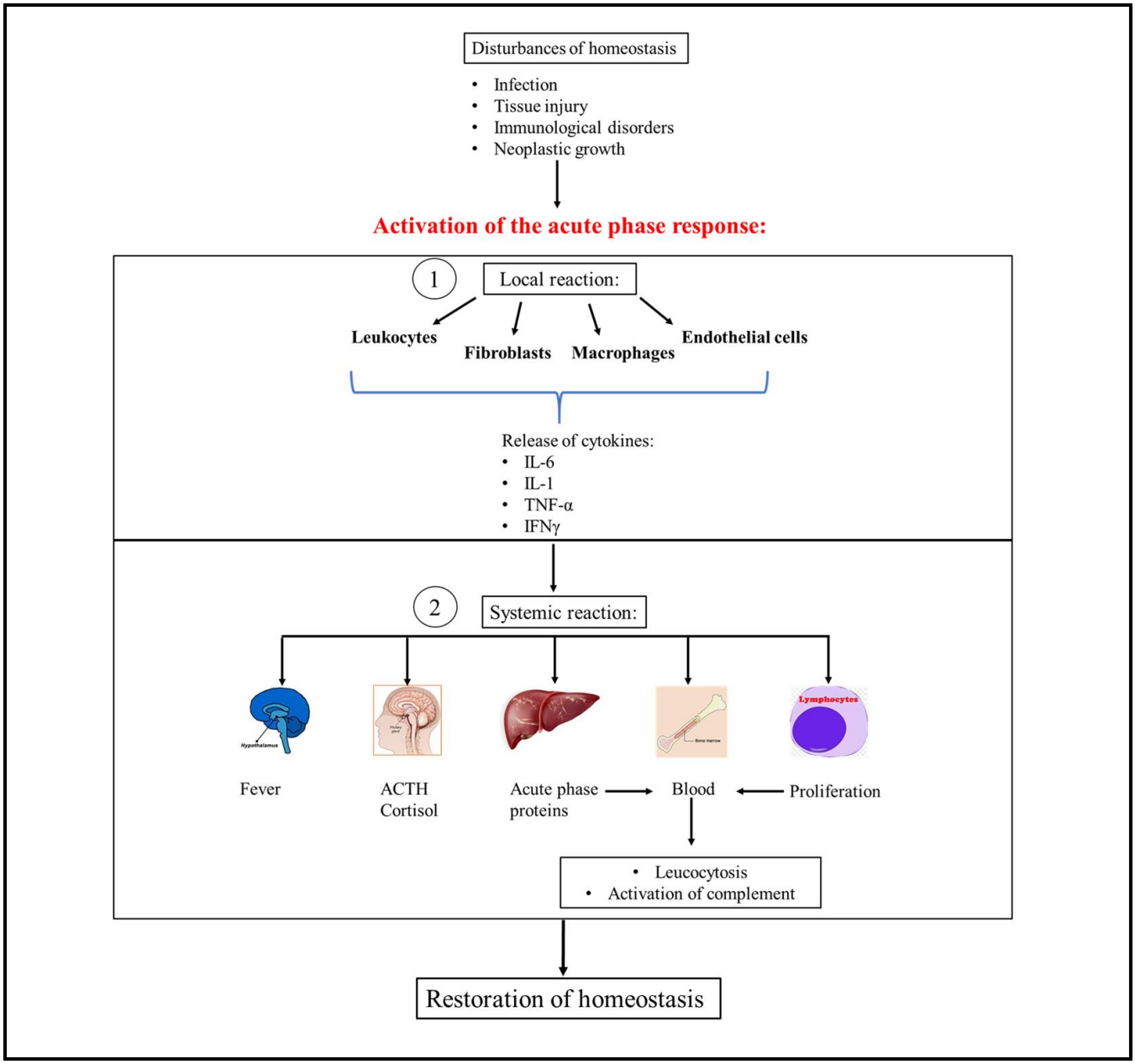

Figure 1.5. Illustration of the different phases that occur during the acute phase response. In response to various disturbances (infection, tissue injury, neoplastic growth and immunological disorders), the acute phase response is activated and results in two reactions: the local (1) and systemic (2) reaction. The local reaction results in the release of pro-inflammatory cytokines from the site of invasion or injury. The systemic reaction results in a number of physiological processes which, most importantly, includes the increase in the production of acute phase proteins in the liver. Image was redrawn and adapted from Heinrich *et al.* 1990 (214).

Table 1.3. Relevant positive acute phase proteins secreted in mammals and their physiological role in the APR

Acute phase protein	Role in the acute phase response
Major (increase 10-1000 fold)	
C-Reactive Protein	Opsonin, activation of complement, and immunomodulation. Enhances phagocytosis. (210, 213, 217).
Serum Amyloid A	Activation of leukocytes, chemotaxis and phagocytosis (210, 213, 217).
Moderate (increase up to 50%)	
Fibrinogen	Involved in tissue repair through endothelial-cell adhesion, spreading and proliferation. Promotes clot formation (210, 213, 217).
Ceruloplasmin	Scavenges free radicals (210).
Haptoglobin	Antioxidant that protects against reactive oxygen species (206, 217). Reduces oxidative damage associated with haemolysis (210).
α1-acid glycoprotein	Inhibits LPS activity (210).
Plasminogen Activator Inhibitor-1	Inhibits the activation of plasminogen (thus inhibiting fibrinolysis) (213).
Minor (increase 2-4 fold)	
α2-macroglobulin	Protease inhibitors and removal of enzymes released during injury (210).

1.5.2 Plasminogen activator inhibitor-1 (PAI-1)

The coagulation system plays an important role in the APR and the maintenance of homeostasis. It allows for blood flow to continuously be under surveillance and ensures rapid formation of blood clots at sites of injury, and thus prevents extreme blood loss from the circulation (224). Blood clots are stabilized by fibrin, which is formed from fibrinogen (224). In order to regulate this process of clot formation, an enzymatic system is in place, known as the fibrinolytic system, that is capable of dissolving blood clots (225). The fibrinolytic system comprises the formation of the active serine protease, plasmin, which can dissolve blood clots by cleaving multiple peptide bonds in the fibrin matrix (224, 225). An integral part of the fibrinolytic system is the formation of active plasmin from inactive plasminogen by the action of two plasminogen activators: tissue-type plasminogen activator (t-PA) and urokinase-type plasminogen activator (u-PA) (225–227), through their serine protease activity. PAI-1 binds and inhibits these two plasminogen activators and thus serves as a checkpoint in the regulation of fibrinolysis (226). Additionally, plasmin is known to degrade extracellular matrix (ECM) components, and therefore PAI-1 indirectly regulates ECM degradation (228), which is an important factor to consider when understanding the role of PAI-1 in different disease states.

PAI-1, also referred to as serpin E1, is a 45-kDa glycoprotein and a member of the serine protease inhibitors (SERPIN) superfamily (225–227, 229). Under physiological conditions it is synthesized in

most tissues and cell types of which the major sources include liver cells, adipocytes, vascular smooth muscle cells, and platelets (226–228). Additionally, under pathological conditions, PAI-1 is released from endothelial cells in response to inflammatory stimuli and other inflammation-activated cells including macrophages (227). Once synthesized, PAI-1 is released into the bloodstream where it spontaneously converts to a latent conformation and this process involves structural rearrangement of the protein (230). Active PAI-1 has a half-life of approximately 2 hours (226, 230), thereby indicating that this protein is fast-acting (231, 232). However, it can be stabilized through binding with vitronectin, a thermostable glycoprotein, which is able to convert PAI-1 into an active form (226, 230, 233). Therefore, the physiologically relevant form of PAI-1 is in complex with vitronectin (226, 227, 234). Additionally, a wide range PAI-1 levels in human plasma are observed: for instance, it was reported that physiological levels of PAI-1 range between 6 to 80 ng/ml, with a mean value of 24 ng/ml (225, 226). Furthermore, De Taeye *et al.*, (234) stated that mean PAI-1 levels in healthy individuals ranged between 15 to 30 ng/ml, while several studies ranging from 1993 to 2006 reported mean PAI-1 levels of 34 ng/ml (235), 9.4 ng/ml, (236), and 14.7 ng/ml (35). Although literature describes a variation in concentrations of PAI-1 in normal, healthy subjects, the levels of PAI-1 play an important role in understanding its role in disease.

PAI-1 has been extensively studied in relation to obesity, insulin resistance, and T2D (studies summarised in Table 1.4). Elevated plasma PAI-1 levels are observed throughout the spectrum of insulin resistance, from obese subjects (237) to T2D patients (34, 35), and a strong correlation exists between body mass index (BMI) and plasma PAI-1 levels (234). The high expression levels of PAI-1 in these disease states raises the question as to its contribution to the phenomenon. Indeed, PAI-1 was shown to be overexpressed in the adipose tissue of obese mice (238–240) and humans (228, 241). Therefore, it is considered a biological marker of obesity (234). However, whether this protein could contribute to the development of obesity is unclear?

As described previously in section 1.4, obesity involves dynamic changes in adipose tissue mass and number. In addition, adipocyte differentiation plays an important role. During adipocyte differentiation, extensive ECM remodelling occurs. It is believed that the established role of PAI-1 in tissue remodelling, i.e. inhibition of ECM degradation, facilitates its role in the modulation of adipocyte differentiation (242). Indeed, several studies, most conducted in mice, support this hypothesis (242, 243). Liang and colleagues (242) demonstrated that overexpression of PAI-1 in mice inhibited murine adipocyte differentiation, while PAI-1 deficiency promoted it. In accordance with this, Lijnen *et al.*, (243) showed that overexpression of PAI-1 *in vivo* impaired adipose tissue growth. Conversely, Crandall *et al.*,(244) showed that pharmacological inhibition of PAI-1 through a small molecule inhibitor, PAI-039, inhibited human pre-adipocyte differentiation. These studies indicate distinct differences in PAI-1-induced effects in murine versus human adipocytes. This study also demonstrated that in a diet-induced model of obesity, the inhibition of PAI-1, through the PAI-039 inhibitor, resulted

in reduced body weight, adipose tissue weight, and volume (244). In agreement with this result, two studies have shown that PAI-1 deficiency prevented fat accumulation and enhanced insulin sensitivity both in a genetic (245) and diet-induced (246) model of obesity, which suggests that PAI-1 protects against the development of obesity. Taken together, these findings suggest that PAI-1 plays a role in the development of obesity. Differences observed between these *in vivo* studies may be due to differences in age, fat composition of diet and genetic background of the mice (247).

In addition to its role in obesity, it is well established that elevated plasma PAI-1 levels is a core feature of insulin resistance (228, 237, 248), which is of particular relevance to the current study. Increased plasma PAI-1 levels are observed in patients with insulin resistance and T2D (34, 35, 228, 248). Indeed, in the Insulin Resistance Atherosclerosis Study (IRAS) study, Festa and colleagues observed elevated levels of PAI-1 (±24 ng/ml) in patients that developed T2D, in comparison to the 16 ng/ml observed in non-diabetic healthy subjects (34) . Additionally, these authors showed that increased PAI-1 levels over time, in addition to high baseline levels (defined as 23.7 ng/ml), are associated with the onset of T2D (35, 249). Elevated PAI-1 levels and hyperinsulinemia are also correlated (248, 250). Hyperinsulinemia of course occurs as a result of peripheral insulin resistance as described in section 1.4. Clinically, improved control of hyperglycaemia in patients with T2D has been shown to decrease PAI-1 activity (173). Improving insulin resistance by diet, exercise, or oral antidiabetic drugs results in a decrease in plasma PAI-1 levels (173, 225). Troglitazone, an antidiabetic drug that improves insulin sensitivity, was shown to decrease plasma PAI-1 antigen levels and activity in diabetic patients (251). The *in vitro* study performed by Liang and colleagues (242) also showed that inhibition of PAI-1 in 3T3-L1 adipocytes protected the cells against becoming resistant to insulin by blocking the effects of TNF-α on insulin sensitivity and glucose uptake. Therefore, PAI-1 may influence the development of obesity-related insulin resistance through TNF-α. In agreement, PAI-1 was shown to inhibit insulin signalling in the hepatoma HepG2- (252) and endothelial cells isolated from aortic tissues in mice (253), by affecting the central protein of the insulin signalling pathway, Akt. Additionally, Tamura *et al.*, (252) showed that PAI-1 affects hepatic glucose metabolism. The role of PAI-1 in developing insulin resistance was also demonstrated *in vivo* in mice lacking PAI-1, which showed improved hyperglycaemia and hyperinsulinemia associated with insulin resistance (245, 246), and also increased glucose uptake (254).

In summary, in addition to being increased in response to insulin resistance, PAI-1 may also contribute to the development thereof. However, much work is still required to determine its contribution to the development of the disease state, and additionally the molecular mechanism through which it occurs.

Table 1.4. Studies supporting the role of PAI-1 in the development of obesity, insulin resistance and type-2 diabetes.

Disease state	Model system	Supporting data	Reference
Obesity	***In vivo*** Primary cultured adipocytes from PAI-1-deficient ($PAI^{-/-}$) mice and overexpressed ($PAI^{+/+}$) mice	• PAI-1 deficiency enhanced adipocyte differentiation and insulin-stimulated glucose uptake. • Conversely, PAI-1 overexpression inhibited differentiation and reduced PPARγ expression.	Liang *et al.* 2006 (242)
	In vivo High-fat diet-induced obesity in PAI-1 knockout mice	• Fat accumulation was prevented in PAI-1 knockout mice, which additionally maintained PPARγ expression in adipocytes.	Ma *et al.* 2004 (246)
	In vivo Diet-induced obesity in mice, administered the PAI-1 inhibitor, PAI-039 ***In vitro*** Human pre-adipocytes treated with the PAI-1 inhibitor, PAI-039	• Inhibition of PAI-1 attenuated dietary fat-induced obesity and showed lower glycemia and triglyceride level. • Inhibition of PAI-1 resulted in attenuation of human pre-adipocyte differentiation	Crandall *et al.* 2006 (244)
	In vivo Genetic model of obesity and diabetic mice lacking the PAI-1 gene	• PAI-1 deficiency reduced murine adiposity.	Schäfer *et al.* 2001 (245)
	In vivo Diet-induced obesity in PAI-1 deficient mice	• PAI-1 containing mice showed marked obesity. PAI-1 deficiency resulted in faster weight gain.	Morange *et al.* 2002 (238)
	In vivo Transgenic mice with overexpression of PAI-1 in adipose tissue, administered the PAI-1 inhibitor, PAI-039	• Overexpression of PAI-1 induced impaired adipose tissue growth. • Inhibition of PAI-1 did not affect adipose tissue development, but improved insulin sensitivity in mice.	Lijnen *et al.* 2005 (243)
Insulin Resistance	***In vivo*** PAI-1 knockout mice fed a high-fat diet	• PAI-1 deficiency decreased the plasma glucose, insulin and cholesterol levels that were markedly increased by the high fat diet	Tamura *et al.* 2014 (252)
	In vitro HepG2 cells were treated with 20 nM for 24 hours	Treatment with PAI-1: • Affected hepatic insulin signalling and resulted in decreased insulin-induced glucose uptake. • Additionally, PAI-1 affected gluconeogenesis by increasing G6Pase and PEPCK mRNA levels	Tamura *et al.* 2015 (254)
	In vitro PAI-1 knockout endothelial cells treated with 10 ng/ml PAI-1 for 24 hours	PAI-1 deficiency: • increased Akt activation Treatment with PAI-1: • decreased Akt activation	Balsara *et al.* 2006 (253)
	In vivo High-fat diet-induced obesity in PAI-1 knockout mice	• PAI-1 knockout mice showed increased glucose uptake and maintained plasma glucose and insulin levels.	Ma *et al.* 2004 (246)

	In vivo Genetic model of obesity and diabetic mice lacking the PAI-1 gene	• PAI-1 deficiency significantly improved the hyperglycaemia and hyperinsulinemia associated with insulin resistance.	Schafer *et al.* 2001 (245)
Type-2 diabetes	***Epidemiological study*** The IRAS study – measured PAI-1 levels in non-diabetic patients in relation to incident diabetes within 5 years	• Elevated levels of PAI-1 (±24 ng/ml) was associated with incident type-2 diabetes	Festa *et al.* 2002 (34)
	Epidemiological study Follow up study to Festa *et al* 2002.	• Increased PAI-1 levels over time, in addition to high baseline levels (23.7 ng/ml), was associated with the onset of T2D	Festa *et al.* 2006 (35)

1.5.3 Serum Amyloid A (SAA)

SAA is a well-characterized APP that is predominantly synthesized in the liver (213, 255). It is an apolipoprotein that can bind and transport lipids in the blood and is mainly associated with high-density lipoproteins (HDLs) (255, 256). The important functional role of SAA during the APR, in host defence, has made it a sensitive marker of inflammation, in addition to CRP (217, 219). Indeed, during the APR, the plasma levels of SAA increase up to 1000-fold (as discussed in section 1.5.1), from 1-5 µg/ml in healthy individuals, to an exceeding 1 mg/ml (256, 257). There are four different isoforms of the SAA genes (SAA1-4) of which SAA1 and SAA2 encode acute-phase SAA (A-SAA) proteins and SAA4 is a constitutively expressed protein (256–259). In humans, SAA3 is a pseudogene, but is functionally expressed in the adipose tissue of mice (259), particularly obese mice (260). A study by Lin *et al.*, (261) found that SAA3 is expressed at very low levels in the liver of mice. Although, in humans, the liver is the main site of synthesis during the APR, a study by Sjoholm *et al.*, (262) in 2005 showed that adipose tissue is the major expression site of A-SAA during non-acute phase conditions with the liver showing the second highest expression. In agreement with this result, Yang *et al.*, (263) showed, in 2006, that A-SAA is highly expressed in human adipocytes.

During the APR, A-SAA is secreted into circulation as a free protein and rapidly associates with HDLs, its physiological carrier (256). The amphipathic structure of SAA facilitates its binding to HDLs and its ubiquitous diffusion *via* the circulation to all organs and tissues, to perform its biological function (213). During the APR, SAA has immune-related functions that include acting as a chemoattractant for monocytes, leukocytes, and polymorphonuclear cells to inflammatory sites, resulting in the extension of inflammation (255, 259, 264). The immune-related functions of SAA are mediated by its ability to bind to various cell surface receptors (255, 265), which can result in the activation of various inflammatory signalling pathways, such as the MAPK and ERK1/2 pathways (discussed in section 1.3.1.5) (265, 266).

Like PAI-1, SAA is a marker of obesity (263) and has been extensively studied in relation to this inflammatory condition as summarised in Table 1.5. Increased circulating levels of SAA has been observed in obese individuals (263, 267, 268), which positively correlates with an increased BMI and decreased weight loss. The concentrations observed in the obese individuals ranged from approximately 11-20 µg/ml (263, 267, 268). Poitou *et al.*, (267) also observed increased levels of hSAA1 and hSAA2 mRNA and protein expression in adipose tissue of these obese individuals. Additionally, like PAI-1, SAA has been shown to affect adipocyte differentiation *in vitro* by reducing the mRNA expression of two adipogenic transcription factors: PPARγ and C/EBPα (260, 269). Dysregulation of lipid metabolism (such as increased basal lipolysis and decreased lipid synthesis in adipose tissue) is also associated with obesity (263). It was shown by three independent studies that SAA increased lipolysis *in vitro* (260, 263, 269) and additionally reduced the mRNA expression of a transcription factor involved in lipid synthesis, namely SREPB-1c (269). Recently a study reported that mice fed a high-fat diet was protected from weight gain when treated with an anti-sense oligonucleotide that inhibits SAA mRNA expression (270). Furthermore, inhibiting SAA levels prevented adipose tissue expansion as well as macrophage infiltration into adipocytes, both of which are associated with obesity (270). Thus, not only are SAA levels increased during obesity, it appears to also play a role in the development thereof.

In addition to obesity, SAA is also a marker of T2D and insulin resistance (271). Indeed, measurement of SAA concentrations in serum of patients with T2D showed significantly higher levels (38, 268, 272, 273) (Table 1.5). SAA concentrations measured in T2D patients ranged from 2.1-24 µg/ml (38, 268, 272, 273), comparable to levels observed in obese individuals. Additionally, elevated SAA levels (as well as other markers of inflammation including TNF-α, IL-6, and CRP) were observed in the plasma of previously healthy individuals, who presented with onset T2D (36, 37). Also in diabetic (*ob/ob*) mice, increased SAA mRNA levels strongly correlated with chronic hyperglycaemia observed in the mice (261). Treatment of T2D patients with the anti-diabetic drug, troglitazone, not only inhibited hyperglycaemia but also significantly reduced SAA levels (273). These findings raise the question of whether SAA is more than just a biological marker for T2D i.e. is an increase in SAA levels a result of T2D, or is T2D a result of an increase in SAA, or perhaps both scenarios are possible. Scheja and colleagues (271) investigated this hypothesis in both *in vivo* (insulin-resistance prone mouse model) and *in vitro* (3T3-L1 adipocytes) models. Insulin-resistance prone mice, which were fed a high-fat diet, showed a significant increase in SAA1 and SAA2 mRNA levels in the liver, and SAA3 mRNA levels in adipose tissue (271). The authors next treated 3T3-L1 adipocytes with SAA (12.5 µg/ml) which resulted in decreased IRS-1- and GLUT-4 mRNA expression (271). In accordance, Ye *et al.*, (274) showed decreased tyrosine phosphorylation of the IRS-1 protein as well as decreased GLUT-4 protein expression in 3T3-L1 adipocytes treated with SAA (20 µg/ml). Additionally, SAA (10 and 20 µg/ml) treatment decreased insulin-stimulated glucose uptake by 3T3-L1 adipocytes (274). Similarly, Filippin-

Monteiro and colleagues, showed that treatment of 3T3-L1 adipocytes with SAA (5 and 10 µg/ml) significantly reduced insulin-stimulated glucose uptake as well as GLUT4 mRNA expression (260). Taken together, these studies support the hypothesis that SAA may play a role in the development of insulin resistance, which could consequently lead to T2D. However, most of the studies investigated the effect of SAA in adipose tissue, and little research exists on how the liver or skeletal muscle is affected by SAA. Not much is known about the effect of SAA on the development of hepatic insulin resistance, which plays a key role in the progression to T2D. Additionally, the effect of SAA on other nodes of the insulin signalling pathway, such as the IR and Akt, have not yet been established.

Table 1.5. Studies supporting the role of SAA in the development of obesity, insulin resistance and type-2 diabetes

Disease state	Model system	Supporting data	Reference
Obesity	***In vitro*** 3T3-L1 adipocytes	• SAA decreased adipocyte differentiation, by decreasing adipogenic transcription factors (PPARγ, C/EBPα) • SAA significantly increased lipolysis	Filippin-Monteiro *et al.* 2012 (260)
	In vivo SAA mRNA inhibition in mice fed a high-fat diet	• Inhibition of SAA promoted a lack of adipose tissue expansion as well as macrophage infiltration into adipose tissue.	De Oliveira *et al.* 2016 (270)
	In vivo Serum SAA levels in obese individuals ***In vitro*** Human adipocytes treated with SAA (2.34 µg/ml) for 24 hours	• SAA levels increased in obese individuals • SAA levels decreased after weight loss • Treatment with SAA increased lipolysis	Yang *et al.* 2006 (263)
	In vitro Human adipocytes treated with SAA for 24 hours	SAA treatment resulted in: • increased lipolysis • reduced mRNA expression of transcription factors involved in adipocyte differentiation (PPARγ, C/EBPα) and lipid synthesis (SREPB-1c)	Faty *et al.* 2012 (269)
	In vivo Gene expression in obese individuals	• Increased expression of SAA1 and SAA2 mRNA and protein expression in obese individuals	Poitou *et al.* 2005 (267)
Insulin resistance	***In vitro*** 3T3-L1 adipocytes	• SAA significantly decreased insulin-stimulated glucose uptake	Filippin-Monteiro *et al.* 2012 (260)
	In vitro 3T3-L1 adipocytes	• SAA significantly decreased mRNA expression of Glut4 and IRS-1	Scheja *et al.* 2008 (271)
	In vitro 3T3-L1 adipocytes	SAA significantly reduced: • insulin-stimulated glucose uptake • activation of IRS-1 • GLUT4 expression	Ye *et al.* 2009 (274)
	In vivo SAA mRNA inhibition in mice fed a high-fat diet	• Inhibition of SAA protected mice from weight gain and insulin resistance	de Oliveira *et al.* 2016 (270)
Type-2 diabetes	***In vivo*** Diabetic (*ob/ob*) mice. Measured SAA3 mRNA in adipose tissue	• Isolated adipose tissue of T2D mice showed drastically increased SAA3 mRNA levels	Lin *et al.* 2001 (261)
	Epidemiological study Patients with T2D who received daily treatment with troglitazone (anti-diabetic drug)	• SAA levels were above the range for healthy subjects (approx. 6.2 µg/ml) • Troglitazone reduced SAA levels (by 25% down to 4.0 µg/ml)	Ebeling *et al.* 1999 (273)
	Epidemiological study Measured SAA levels in patients with impaired glucose tolerance	• Plasma levels of SAA were significantly higher in patients with T2D and in those with impaired glucose tolerance (approx. 6 µg/ml).	Müller *et al.* 2002 (36)

	in comparison to individuals with and without T2D		
	Epidemiological study Measured SAA levels in non-diabetic individuals who participated in a 7-year follow-up	• SAA levels were significantly associated with the onset of T2D (approx. 4.0 µg/ml)	Marzi *et al.* 2013 (37)
	Epidemiological study Measured SAA levels in T2D patients	• Insulin resistance and T2D was significantly correlated with SAA levels (approx. 24 µg/ml)	Leinonen *et al.* 2003 (38)

1.5.4 C-Reactive Protein (CRP)

Discovered in 1930 in the serum of patients with acute pneumococcal pneumoniae (275), CRP was the first described APP. It was named for its capacity to bind the C polysaccharide of *Streptococcus pneumoniae* (209, 219, 276, 277) and subsequently played a significant role in the identification of the APR (277). CRP is primarily synthesized by hepatocytes in response to an inflammatory stimulus and its synthesis is mainly regulated by the pro-inflammatory cytokines TNF-α, IL-6, and IL-1 (29, 278, 279). As a member of the pentraxin family of calcium-dependent ligand binding proteins (276), CRP is produced as a homopentameric protein, consisting of five identical subunits (Mr = 23 kDa) (209, 276, 280), which is termed native CRP (nCRP) (280). Additionally, this protein can irreversibly dissociate into its monomeric form (mCRP) which has been observed when the protein is exposed to harsh damaging conditions (276). In the presence of calcium, CRP binds to polysaccharides such as phosphocholine on microorganisms, with high affinity (276), and triggers the classical complement pathway of the innate immune system (280) (summarised in Table 1.3). The two isoforms have shown distinct functions in the inflammatory process with nCRP tending to exhibit more anti-inflammatory activities relative to the mCRP isoform (276, 280).

The CRP levels in healthy individuals is generally below 2 mg/l (277), but can be as high as 10 mg/l (217, 219). This level can increase with illnesses such as rheumatoid arthritis or sepsis, in the first 6-8 hours of the APR and can reach peak levels of 300 mg/l after 48 hours (277). Indeed, a review by Suffredini *et al.*, (213) reported that during the APR, CRP increases from 1 mg/l up to 1000 mg/l in plasma. Additionally, CRP values between 2 and 10 mg/l may be seen with metabolic inflammatory states, such as uremia, cardiac ischemia, and other low non-infectious inflammatory conditions (219). Upon resolution of the inflammatory stimulus, CRP levels rapidly decline with a half-life on average of approximately 19 hours (276, 281). This is consistent under all conditions and disease states, therefore the sole determinant of circulating CRP concentrations is the synthesis rate (276). Additionally, few drugs affect the circulating levels of CRP unless they also affect the underlying pathology providing the inflammatory/acute-phase stimulus (276).

In addition to PAI-1 and SAA, circulating levels of CRP have been studied in relation to insulin resistance and T2D, due to its role as a sensitive inflammatory marker (summarised in Table 1.6). This is important especially when establishing a link between inflammation and the development of insulin resistance and T2D. Several cross-sectional studies have shown that high sensitivity CRP levels (hsCRP) (CRP levels measured using high sensitivity immunoassays) are associated with obesity (282, 283), increased fasting blood sugar levels (283), and impaired insulin sensitivity (284, 285), all components of insulin resistance. These findings fuelled the speculation that elevated hsCRP levels might be able to identify individuals in a prediabetic, insulin resistant-state (286).

In addition, significant epidemiological studies have shown that increased hsCRP levels may predict the development of future T2D. Firstly, the Women's Healthy Study (WHS) (40) demonstrated an association between hsCRP and insulin-resistant states, showing that among healthy women, high levels of IL-6 and hsCRP were associated with an increased risk for the development of T2D. In addition, the Cardiovascular Health Study (CHS) (41) also demonstrated that in a population of elderly men and women, elevated baseline hsCRP levels predicted the development of T2D. Finally, the IRAS study performed by Festa and colleagues (34), showed that high hsCRP baseline levels (>2.4 mg/l) amongst patients diagnosed with insulin resistance were associated with a higher risk of developing T2D. In addition to this, in a later study by the same authors, a significant correlation between CRP and components of insulin resistance were recognised (39).

In addition to establishing CRP as a predictive risk factor for insulin resistance and the development of T2D, numerous studies also investigated whether CRP could a play a role in the development of the disease state (summarised in Table 1.6). Alessandris and colleagues (287) demonstrated using rat skeletal muscle cells, that high concentration of CRP (10 mg/l) impaired insulin signalling by increasing the serine phosphorylation of IRS-1 and reducing the activation of Akt. Additionally, this resulted in reduced glycogen synthesis and glucose uptake, thus, showing that CRP has an overall effect on the regulation of glucose metabolism. In support of this study, Xu *et al.*, (288) showed a similar effect of CRP on insulin signalling in endothelial cells. Treatment with concentrations of CRP (ranging from 1, 5, 10, and 25 mg/l) increased serine phosphorylation of IRS-1 and decreased the activation of Akt (288). Furthermore, similar effects were observed on insulin signalling in primary cultured rat hepatocytes when treated with CRP (30 mg/l), which resulted in decreased tyrosine phosphorylation of IRS-1 and its association with PI3K, as well as increased serine phosphorylation of IRS-1 (289). Additionally, this study demonstrated the same effect *in vivo* in rats administered CRP.

In summary, like the other APPs mentioned, CRP is described as a strong predictor for the development of T2D (40, 41, 286, 290, 291). Additionally, the role of CRP in the development of insulin resistance by affecting the insulin signalling pathway in hepatocytes, skeletal muscle, and endothelial cells have

been described (287, 288, 292). However, the effect of CRP on other key nodes in the insulin signalling pathway, such as the IR, have not been researched to fully elucidate its role in insulin resistance.

Table 1.6. Studies supporting the role of CRP in the development of insulin resistance and type-2 diabetes.

Disease state	Model system	Supporting data	Reference
Insulin resistance	***In vitro*** Rat skeletal muscle (L6) cells treated with 10 mg/l CRP	CRP induced insulin resistance in skeletal muscle cells by: • increasing serine phosphorylation of IRS-1 • reducing activation of Akt • reducing glycogen synthesis • impairing glucose uptake	Alessandris *et al.* 2007 (287)
	In vitro Mouse endothelial cells treated with recombinant CRP at various doses and times	Overall CRP impaired insulin signalling in endothelial cells by: • increasing serine phosphorylation of IRS-1 • decreasing activation of Akt	Xu *et al.* 2007 (288)
	In vitro Primary cultured rat hepatocytes treated with 30 mg/l hCRP ***In vivo*** Rats treated with CRP	CRP induced hepatic insulin resistance both *in vivo* and *in vitro* by: • reducing the activation of IRS-1 and Akt • impairing the association of IRS-1 with PI3K. • inducing the inhibition of IRS-1 (through serine phosphorylation)	Xi *et al.* 2011 (292)
Type-2 diabetes	***Epidemiological study*** The IRAS study – measured CRP levels in non-diabetic patients in relation to incident diabetes within 5 years	• Elevated CRP levels (>2.4 mg/l) was associated with incident T2D	Festa *et al.* 2002 (34)
	Epidemiological study Measured insulin sensitivity and CRP levels in the non-diabetic population of the IRAS study	• Elevated CRP levels (>3.53 mg/l) was strongly associated with components of insulin resistance and T2D	Festa *et al.* 2000 (39)
	Epidemiological study Women's Health Study	• High hsCRP levels were associated with increased risk for development of T2D	Pradhan *et al.* 2001 (40)
	Epidemiological study Cardiovascular Health Study	• High baseline levels (2.8 mg/l) of CRP predicted T2D	Barzilay *et al.* 2001 (41)

1.5.5 Regulation of acute phase proteins

Thus far it has been established that the APPs, PAI-1, SAA, and CRP are strongly associated with insulin resistance and T2D due to their elevated levels in these disease states. It is thus important to establish what signalling molecules regulate the levels of these APPs as this might provide insight into how and why APPs are associated with insulin resistance and T2D. For this reason, the regulation of the three APPs of interest will be discussed next.

Studies investigating PAI-1 expression have shown that PAI-1 is regulated by a variety of factors including: insulin, TNF-α, IL-6, IL-1, GCs, glucose, epidermal growth factor (EGF), transforming growth factor-β (TGF-β) and very low density lipoproteins (VLDLs) (228), as summarised in Table 1.7.

The effect of insulin on PAI-1 regulation has been extensively studied (293–299). As discussed previously in section 1.5.2, PAI-1 levels is associated with hyperinsulinemia (248, 250). Several *in vitro* studies have shown that insulin stimulates PAI-1 transcription and protein synthesis in HepG2- (293, 294), 3T3-L1 adipose- (298), and endothelial cells (299). Banfi *et al.*, (294) demonstrated a possible mechanism through which insulin could regulate PAI-1 transcription in HepG2 cells. By using a tyrosine kinase inhibitor, the authors showed that tyrosine phosphorylation is required for PAI-1 biosynthesis as well as interaction of insulin with its cognate receptor (294). Further investigations, using an inhibitor of a key protein in the insulin signalling pathway, PI3K, as well as a protein that regulates the pathway, PKC (as described in section 1.3.1.5), demonstrated that the presence of these inhibitors attenuated insulin stimulation of PAI-1 transcription and biosynthesis. Therefore, activation of PI3K, followed by PKC is required for insulin-induced biosynthesis of PAI-1 in HepG2 cells (294). However, the involvement of the PI3K pathway in the regulation of PAI-1 synthesis seems tissue-specific, as Mukai and colleagues (299) demonstrated in vascular endothelial cells that treatment with PI3K inhibitors increased the TNF-α and insulin-induced expression of PAI-1. Finally, inhibition of MAPK and ERK (section 1.3.1.5) inhibited both basal and insulin-stimulated PAI-1 secretion and gene transcription (>75%) in HepG2 cells, thus suggesting that the MAPK pathway also regulates PAI-1 expression in the liver (228, 294). Finally, the precursor of insulin, proinsulin, also increased the mRNA expression as well as activity of PAI-1 in HepG2 (295) and endothelial cells (296). The effect on PAI-1 by proinsulin was mediated by the insulin receptor in HepG2 cells, whereas in endothelial cells it was not (295, 296). These studies suggest that insulin itself, through activation of its own signalling pathway, could upregulate PAI-1 synthesis in the liver. Furthermore, it was shown that even in an insulin-resistant state, PAI-1 continues to be induced to an even greater extent in comparison to control mice by insulin in diabetic mice (297). The effect of insulin on the regulation of SAA and CRP on the other hand, has not been investigated. Finally, PAI-1 can also be upregulated by metabolic disturbances such as VLDLs, triglycerides (300, 301), and increased glucose levels (302).

In vitro studies in the hepatoma cell lines, AML-12 and HepG2, showed enhancement of PAI-1 transcription by the pro-inflammatory cytokines, IL-6 and IL-1 (303, 304). Additionally, whereas IL-6 only showed a modest effect on PAI-1 mRNA levels, IL-6 in combination with IL-1 showed a synergistic effect (303, 304). TNF-α seemed to affect PAI-1 mostly in adipose tissue, both *in vitro* and *in vivo* (298, 305, 306) by increasing mRNA levels in mice (305) as well as PAI-1 activity and protein expression in 3T3-L1 adipocytes (298, 306). Interestingly, the effect observed in 3T3-L1 adipocytes was enhanced in combination with insulin (298). These studies suggest that TNF-α (which is related to obesity) might be the key inducer of PAI-1 expression in adipose tissue in obesity-related insulin resistance. Additionally, TNF-α enhanced PAI-1 mRNA and protein expression in endothelial cells (299, 307). Furthermore, the anti-inflammatory GCs have also been shown to regulate PAI-1 expression (33, 254, 308–310). Using the synthetic GC, Dex, several studies have shown an increase in PAI-1 mRNA and protein expression in response to Dex, in human visceral adipose tissue (308), primary hepatocytes (309), epithelial cells (33), and human bone marrow adipocytes (311). Interestingly, in epithelial cells, Kimura and colleagues (33) showed that Dex further enhanced the TNF-α induced mRNA expression of PAI-1. Thus, raising the question of whether these antagonizing mediators could work together to upregulate the expression of APPs, such as PAI-1? However, it is not yet known whether this combinational effect is observed in other cell types, or if Dex can enhance the effect of IL-6 and IL-1 on PAI-1 expression. Furthermore, corticosterone, the endogenous GC in mice, increased the mRNA as well as circulating level of PAI-1 *in vivo* (254). In addition to these pro- and anti-inflammatory mediators, several growth factors have been shown to enhance the expression and activity of PAI-1 (310, 312), for example, EGF in HepG2 cells increased PAI-1 mRNA levels (310). Two additional growth factors, platelet-derived growth factor and TGF-β, have also been described as enhancing PAI-1 mRNA and protein expression in vascular smooth muscle cells (VSMC's) (312).

As markers of inflammation and major positive APPs, A-SAA and CRP expression are mainly regulated by the pro-inflammatory cytokines IL-6, IL-1, and TNF-α (summarised in Table 1.7). However, several *in vitro* studies investigating A-SAA and CRP mRNA and protein expression in hepatoma cell lines, show differential regulation by these aforementioned cytokines (Table 1.7). For instance, SAA mRNA expression is induced by all three cytokines (TNF-α, IL-1, and IL-6), however to different extents (26-28, 32, 278, 313–315). IL-1 was shown to be a strong inducer of SAA mRNA expression (32, 314), whilst IL-6 stimulates SAA mRNA expression to a lesser extent (315, 316). SAA mRNA was induced modestly by TNF-α and IL-6 alone in HepG2 cells, and this induction was enhanced when these cytokines were present in combination (28). Furthermore, TNF-α, IL-1, and IL-6 in combination were able to enhance the transcription of SAA in HepG2 cells to a greater extent compared to treatments with one cytokine alone (316). CRP synthesis, on the other hand, was shown to be mainly regulated by IL-6 in the hepatoma cell lines, Hep3B and HepG2 (29, 278). Additionally, in primary human hepatocytes, IL-1 was able to upregulate CRP synthesis, *via* inducing the synthesis of IL-6, strengthening the

argument that CRP levels are mainly upregulated by IL-6 in the liver (29). Interestingly, TNF-α alone, or in combination with IL-6, had no effect on CRP synthesis in Hep3B cells (26).

The induction of SAA and CRP is not limited to the liver. CRP production was induced by IL-1 and IL-6, alone, and in combination in human adipocytes (279). The mRNA expression of SAA3, the SAA isoform mainly produced in adipose tissue, is increased, by TNF-α and IL-6 in 3T3-L1 adipocytes (317) as well as IL-1 (30). It was found that the positive effect on SAA3 mRNA expression induced by IL-6 and IL-1 was mediated by JNK-2 and NFκB, respectively (30, 317). These two proteins are involved in the negative regulation of the insulin signalling pathway, as discussed in section 1.3.1.5. In addition, the adipokine, resistin, also induced CRP synthesis in adipocytes (279).

Like PAI-1, the cytokine-driven production of SAA and CRP in hepatoma cell-lines can be enhanced by the GC, Dex (26–30). GCs were also able to increase SAA3 mRNA levels in 3T3-L1 adipocytes, suggesting this effect is not tissue specific (317). Interestingly, Dex treatment in combination with TNF-α, IL-1 or IL-6 increased SAA and CRP production to a greater extent in comparison to the respective cytokine alone (26, 27, 29). Depraetere *et al.*, (29) showed that in HepG2 cells, pre-treatment with Dex primed the cells to be more responsive to IL-6. In addition to Dex, another synthetic GC, prednisolone, enhanced the cytokine-driven production of SAA in HepG2 cells, but not that of CRP (32).

Overall, the APPs, PAI-1, SAA, and CRP are regulated by pro-inflammatory cytokines and anti-inflammatory GCs. Both these signalling molecules are known to play a significant role in the development of T2D and the insulin resistant state (see section 1.4). It thus begs the question of whether GC- and pro-inflammatory cytokine-induced insulin resistance develops as a result of an increase in these APPs?

Table 1.7. Effects of various components on the regulation of PAI-1, SAA, and CRP.

APP	Pro-inflammatory cytokines (Inflammation)	Glucocorticoids (GCs)	Insulin and other growth hormones	Other
PAI-1	**TNF-α:** • Increased PAI-1 mRNA and protein expression in both adipocytes (298, 305) and endothelial cells (299, 307)	**Dex:** • Increased PAI-1 mRNA levels and secretion in adipose tissue (308, 311), primary hepatocytes (309) and epithelial cells (33)	**Insulin**: • Stimulates PAI-1 transcription and protein expression in HepG2 (293, 294), adipose (298) and endothelial cells (299) **Proinsulin:** • Stimulates PAI-1 mRNA and activity in HepG2 (295) and endothelial cells (296)	**VLDL:** • Enhanced release of PAI-1 antigen and PAI-1 activity in HepG2 cells (300, 301)
	IL-1: • Enhanced PAI-1 transcription in hepatocytes (303, 304)	**Corticosterone:** • Increased PAI-1 mRNA as well as circulating levels (254)	**Platelet-derived growth factor and TGFβ:** • Induce PAI-1 mRNA and protein expression and activity in VSMC's (312)	**Glucose:** • Elevated glucose concentrations increased PAI-1 secretion in endothelial cells (302)
	IL-6: • Modestly enhanced PAI-1 transcription in hepatocytes (303, 304) **IL-6 and IL-1** • Synergistically enhanced PAI-1 transcription in hepatocytes (303, 304)		**EGF:** • Increased PAI-1 mRNA in HepG2 cells (310)	
SAA & CRP	**TNF-α:** • Increases SAA mRNA in HepG2 cells (28) and SAA3 mRNA in 3T3-L1 adipocytes (317) • No effect on CRP production (26)	**Dex:** • Enhances the cytokine-induced production of SAA and CRP, in liver cells (26–30), and 3T3-L1 adipocytes (317) • Has no effect on its own (192, 196, 200	**Unknown in the liver** (no effect on SAA3 mRNA expression in 3T3-L1 adipocytes) (317)	• Resistin (an adipokine) induced CRP production in human adipocytes (317)
	IL-1: • Strong inducer of SAA mRNA expression in	**Prednisolone:** • Enhanced SAA production, induced by IL-1 in HepG2 cells (32)		

	hepatoma cell lines (32, 314) • Increases SAA3 mRNA in 3T3-L1 adipocytes (30) • Induces CRP production in primary human hepatocytes (29) and human adipocytes (279)	• No effect on CRP synthesis (32)		
	IL-6: • Induces SAA to a lesser extent in hepatoma cells (313, 315) • Increases SAA3 mRNA in 3T3-L1 adipocytes (317) • Strong inducer of CRP synthesis in hepatoma cells (29, 278) and human adipocytes (279)	**Combinatorial effects with Dex:** **Dex+TNF-α+IL-6:** • Dex enhanced SAA mRNA expression in Hep3B cells (26) **Dex+IL-1+IL-6:** • Dex enhanced the synthesis of SAA and CRP in Hep3B cells (26) and SAA gene expression in HepG2 cells (31)		
	Combinatorial effect of the three cytokines: **TNF-α+ IL-1+ IL-6:** • Induces SAA synthesis in hepatoma cells (316) **TNF-α+IL-6:** • Increases SAA3 mRNA in 3T3-L1 adipocytes (317) **IL-1+IL-6:** • Increases CRP production in hepatoma cell lines (29)			

1.6 Conclusion

T2D is a state of heightened inflammation and although numerous factors contribute to the development of insulin resistance and subsequently T2D, such as obesity and stress, a common theme throughout the literature portrays inflammation as a key role player. APPs, which are markers of inflammation, have been closely associated with T2D as their serum levels are elevated in T2D patients (34, 35, 37–41, 268, 272, 273). These include, PAI-1, SAA, and CRP, which all play different roles during the APR. Whether these APPs are more than just biological markers for T2D and actually influence the development of insulin resistance is still unclear. Some studies do support the possibility that PAI-1, SAA, and CRP impair insulin signalling (252–254, 271, 274, 287–289), whilst others believe APPs are only a by-product of T2D (67, 318–320). The major source of these APPs is the liver, a central target for insulin and believed to be the first peripheral tissue to become insulin resistant. The liver, when in an insulin resistant state, is an important contributor to hyperglycaemia, which contributes further to the systemic progression of insulin resistance. Very few studies have examined how APPs affect the ability of the liver to respond to insulin. Understanding whether these APPs play a role in insulin resistance and T2D progression could provide insight into novel mechanisms leading to the development of insulin resistance and towards the development of innovative drug targets.

1.7 Hypothesis and aims

It is evident from the literature that the APPs, PAI-1, SAA and CRP are associated with insulin resistance and the development of T2D. However, the current knowledge regarding the role that these APPs may play in the development of insulin resistance is limited. Given that insulin resistance is caused by a defective insulin signalling pathway, and that insulin action in the liver plays an integral role in the progression to T2D, the main aim of this study was to investigate the effects of PAI-1, SAA, and CRP on hepatic insulin signalling. In this study we hypothesize that PAI-1, SAA, and CRP negatively affect the key proteins in the insulin signalling pathway, leading to deficient insulin action in the liver.

Using a murine hepatoma and human liver carcinoma cell line, namely BWTG3- and HepG2 cells, respectively, as *in vitro* model systems to investigate hepatic insulin signalling, the aims of this study were as follows:

(1) To establish optimal activation of the insulin signalling pathway.
(2) Evaluate whether increasing concentrations of PAI-1, SAA, and CRP affect insulin-induced activation of key proteins in the insulin signalling pathway such as the IR, IRS-2, and Akt.

(3) To investigate if the length of exposure to PAI-1, SAA, and CRP affects insulin-induced activation of key proteins (IR, IRS-2 and Akt) in the insulin signalling pathway.
(4) To determine if PAI-1, SAA, and CRP affect gluconeogenesis, a downstream target of insulin, through the transcriptional regulation of key gluconeogenic genes, *G6Pase* and *PEPCK*, as well as hepatic glucose production.

The materials and methods used in this study will be described in detail in Chapter 2. The results of this study will be presented in Chapter 3 followed by the discussion in Chapter 4, which will place the results in a broader context. Limitations and future work will also be discussed in Chapter 4.

CHAPTER 2:

MATERIALS AND METHODS

2.1 Test compounds

Human insulin, human recombinant plasminogen activator inhibitor-1 (PAI-1) and C-reactive protein (CRP) were purchased from Sigma-Aldrich. Human recombinant apo-serum amyloid A (SAA) was purchased from PeproTech. A 10 mg/ml stock solution of insulin was prepared in milliQ water, filter sterilized, and further diluted to a final concentration of 1 mg/ml in low glucose (5 mM) Dulbecco's Modified Eagle's Medium (DMEM) (Sigma-Aldrich) supplemented with 10% fetal bovine serum (FBS). Working solutions were prepared with further dilutions in sterile nuclease-free water and stored at -20 °C. Lyophilized PAI-1 powder was reconstituted in sterile 100 µl ultrapure water to a stock concentration of 0.25 mg/ml. A working solution of 0.25 µg/ml was prepared using low glucose DMEM supplemented with 10% FBS and stored at -80 °C. Lyophilized SAA powder was dissolved to a stock concentration of 1 mg/ml and CRP was diluted to a working solution of 100 µg/ml in low glucose DMEM supplemented with 10% FBS, respectively. SAA was stored at -20 °C and CRP at 4 °C.

2.2 Mammalian cell culture

2.2.1 Cell Growth and Maintenance

Murine hepatoma (BWTG3) cells were obtained from the University of Gent, Belgium, and human liver carcinoma (HepG2) cells were purchased from Cellonex. Both BWTG3- and HepG2 cells were cultured and maintained in low glucose (5 mM) DMEM, containing 1 mM sodium pyruvate and 17.9 mM sodium bicarbonate purchased from Sigma-Aldrich. In addition, the culture medium was supplemented with 10% (v/v) fetal bovine serum (FBS) (Merck) and 1% (v/v) penicillin/streptomycin (Pen/Strep) (50 IU/ml penicillin and 50 µg/ml streptomycin) (Sigma-Aldrich). Both cell lines were maintained in 75 cm^2 tissue culture flasks (Bio-Smart Scientific) and regularly tested for mycoplasma infection using Hoechst Staining (321) and only mycoplasma negative cells were used for further experiments (see Addendum A, Fig.A1). Cells were maintained at a temperature of 37 °C, 5% CO_2 atmosphere, and 95% humidity.

2.2.2 Treatment Conditions

For dose response experiments, BWTG3 and HepG2 cells were seeded, in culture medium, into 12-well plates (BioSmart Scientific) at a density of $2x10^5$ cells/well and grown to a confluency of 70-80%. This was followed by serum starving the cells for 24 hours in un-supplemented culture medium. The serum starved cells were subsequently treated with PAI-1 (5, 10, and 20 ng/ml), SAA (5, 10, and 20 µg/ml), and CRP (2.5 and 4.5 µg/ml) for 24 hours. Treatments were prepared in unsupplemented culture medium. Because the test compounds were prepared in supplemented low glucose DMEM, the vehicle control for each experiment consisted of 0.1% of supplemented low glucose DMEM. Prior to cell lysis, the cells were treated with 100 ng/ml insulin for 30 minutes to stimulate the insulin signalling pathway. For time course experiments, BWTG3 and HepG2 cells were seeded into 6-well plates (BioSmart Scientific) at a density of $5x10^5$ cells/well (BWTG3) and $1x10^6$ cells/well (HepG2), respectively, followed by serum starving the cells for 24 hours in un-supplemented culture medium. Cells were treated with 10 ng/ml PAI-1, 10 µg/ml SAA, and 4.5 µg/ml CRP for 2, 24 and 48 hours, followed by a treatment with 100 ng/ml insulin for 30 minutes prior to cell lysis.

2.3 Total RNA extraction

BWTG3 and HepG2 cells were maintained as described in section 2.2.1 and treated as described in 2.2.2 for time course experiments. Total RNA was extracted using Tri-Reagent (Sigma-Aldrich) as per the manufacturer's instructions. Briefly, the cells were lysed with 400 µl Tri-reagent and cell lysis was promoted by placing the cells at -20 °C overnight. The cells were then allowed to thaw, and the cell lysates were transferred into clean 1.5 ml microcentrifuge tubes followed by the addition of 80 µl chloroform to extract total RNA. The cells were vortexed for one minute, followed by centrifugation at 14000 x g for 15 minutes at 4 °C. The aqueous phase containing the RNA was removed (130 µl) and transferred into a clean 1.5 ml microcentrifuge tube followed by the addition of 200 µl ice-cold isopropanol. The samples were vortexed for one minute and RNA precipitation was facilitated by placing the samples at -20 °C for 1-7 days. This was followed by centrifugation at 14 000 x g for 30 minutes at 4 °C to pellet the RNA. The supernatant was removed, and the pellet was washed with 500 µl ice-cold 70% EtOH (diluted in diethyl pyrocarbonate (DEPC) treated water) and vortexed for one minute followed by centrifugation at 14000 x g for 5 minutes at 4°C. This wash step was repeated at least once to ensure the removal of any contaminants. With the final wash step, the supernatant was removed, and the pellet air-dried for 10 minutes. RNA pellets were dissolved in 15 µl DEPC-treated water and incubated at 55 °C for 5 minutes. RNA samples were stored at -20 °C. The RNA concentration as well as purity was assessed using the NanoDrop (ND-100 Spectrophotometer). The integrity of the isolated RNA was confirmed by assessing the presence of intact 28S and 18S ribosomal RNA on a 1% (w/v) agarose denaturing gel stained with Nancy-520 (322) (Addendum A, Fig.A2) (Sigma-Aldrich).

2.4 cDNA synthesis

The cDNA was synthesized using the ImProm-II Reverse-Transcription kit (Promega) as per the manufacturer's instructions. Briefly, 2 µg RNA was added into a thin-walled PCR tube followed by the addition of 50 µg/ml oligoDT primers. Nuclease-free water was then added to a final volume of 5 µl. This mixture was incubated at 70 °C for 5 minutes. Thereafter, a master mix containing the following reagents was added to each sample to a final volume of 20 µl: 7.6 µl of nuclease-free water, 4 µl ImProm-II 5X reaction buffer, 1.5 mM $MgCl_2$, 0.67 mM dNTP's, 20U of recombinant RNasin® ribonuclease inhibitor and 160U ImProm-II reverse transcriptase. This mixture was placed at 25 °C for 5 minutes to allow annealing of the oligoDT primers, followed by an incubation step at 45 °C for 1 hour for extension. The final step involved placing the mixture at 70 °C for 15 minutes to inactivate the reverse transcriptase and placing the samples on ice for 5 minutes. The cDNA samples were stored at -20 °C.

2.5 Quantitative real-time polymerase chain reaction (qPCR)

Quantitative real-time PCR (qPCR) was performed using the Lightcycler 96 system (Roche Applied Science). For each cDNA sample, a master mix containing the following reagents was prepared: 6.25 µl SYBR green (Kapa SYBR Fast qPCR mastermix, containing the DNA polymerase enzyme and necessary reagents for the PCR reaction, Roche Applied Science), 0.25 µM forward and reverse primers and 2.25 µl nuclease-free water to a final volume of 9 µl. Lightcycler multiwell plates were used (Celtic Molecular Diagnostics) for the qPCR reaction in which 9 µl of the mastermix was added to each well and 1 µl of the cDNA sample or nuclease-free H_2O (for the non-template control). The details of the primer sets used in this study are shown in Table 2.1. LightCycler® 96 software (Roche Applied Science) was used to set the PCR conditions which were as follows: pre-incubation at 95 °C for 3 seconds, followed with 45 cycles of amplification: 95 °C for 3 seconds, 60 °C (or 61 °C for the mouse PEPCK primer set) for 20 seconds and 72 °C for 3 seconds. This was followed with a melting step at 95 °C for 10 seconds. The amplicon size was confirmed on a 2% (w/v) agarose denaturing gel (Addendum A, Fig.A3). GAPDH was used as an internal control for BWTG3 samples and 18S and β-actin for HepG2 samples. The mRNA levels of the gene of interest was normalized relative to the respective internal control. Relative quantification of the target genes was performed using the comparative CT method (delta-delta CT method) with the respective vehicles arbitrarily set to 1.

Table 2.3. Details of primers used for real-time quantitative PCR analysis.

Species	Gene	Sequence (5'→3')	Strand	Amplicon Length	Annealing temperature (°C)	Primer efficiency
Mouse	G6Pase	TGCAAGGGAGAACTCAGCAA	Forward	64 bp	60 °C	1.69
		GGACCAAGGAAGCCACAATG	Reverse			
	PEPCK	ATGAAAGGCCGCACCATGTA	Forward	576 bp	61 °C	2.55
		AGCCCTTAAGTTGCCTTGGG	Reverse			
	IRS-2	GCACCTATGCAAGCATCGAC	Forward	70 bp	60 °C	1.65
		GCGCTTCACTCTTTCACGAC	Reverse			
	GAPDH	ACATGCCGCCTGGAGAAACCT	Forward	90 bp	60 °C	2.08
		GCCCAGGATGCCCTTTAGTGG	Reverse			
Human	PEPCK	CTGGCCTGCGGCTTAACT	Forward	246 bp	60 °C	2.0*
		ACTTGGGGAGCTTTCGGATG	Reverse			
	IRS-2	GCCACCATCGTGAAAGAGTG	Forward	224 bp	60 °C	1.76
		CCATCCGGGAACAAGGGAAA	Reverse			
	18S	GAGAAACGGCTACCACATCCAAG	Forward	158 bp	60 °C	2.05
		CCTCCAATGGATCCTCGTTA	Reverse			
	β-actin	CATGTACGTTGCTATCCAGGC	Forward	242 bp	60 °C	2.13
		CTCCTTAATGTCACGCACGAT	Reverse			

* = primer efficiency could not be determined and was thus assumed to be 2.0

2.6 Western Blot analysis

2.6.1 Preparation of protein lysates

For western blot analysis, BWTG3 and HepG2 cells were treated as described in section 2.2.2 for dose response and time course experiments. Whole cell lysates were prepared: briefly, cells were washed with 1x ice-cold PBS, then lysed in 100 µl passive lysis buffer containing 0.09 M Tris pH 8.0, 0.5 M EDTA, 10% glycerol, 0.2% (v/v) TritonX-100, 0.125 M sodium fluoride (NaF), 50 mM sodium orthovanadate (Na_3VO_4), and 1% (v/v) phenylmethylsulphonyl fluoride (PMSF). Additionally, protease and phosphatase inhibitor tablets (both purchased from Roche Applied Science) were added. Cell lysis was promoted with an overnight freeze-thaw cycle, followed by the addition of 5x SDS-reducing lysis buffer (1 M Tris-HCl (pH 6.8), 10% SDS, 0.1% (w/v) bromophenol blue and 20% (v/v) glycerol). Protein lysates were boiled at 95°C for 15 minutes, to denature the proteins, and stored at -20 °C until further analysis.

2.6.2 SDS-PAGE Electrophoresis and Western Blot

For gel electrophoresis, protein lysates were separated on a 10% polyacrylamide gel at a constant voltage of 100 V for 15 minutes, and 200 V for 90 minutes, in 1X running buffer (3.03% (w/v) Tris, 14.41% (w/v) glycine, 1% SDS). Proteins were transferred onto a HybondTM ECLTM nitrocellulose membrane (AEC Amersham) for 2 hours at a constant current of 0.18 A in cold 1X transfer buffer (3.03% (w/v) Tris, 14.41% (w/v) glycine, 1% SDS and 10% (v/v) methanol). Membranes were blocked in 5% (w/v) fat-free milk powder prepared in 1X Tris Buffered Saline (TBS) (0.05 M Tris, 0.15 M NaCl) containing 0.1% (v/v) Tween-20 (1X TBST), for 90 minutes at room temperature. Membranes were rinsed with 1X TBST and incubated with the primary antibodies overnight at 4 °C (Table 2.2), while agitating. Anti-phospho-insulin receptor (Tyr1150 & Tyr1151) (1:1000, cat# 81500, Santa Cruz Biotechnology), anti-phospho-insulin receptor substrate-2 (Ser731) (1:500, cat# ab3690, Abcam), anti-phospho Akt (Ser473) (1:1000, cat# 4060, Cell Signalling Technology), anti-phospho Akt (Thr308) (1:700, cat# 13038, Cell Signalling Technology) were used to probe for phosphorylated proteins. Anti-insulin receptor (1:500, cat# CT-1, ThermoFisher Scientific) and anti-AKT (1:1000, cat# 9272, Cell Signalling Technology) were used to probe for total proteins. Anti-EF-1α1 (1:1000, cat# 21758, Santa Cruz Biotechnology) and anti-Hsp90 (1:1000, cat# 7647, Santa Cruz Biotechnology) were used for loading controls to normalize for equal loading of proteins. All primary antibodies were prepared in 1X TBST and stored at 4 °C. After incubating with the primary antibodies, the membranes were rinsed twice in 1X TBST for 5 minutes followed by one rinse with 1X TBS for 5 minutes, prior to incubation with the appropriate secondary antibody conjugated to HRP for 90 minutes at room temperature (Table 2.2). Goat anti-rabbit IgG-HRP (cat# ab6791) and rabbit anti-mouse IgG-HRP (cat# ab97046) were purchased from Abcam and goat anti-mouse IgG-HRP (cat# A9917) was purchased from Sigma-Aldrich. The secondary antibodies were prepared in 5% (w/v) fat-free milk powder. After incubation

with secondary antibodies, the membranes were washed as previously described and visualized using the Western ECL substrate (BioRad) for 5 minutes. Chemiluminescence was detected using the MyECL Imager (Thermo-Scientific). The MyImageAnalysis® software version 2.0 (Thermo-Scientific) was used to quantify all western blot images.

Table 2.4. Specific antibodies and dilutions used for Western Blot analysis.

Protein	Primary (1°) antibody	Secondary (2°C) antibody
Phosphorylated insulin receptor	1:1000 p-IR (Tyr1150 & 1151)[1]	1:2000 goat anti-mouse[3]
Total insulin receptor	1:500 Total-IR[2]	1:2000 goat anti-mouse[3]
Phosphorylated IRS-2	1:500 Phospho-IRS-2 (Ser731)[4]	1:10 000 goat anti-rabbit[4]
Phosphorylated Akt	1:700 p-Akt (Thr308)[5]	
	1:1000 p-Akt (Ser473)[5]	
Total Akt	1:1000 Total Akt[5]	
Hsp90	1:1000 Hsp90[1]	
EF-1α1	1:1000 EF-1α1[1]	1:10 000 rabbit anti-mouse[4]

[1]Santa Cruz Biotechnology Inc

[2]ThermoFisher Scientific

[3]Sigma-Aldrich

[4]Abcam

[5]Cell Signalling Technology

2.7 Hepatic glucose production

2.7.1 Induction of glucose production

In order to measure hepatic glucose production, a protocol previously optimized for primary mouse hepatocytes was followed (323). BWTG3 and HepG2 cells were plated into 24-well plates at a density of $2x10^5$ cells/well and grown to 70-80% confluency. Cells were serum-starved for 24-hours, followed with a pre-treatment with 10ng/ml PAI-1, 10 µg/ml SAA, and 4.5 µg/ml CRP for 48 hours. A one-hour pre-treatment with 100 ng/ml insulin was used as a negative control, as insulin is known to decrease *de novo* glucose synthesis. Cells were washed twice with pre-warmed sterile 1X PBS followed with an incubation in 250 µl glucose production buffer (consisting of phenol red free DMEM without glucose, 2 mM L-glutamine, 15 mM HEPES, 20 mM sodium lactate and 2 mM sodium pyruvate as substrates for gluconeogenesis) for 6 hours in the presence of the test compounds (10 ng/ml PAI-1, 10 µg/ml SAA, and 4.5 µg/ml CRP), with or without 100 ng/ml insulin. The medium was collected, and extracellular glucose content was measured using a fluorometric glucose assay method based on the principles of the Amplex/Glucose Oxidase assay kit (ThermoFisher Scientific), discussed in detail in Addendum B.

2.7.2 Glucose measurement assay

To measure the extracellular glucose output, a fluorometric glucose detection method was utilised, which is based on the principle of the Amplex Red/Glucose oxidase kit (ThermoFisher Scientific). This assay is based on two reactions: 1) the conversion of glucose to D-gluconolactone and hydrogen peroxide (H_2O_2) by glucose oxidase and 2) the oxidation of a substrate by H_2O_2 catalysed by horseradish peroxidase (HRP). In this assay AmpliFlu (similar to Amplex Red) (Sigma-Aldrich, cat#90101) was used as a substrate for HRP to produce the red fluorescent product, resorufin (324, 325). After collection of 200 µl of the medium, 50 µl was added into each well of a 96-well microplate. A working reagent was freshly prepared each time before an experiment containing 10 µM AmpliFlu, 0.2 U/ml HRP (Sigma-Aldrich, cat#SRE0082) and 2 U/ml glucose oxidase (Sigma-Aldrich, cat#G7141) in glucose production buffer and 50 µl was added to each well. The microplate was incubated for 30 minutes at room temperature and protected from light (AmpliFlu is light sensitive). The fluorescence was measured at an excitation wavelength of 571 nm and emission wavelength of 585 nm (Addendum A, Fig.A4). A no-glucose containing control (glucose production buffer) was used to correct for background fluorescence. The relative fluorescence measured was normalized to total protein content of each sample, measured using the bicinchoninic acid assay (BCA) (Pierce, ThermoFisher Scientific).

2.8 Protein determination

To quantify the total protein content of the cell lysates, the Pierce™ BCA (Bicinchoninic acid) protein assay (ThermoFisher Scientific) was utilised, which essentially measures the reduction of Cu^{2+} to Cu^{1+} by proteins in an alkaline solution, which is detected by bicinchoninic acid (326). Firstly, bovine serum albumin (BSA) standards were prepared by performing 8 serial dilutions of 1 ml BSA stock (2 mg/ml dissolved in H_2O) in RIPA buffer (56 mM 1M Tris-HCl pH 7.4, 150 mM NaCl, 1 mM EDTA and 0.1% SDS) to concentrations ranging from 25-2000 µg/ml. Subsequently, the BCA working reagent was prepared: for each cell lysate, reagent A (containing sodium carbonate, sodium bicarbonate, bicinchoninic acid and sodium tartrate in 0.1 M sodium hydroxide) and reagent B (containing 4% cupric sulphate) was mixed in a 50:1 ratio. For the reaction in the 96-well microplate, 10 µl of cell lysate (in an appropriate dilution made in RIPA buffer) or the prepared standards was added to each well as well as 200 µl of working reagent. The microplate was incubated at 37 °C for 30 minutes and protected from light. The reaction forms a purple colour and the BCA/Cu^{1+} complex exhibits a strong absorbance at 562 nm. The absorbance was measured at 562 nm and a standard curve was composed using GraphPad Prism® version 5 software. The protein concentration of each cell lysate was measured by interpolating the absorbance readings of each cell lysate into the standard curve and using the equation of the linear region, taking the Beer-lambert law into account.

2.9 Statistical analysis

Visual representation of data and statistical analysis was conducted using GraphPad Prism® version 5 software. For western blot analysis, specifically dose response experiments, a student t-test was used to compare the specific treatment to the vehicle and insulin control. For time course experiments, one-way ANOVA with Tukey's Multiple Comparison's post-test was used to compare between the different treatment times. Additionally, two-way ANOVA was used to compare the two data sets for the time course experiment. For real-time qPCR, one-way ANOVA with Tukey's Multiple Comparison's post-test was used to compare the different treatment times with the vehicle and insulin control. Statistical significance was indicated by *, ** or ***, to indicate $p<0.05$, $p<0.01$ or $p<0.0001$, respectively. No statistical significance (ns) indicates $p>0.05$. All data shown represents two or three independent experiments, with the error bars indicating standard deviation (SD) for two independent experiments and standard error of the mean (SEM) for three independent experiments.

CHAPTER 3:

RESULTS

3.1 Establishing an experimental model that displays maximal sensitivity to insulin

Activation of the insulin signalling pathway is initiated when insulin binds to the insulin receptor (IR), initiating a phosphorylation cascade. Nodes within this phosphorylation cascade include the PI3K/Akt pathway, linked to the insulin receptor signalling *via* adaptor proteins, such as the insulin receptor substrates (IRSs) (Fig.3.1). Unperturbed insulin signalling eventually leads to the transcriptional regulation of various genes in addition to regulating the activity of various proteins involved in glucose metabolism *via* post-translational modifications. The ability of insulin to activate these key proteins in the pathway determines the cells responsiveness to insulin.

Most studies use 100 nM insulin which correlates to 580 ng/ml to stimulate the insulin signalling pathway, irrespective of the tissue-or cell type (149, 260, 274, 287, 327). To confirm active insulin signalling in the murine hepatoma (BWTG3) cells, two insulin concentrations, 100 ng/ml and 500 ng/ml were used to determine the optimal conditions required for the activation of key proteins in the insulin signalling pathway. Additionally, whether a high glucose concentration, as found in traditional culture medium, could affect insulin signalling was also considered. Consistent exposure to high glucose levels are known to inhibit insulin signalling (328, 329). For this reason, a comparative study between the traditional culture medium, which contains 25 mM glucose (high glucose), and culture medium with 5 mM glucose (low glucose) was included to further determine the optimal conditions for the activation of the insulin signalling pathway. More specifically, the phosphorylation status of the IR at Tyr1150 & 1151, Akt at Ser473, and IRS-2 at Ser731 was measured. The total Akt levels was also determined in response to insulin treatment.

Firstly, western blot analysis showed that 100 ng/ml insulin was sufficient for maximal induction of IR -and Akt phosphorylation in the BWTG3 cells (Fig.3.2A & C). There was no significant difference ($p>0.05$) between the two insulin concentrations used, no matter the glucose concentration of the culture medium (Fig.3.2A, C & D). Lastly, high glucose culture medium affected the ability of insulin to optimally activate the IR and Akt (Fig.3.2A & C). For example, both insulin concentrations caused a greater increase in the phosphorylation of IR in low glucose medium (Fig3.2A). Additionally, culturing the cells in high glucose resulted in a significant ($p<0.01$) increase in IRS-2 Ser731 phosphorylation (4.2-fold) (Fig3.2B). Furthermore, whilst insulin at both concentrations used was unable to induce Akt phosphorylation at Ser473 in cells cultured in high glucose medium, insulin did significantly ($p<0.001$) increase Akt phosphorylation at Ser473 by 163-fold (Fig.3.2C) when cells were grown in low glucose culture medium as well as slightly decrease the phosphorylation of IRS-2 at Ser731 (Fig.3.2B), which was expected. As a result, going forward, the BWTG3- and HepG2 cells were maintained in low glucose culture medium and a 100 ng/ml insulin was used to activate the insulin signalling pathway.

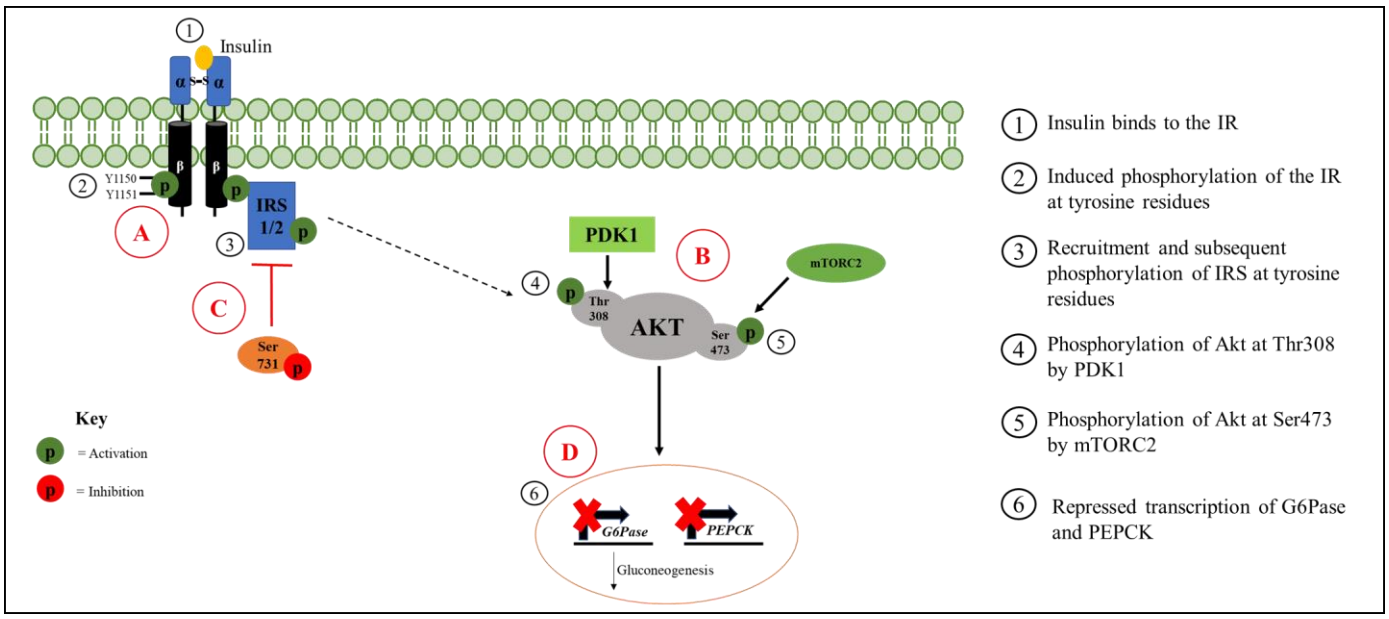

Figure 3.1. Simplified illustration of key nodes in the insulin signalling pathway, specifically the PI3K/Akt pathway. Insulin binding to the IR results in autophosphorylation at its tyrosine residues and thus activation of the protein, leading to subsequent recruitment and activation of IRS-1 and 2. This results in the phosphorylation of the central protein, Akt, at its Thr308, by PDK1 which involves the recruitment of various intermediate proteins (represented by the dotted arrow). Finally, mTORC2 phosphorylates Akt at its Ser473 residue resulting in the full activation of the protein, resulting in the regulation of various downstream targets. Finally, the pathway can be regulated by phosphorylation of the IRS proteins at their serine residues, resulting in the inhibition of downstream targets which include the transcription of gluconeogenic genes, *G6Pase* and *PEPCK*. **(A)**, **(B)** and **(C)**, represents the three nodes that will be investigated in this study as well as **(D)** which represents the downstream target that will be investigated. These include **(A)** tyrosine phosphorylation of the IR at Tyr1150 & 1151, **(B)** phosphorylation of Akt at Thr308 and Ser473, **(C)** Ser731 phosphorylation of IRS-2 and **(D)** transcriptional regulation of G6Pase and PEPCK. IR = insulin receptor; IRS1/2 = insulin receptor substrates 1 and 2; PDK1= 3-phosphoinositide-dependent protein kinase 1; mTORC2 = mammalian target of rapamycin 2; G6Pase = glucose-6 phosphatase; PEPCK = phosphoenolpyruvate carboxykinase.

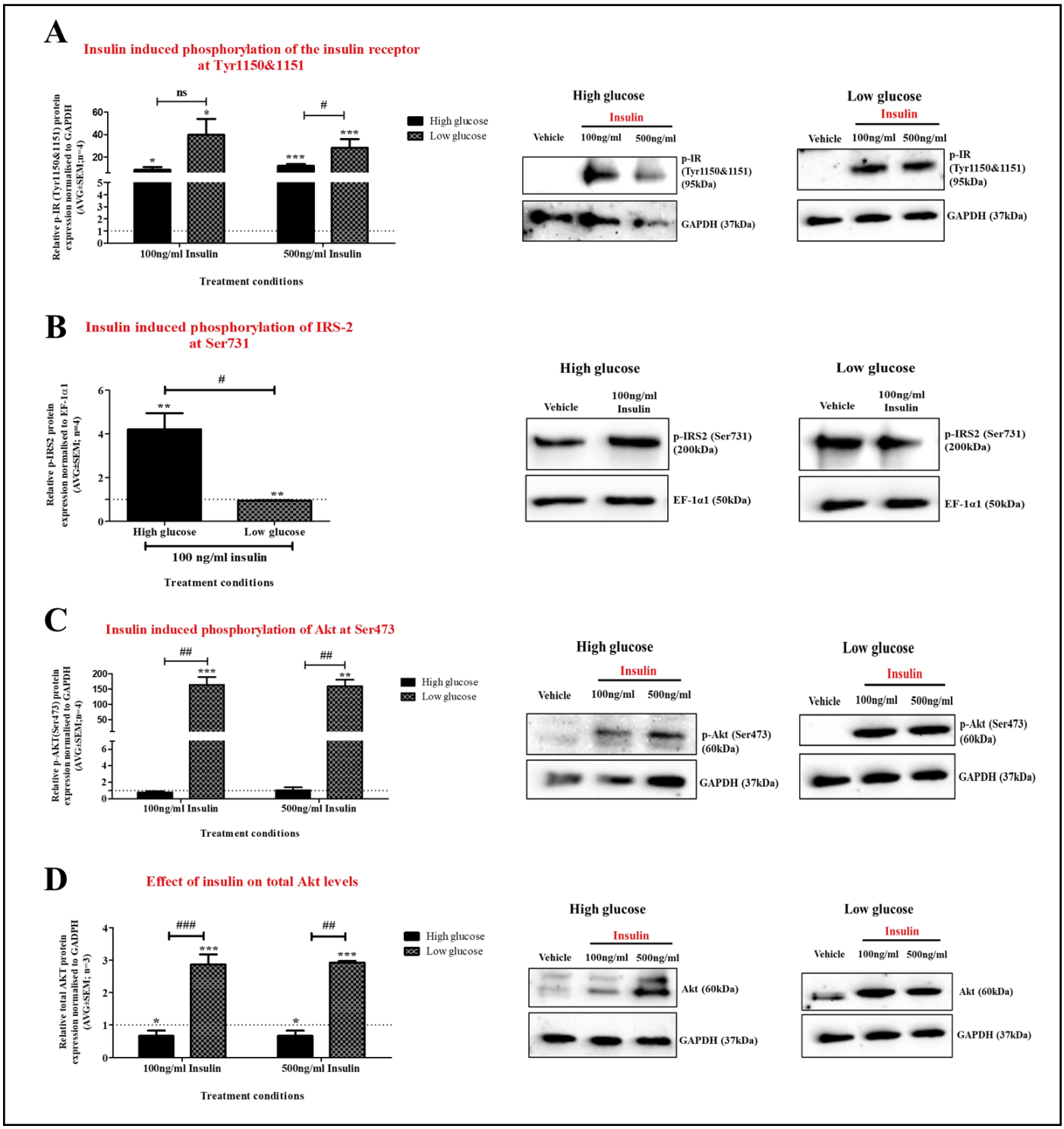

(Figure legend on next page)

Figure 3.2. An experimental model system that displays optimal activation of the insulin signalling pathway was established in murine hepatoma cells. BWTG3 cells were cultured and maintained in either traditional culture medium containing high glucose (25 mM) or culture medium containing low glucose (5 mM). Following serum-starving for 24 hours, the cells were treated with 100 ng/ml and 500 ng/ml insulin for 30 minutes prior to cell lysis. Phosphorylation of the insulin receptor (IR) at Tyr1150 & 1151 **(A)**, insulin receptor substrate-2 (IRS) at Ser731 **(B)**, Akt at Ser473 **(C)** as well as total Akt levels **(D)** were measured using western blot analysis and quantified relative to the loading control GAPDH and EF-1α1. Statistical analysis comparing the insulin treatment relative to the vehicle (*), which was set to 1 (represented as a dotted line), and the glucose concentrations to the insulin treatment (#) was performed using a two-tailed unpaired Student's t-test (*/#$p<0.05$, **/##$p<0.01$, ***$p<0.001$).

3.2 Activation of the insulin signalling pathway

Having established the model system for this study, the effect of the selected APPs on insulin signalling was investigated. As a control for each experiment, BWTG3 and HepG2 cells were treated with insulin in the absence of the APPs to confirm a functional insulin signalling pathway as determined by western blot analysis, which thus served as a positive control in all subsequent experiments. In BWTG3 cells, phosphorylation of the IR at Tyr1150 & 1151 significantly ($p<0.01$) increased by 8.6-fold upon 100 ng/ml insulin treatment for 30 minutes (Fig.3.3A). A small (1.3-fold) but significant ($p<0.05$) increase was observed in total IR levels (Fig.3.3B). Further downstream activation of the pathway was confirmed as treatment with 100 ng/ml insulin significantly ($p<0.001$) increased Akt phosphorylation at Thr308 by 4.2-fold (Fig.3.3D) and at Ser473 by 81-fold (Fig.3.3E). The total Akt protein levels also significantly ($p<0.05$) increased by 1.7-fold (Fig.3.3F). The inhibitory phosphorylation site of IRS-2 at Ser731 was not affected by 100 ng/ml insulin treatment (Fig.3.3C). In HepG2 cells 100 ng/ml insulin, like in BWTG3 cells, slightly increased total IR levels (1.3-fold increase) (Fig.3.4A). Similarly, insulin, significantly ($p<0.001$), induced phosphorylation of Akt at Thr308 by 31-fold (Fig.3.4C) whilst a 53-fold increase in phosphorylation of Akt at Ser473 (Fig.3.4D) was observed in HepG2 cells. Insulin treatment slightly increased total Akt protein levels (1.2-fold, Fig3.4E) in HepG2 cells albeit not significantly ($p>0.05$). Taken together, both cell lines responded to insulin treatment similarly albeit to different degrees. For example, Akt phosphorylation at Thr308 in the HepG2 cell model was more responsive to insulin (31-fold) when compared to the BWTG3 cell line (4.2-fold). In contrast, insulin-induced Akt phosphorylation at Ser473 was more pronounced in BWTG3 cells (81-fold) than HepG2 cells (53-fold) (Fig3.3E vs Fig3.4.D).

Finally, like in BWTG3 cells, phosphorylation of IRS-2 at Ser731 was not significantly ($p>0.05$) affected by the insulin treatment in HepG2 cells (Fig.3.4B). In summary 30-minute treatment with 100 ng/ml insulin was able to successfully activate key proteins in the insulin signalling pathway, such as the IR and Akt, in both the murine and human liver cell models.

It should be noted that phosphorylation of the IR could not be investigated in HepG2 cells due to difficulty experienced with the commercially obtained antibody used in this investigation, therefore moving forward, phosphorylation of the IR was only investigated in BWTG3 cells.

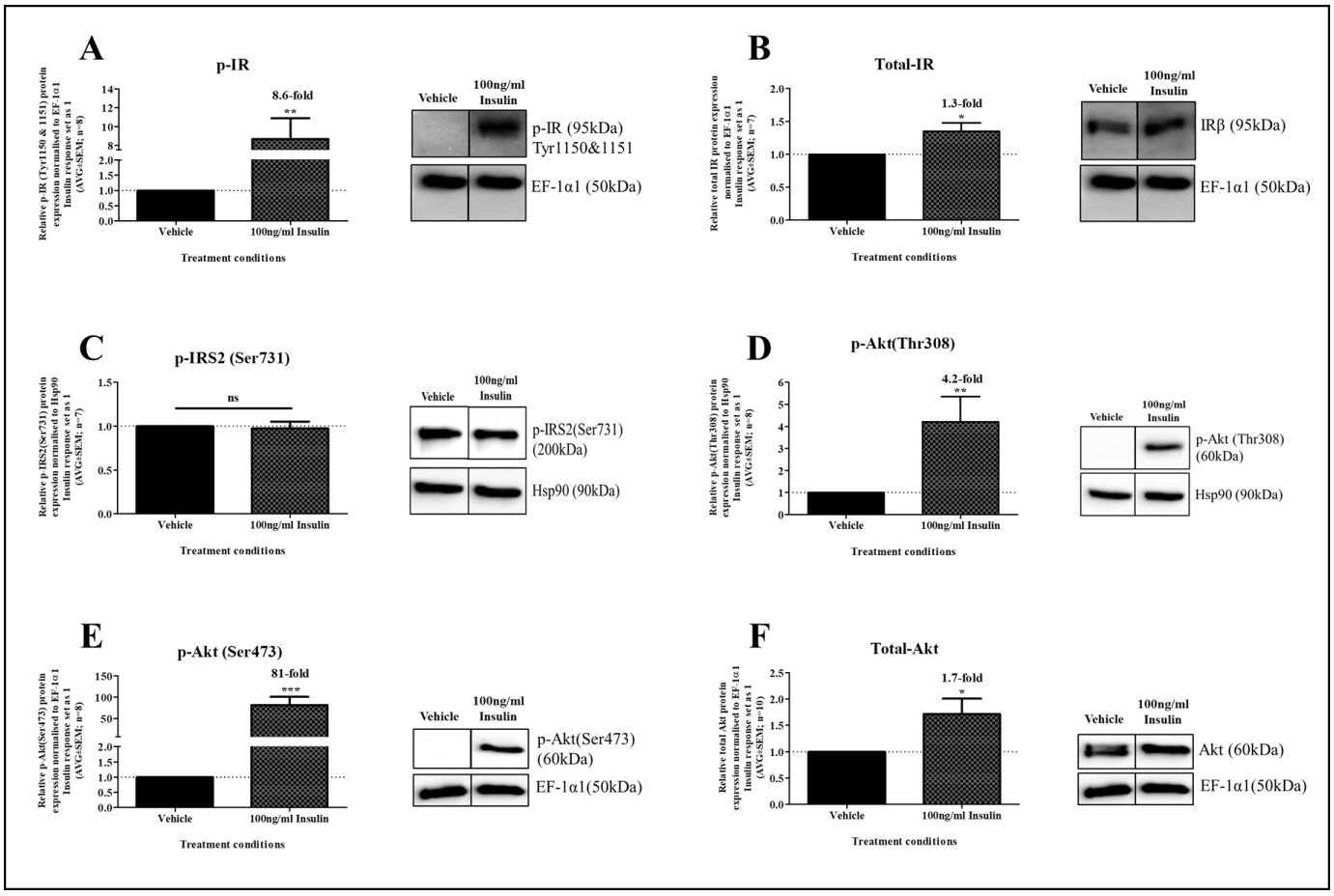

Figure 3.3. Insulin successfully activates the phosphorylation of key regulatory proteins in the insulin signalling pathway in BWTG3 cells. Murine hepatoma (BWTG3) cells, grown in low glucose (5 mM) medium, were serum-starved for 24 hours followed with by a 100 ng/ml insulin treatment for 30 minutes prior to cell lysis. Phosphorylation of the insulin receptor (IR) at Tyr1150 & 1151 **(A)**, insulin receptor substrate-2 (IRS-2) at Ser731 **(C)** and Akt at both the Thr308 and Ser473 site **(D and E)**, as well as the total protein expression (**B and F)** was measured and quantified relative to the loading control, EF-1α1 or Hsp90 **(** representative blots shown next to graphs). The vehicle was set to 1 and statistical analysis comparing the insulin treatment relative to the vehicle control was done using a two-tailed unpaired Student's t-test (*p<0.05, **p<0.01, ***p<0.001).

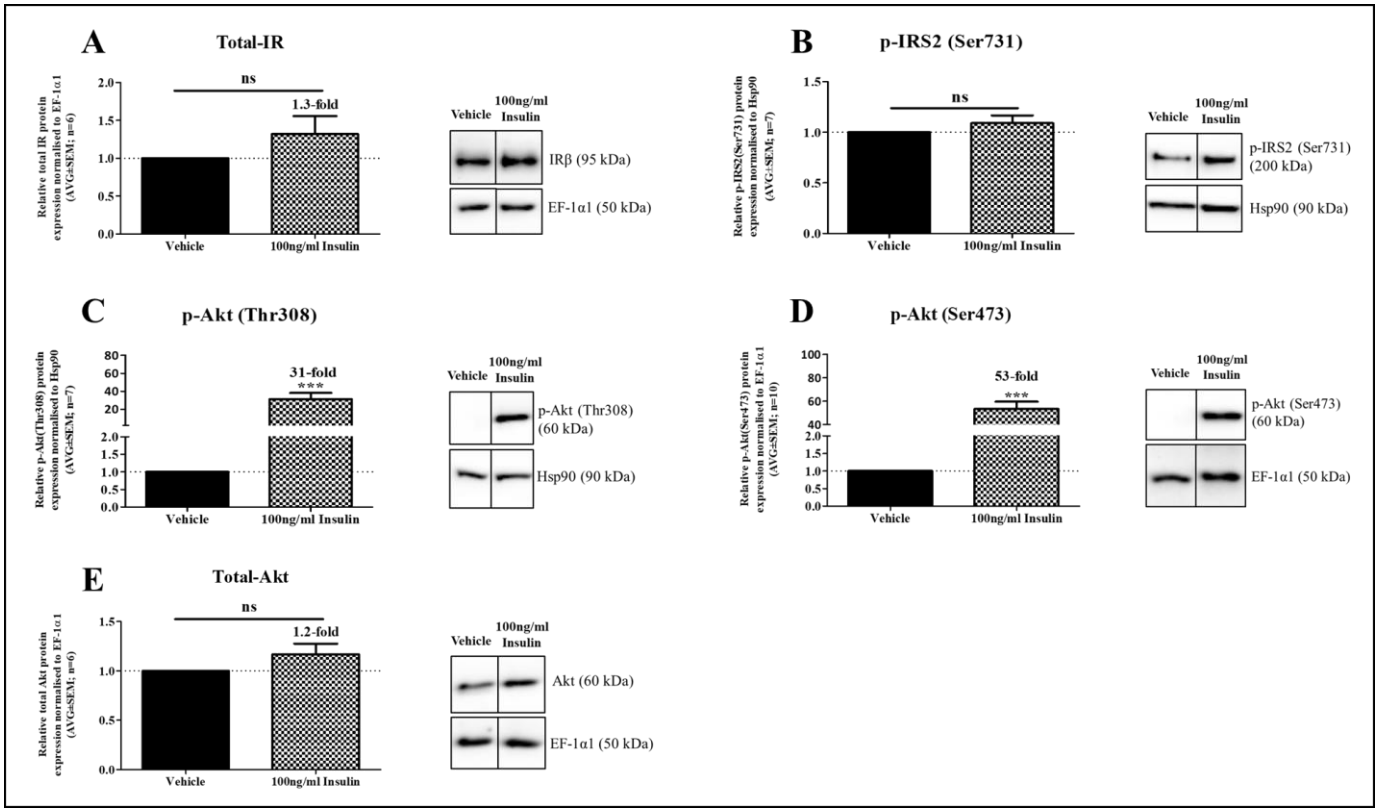

Figure 3.4. Insulin successfully activates key regulatory proteins in the insulin signalling pathway in human hepatoma cells. HepG2 cells, grown in low glucose (5 mM) medium were serum-starved for 24 hours. Cells were then treated with 100 ng/ml insulin for 30 minutes prior to cell lysis. Total insulin receptor (IR) **(A)** expression, as well as phosphorylation of insulin receptor substrate-2 (IRS-2) at Ser731 **(B)** and Akt at both Thr308 **(C)** and Ser473 **(D)** in addition to total Akt **(E)** expression was measured and quantified relative to the loading control, EF-1α1 or Hsp90 (representative blots are shown next to graph). The vehicle was set to 1 and statistical analysis comparing the insulin treatment relative to the vehicle control was done using a two-tailed unpaired Student's t-test (*$p<0.05$, ***$p<0.001$)

3.3 The effects of selected acute phase proteins, PAI-1, SAA, and CRP on insulin-induced activation of the insulin signalling pathway

The central focus of this study was to investigate the effect of three different acute phase proteins (APPs), plasminogen activator inhibitor-1 (PAI-1), serum amyloid A (SAA), and C-reactive protein (CRP) on insulin-induced activation of key nodes in the insulin signalling pathway. Systematic evaluation of the insulin signalling pathway was investigated starting with the insulin receptor, followed by IRS-2, and lastly Akt (Fig.3.1). Activation of the proteins *via* phosphorylation and total protein levels were examined using western blot analysis. Finally, interference of factors, other than the chosen APPs, on the insulin signalling pathway were limited by culturing the cells in medium containing low glucose concentrations (5 mM) and serum-starving for 24 hours prior to APP treatment. Additionally, the insulin concentration used to activate the insulin signalling pathway was optimised as described in section 3.1.

3.3.1 Activation of the insulin receptor is differentially regulated by PAI-1, SAA, and CRP

As previously described, phosphorylation of the IR at tyrosine residues is important for downstream signalling to elicit a biological response, indicative of a receptor tyrosine kinase. Therefore, western blot analysis was performed to investigate the effect of the APPs, PAI-1, SAA, and CRP on insulin-induced phosphorylation of the IR at Tyr1150 & 1151 in BWTG3 cells. As shown previously (Fig.3.3A), insulin alone increased the phosphorylation of IR at Tyr1150 & 1151 in the murine hepatoma cells. This increase in phosphorylation was set to 1 as well as the effect of insulin on total IR levels when compared to the effect of the APPs on the insulin-induced effect (Fig.3.5). Pre-treatment with 5 ng/ml PAI-1 significantly ($p<0.01$) reduced the insulin-induced phosphorylation of the IR by 23% (Fig.3.5A). In contrast, higher PAI-1 concentrations of 10 and 20 ng/ml caused a slight increase in the insulin-induced phosphorylation of the IR, by 1.2- and 24%, respectively (Fig.3.5A). The total IR protein levels, however, were not significantly ($p>0.05$) affected by PAI-1, at any of the three concentrations used (Fig.3.5B). Like PAI-1, SAA pre-treatment for 24 hours showed a similar effect regarding insulin-induced phosphorylation of the IR, with 5 µg/ml SAA causing a 18% decrease in the insulin-induced phosphorylation, and 10 and 20 µg/ml causing a 9- and 25% increase, respectively (Fig.3.5C). Furthermore, SAA was the only selected APP that decreased the total IR protein levels at all three concentrations, by 50%, 32% and 19%, respectively (Fig.3.2D). Interestingly, CRP treatment significantly ($p<0.05$) inhibited insulin-induced phosphorylation of the IR at both concentrations tested,

with 2.5 and 4.5 µg/ml CRP decreasing phosphorylation by 31- and 20%, respectively (Fig.3.5E). CRP at both concentrations used however had no significant effect ($p>0.05$) on the total IR levels (Fig.3.5F).

When investigating the effect of the selected APPs on the total IR expression in HepG2 cells (Fig.3.6), different responses were observed in comparison to the BWTG3 cells. Whilst in BWTG3 cells pre-treatment with PAI-1 at all the concentrations tested had no significant effect on total IR protein levels (Fig3.5B) this was not the case with total IR protein levels in HepG2 cells in response to PAI-1 treatment (Fig.3.6A). The total IR protein levels in HepG2 cells were increased to a similar extent by the different PAI-1 concentrations used, with 5 ng/ml resulting in a 1.4-fold increase ($p<0.001$) and 10 ng/ml and 20 ng/ml causing a 1.6-fold ($p<0.01$) increase (Fig.3.6A). SAA pre-treatment in HepG2 cells showed differential effects on the total IR protein levels, depending on the concentration used. Like PAI-1, pre-treatment with 5 µg/ml SAA caused a significant ($p<0.05$) increase of 1.4-fold, while 10 and 20 µg/ml significantly ($p<0.001$) decreased total IR levels 25- and 53%, respectively (Fig.3.6B). Pre-treatment with both concentrations of CRP, 2.5 and 4.5 µg/ml, significantly ($p<0.05$ and $p<0.01$ respectively) decreased total IR levels by 36- and 43%, respectively, in contrast to what was observed in the BWTG3 cells.

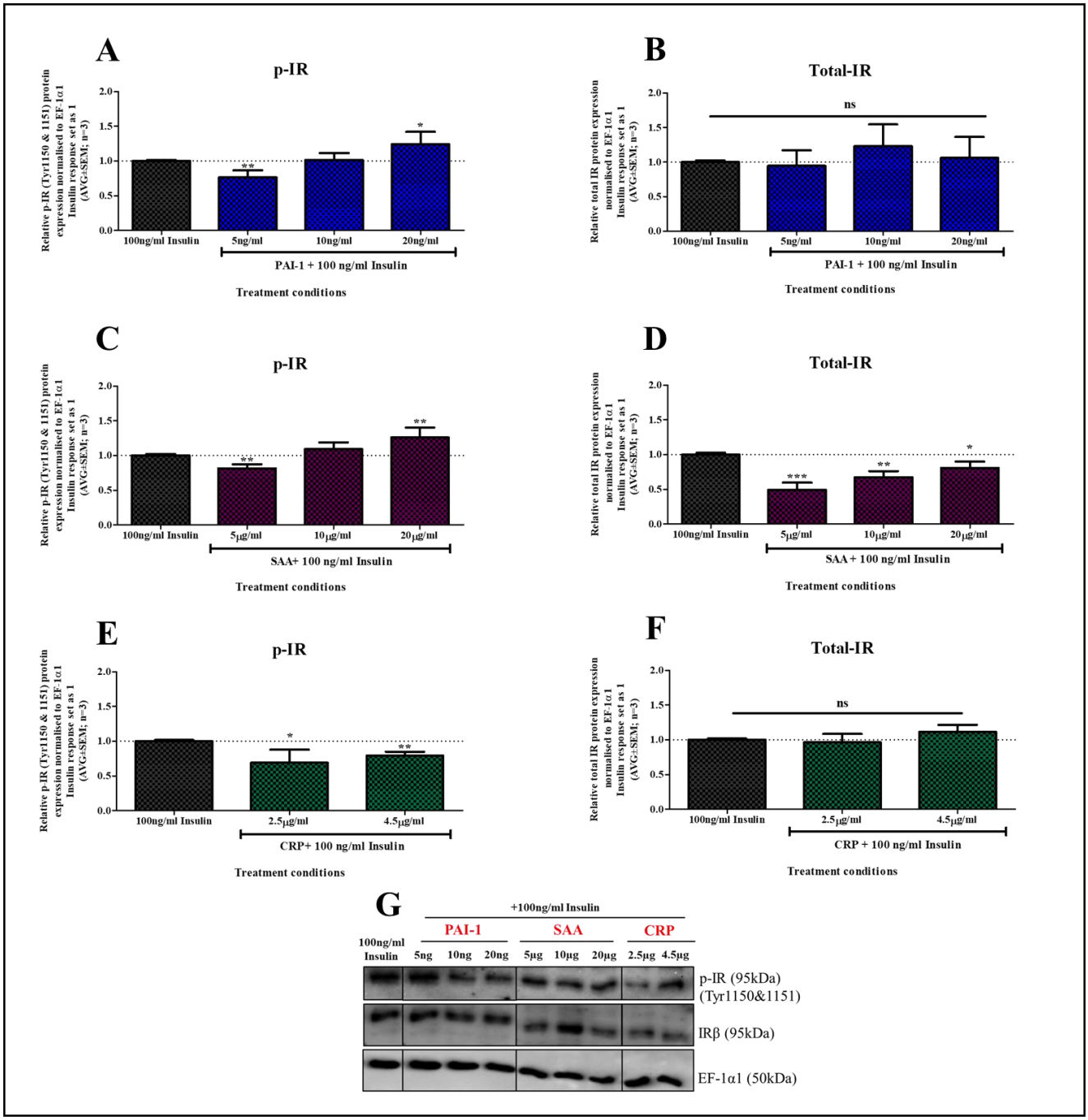

Figure 3.5. The APPs, PAI-1, SAA, and CRP differentially regulate phosphorylation of the insulin receptor as well as its total receptor levels in the mouse hepatoma cell line, BWTG3. BWTG3 cells were serum-starved for 24 hours and treated with physiological concentrations of PAI-1 (5-20 ng/ml) **(A & B)**, SAA (5-20 μg/ml) **(C & D)** and CRP (2.5 and 4.5 μg/ml) **(E & F)** for 24 hours followed by a 30 minute treatment with 100 ng/ml insulin to stimulate the insulin signalling pathway prior to cell lysis. Phosphorylation of the insulin receptor (IR) at Tyr1150 & 1151 **(A, C, E)** and total insulin receptor expression **(B, D, F)** was measured and quantified relative to the loading control, EF-1α1 (**G** shows a representative blot). The response of the APPs used were normalised relative to the insulin control which was set to 1 and represented by the dotted line. Data shown represents three independent experiments. Statistical analysis comparing the relative APP treatments to the insulin control was performed using a two-tailed unpaired Student's t-test (*p<0.05, **p<0.01, ***p<0.001).

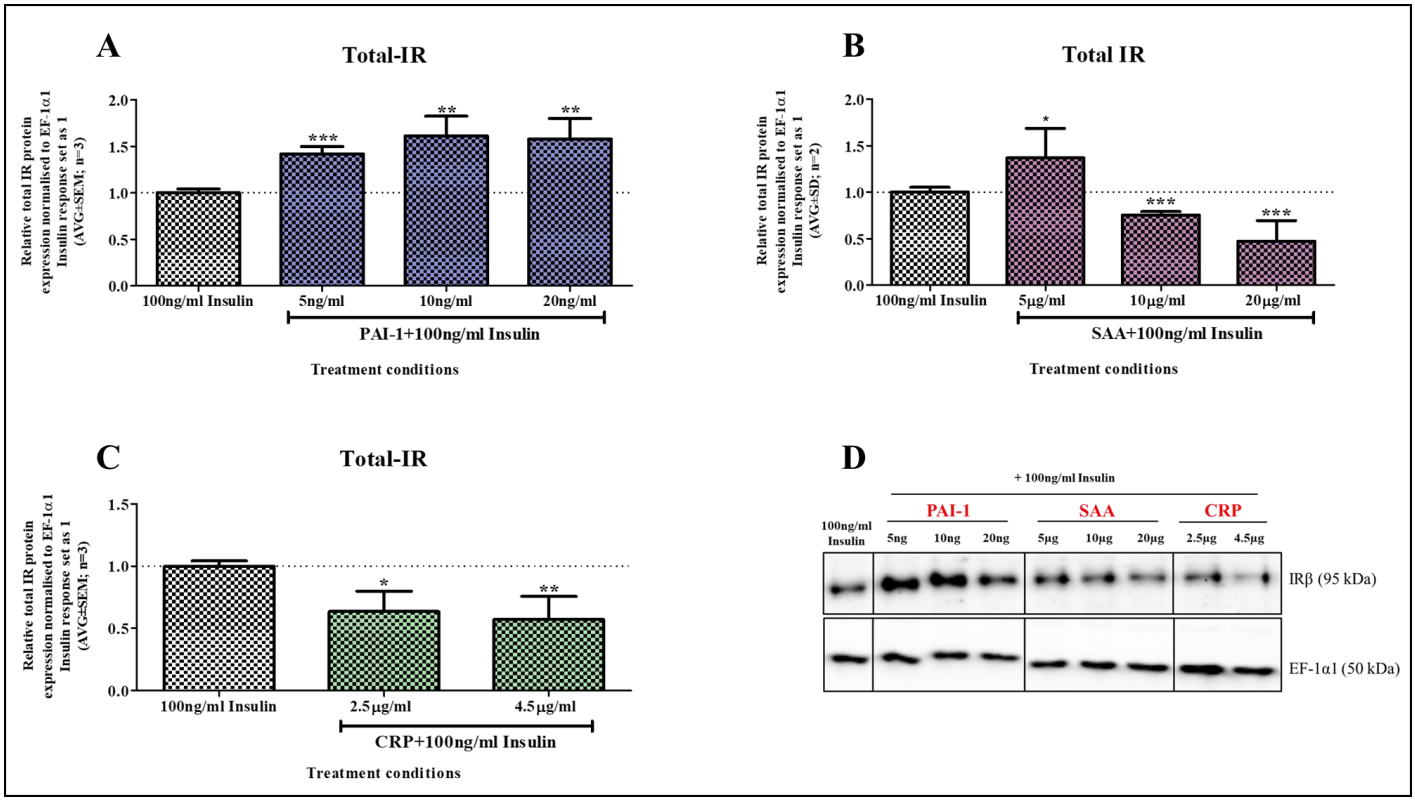

Figure 3.6. The APPs, PAI-1, SAA and CRP differentially regulate expression of the total insulin receptor levels in the human hepatoma cell line, HepG2. HepG2 cells were serum-starved for 24 hours and pre-treated with physiological concentrations of PAI-1 (5-20 ng/ml) **(A)**, SAA (5-10 µg/ml) **(B)**, CRP (2.5 and 4.5 µg/ml) **(C)** for 24 hours followed by a 30 minute treatment with 100 ng/ml insulin to stimulate the insulin signalling pathway prior to cell lysis**.** Total IR protein levels were measured and quantified relative to the loading control, EF-1α1 (**D** shows the representative blot). The response of the APPs used were normalised relative to the insulin control which was set to 1 and represented by the dotted line. Data shown represents three independent experiments. Statistical analysis comparing the relative APP treatments to the insulin control was performed using a two-tailed unpaired Student's t-test (*p<0.05, **p<0.01, ***p<0.001)

3.3.2 The inhibition of IRS-2 is differentially affected by the APPs, PAI-1, SAA, and CRP

Following activation of the IR, IRS-2 is recruited and binds to the IR and is subsequently activated through phosphorylation at its tyrosine residues (Fig.3.1). However, the ability of the IRS to bind to the IR is reduced when certain serine residues are phosphorylated, thereby preventing the IRS-2 from undergoing tyrosine phosphorylation and thus inhibiting its activity (145, 330). It is for this reason that phosphorylation of IRS-2 at Ser731 was investigated in response to the APPs using western blot analysis. Firstly, 100 ng/ml insulin treatment for 30 minutes had no significant ($p>0.05$) effect on the phosphorylation of IRS-2 at Ser731 site in both BWTG3 cells (Fig.3.3C) and HepG2 cells (Fig.3.4B). Subsequently, in BWTG3 cells treatment with PAI-1 for 24 hours prior to insulin exposure showed differential effects, with 5 ng/ml significantly ($p<0.01$) reducing phosphorylation of IRS-2 (35%), while 10 ng/ml caused a slight, although not significant, increase (13%) and 20 ng/ml PAI-1 had no effect (Fig.3.7A). The effect of SAA on Ser731 phosphorylation of IRS-2 was also dependent on the concentration. The lowest concentration SAA (5 µg/ml) used resulted in a 20% decrease although not significant ($p>0.05$), whilst 10 and 20 µg/ml SAA both increased phosphorylation of IRS-2 at Ser731 by 8%, although only 20 µg/ml SAA showed statistical significance ($p<0.01$) (Fig.3.7B). In contrast to PAI-1 and SAA, CRP at 2.5 and 4.5 µg/ml significantly ($p<0.01$ and $p<0.001$, respectively) reduced the phosphorylation of IRS-2 at Ser731 by 28- and 44%, respectively (Fig.3.7C), which suggest unhindered binding to the IR.

In HepG2 cells treatment with 5 ng/ml PAI-1 for 24 hours prior to insulin exposure caused a significant ($p<0.01$) increase in phosphorylation of IRS-2 at Ser731 (1.2-fold), while 10 and 20 ng/ml had no significant effect (Fig.3.8A). Additionally, the effect of SAA treatment on Ser731 phosphorylation of IRS-2 was independent of concentration, with 5 µg/ml causing a 28% decrease, although not significant, and 10 and 20 µg/ml SAA treatment caused a significant ($p<0.05$ and $p<0.01$, respectively) decrease in IRS-2 phosphorylation of 29- and 34%, respectively (Fig.3.8B). Similarly, to what was observed in BWTG3 cells, CRP at the two concentrations tested, 2.5 and 4.5 µg/ml, significantly ($p<0.001$ and $p<0.05$, respectively) decreased the phosphorylation of IRS-2 at Ser731 by 36% and 34%, respectively (Fig.3.8C).

In summation, these results show that in both the murine and human liver cell models, the APPs, PAI-1, SAA, and CRP, affect phosphorylation of IRS-2 at Ser731 to a different extent.

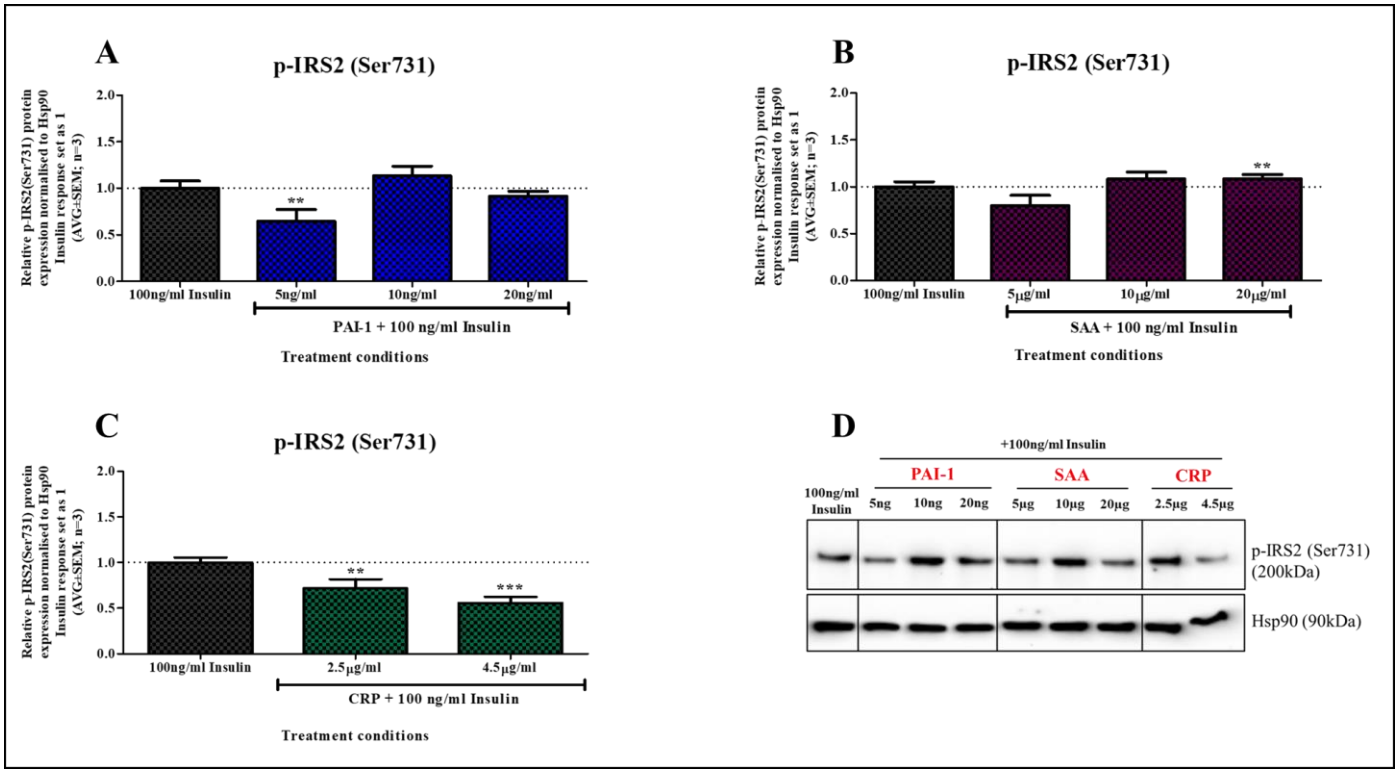

Figure 3.7. The APPs, PAI-1, SAA and CRP regulate the inhibition of the insulin receptor substrate-2 via Ser731 phosphorylation in the mouse hepatoma cell line, BWTG3. BWTG3 cells were serum-starved for 24 hours and pre-treated with physiological concentrations of PAI-1 (5-20 ng/ml) **(A)**, SAA (5-20 µg/ml) (**B),** and CRP (2.5 and 4.5 µg/ml) **(C)** for 24 hours followed by a 30 minute treatment with 100 ng/ml insulin to stimulate the insulin signalling pathway prior to cell lysis. Phosphorylation of the insulin receptor substrate-2 (IRS-2) at Ser731 was measured and quantified relative to the loading control, Hsp90 (**D** shows the representative blot). The response of the APPs used were normalised relative to the insulin control which was set to 1 and represented by the dotted line. Data shown represents three independent experiments. Statistical analysis comparing the relative APP treatments to the insulin control was performed using a two-tailed unpaired Student's t-test (**p<0.01, ***p<0.001).

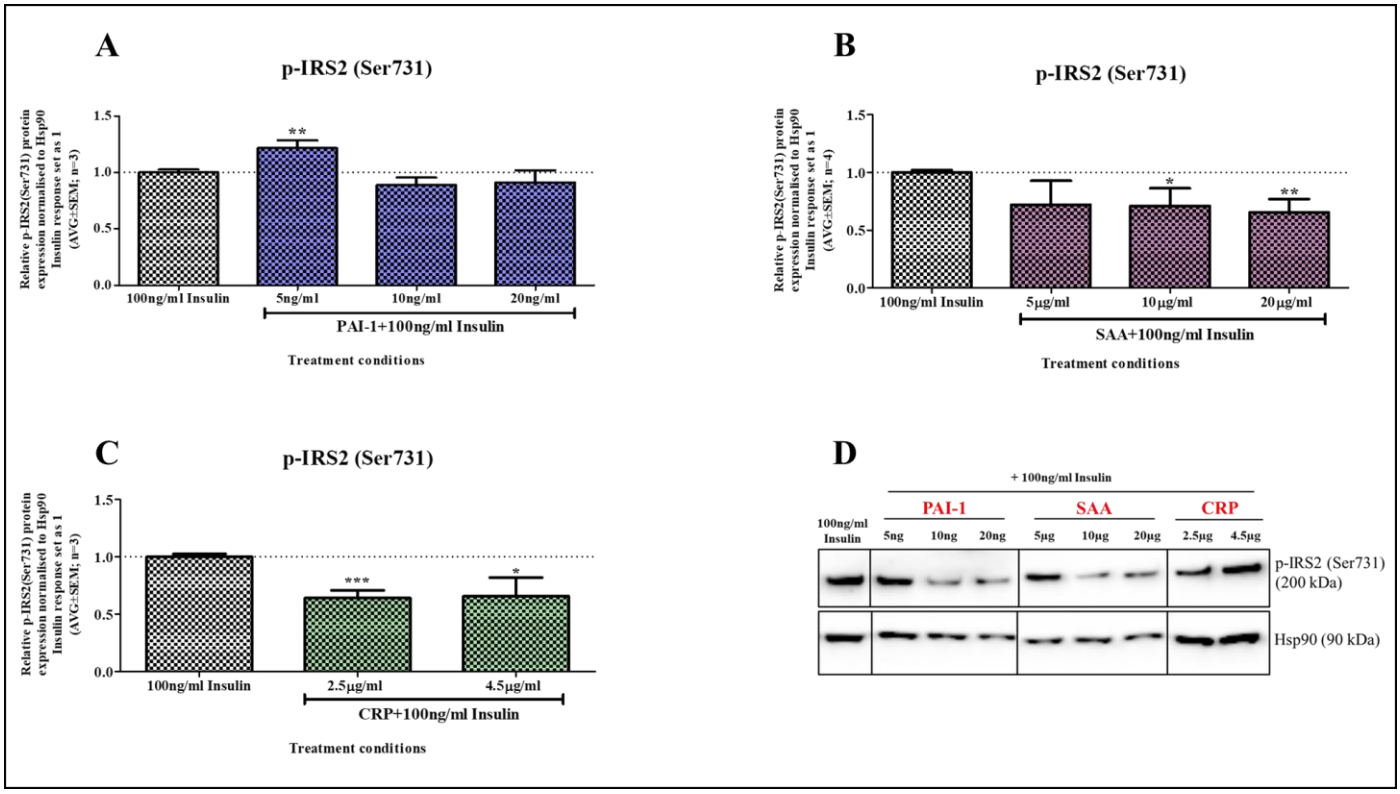

Figure 3.8. The APPs, PAI-1, SAA and CRP regulate the inhibition of the insulin receptor substrate-2 via Ser731 phosphorylation in the human hepatoma cell line, HepG2. BWTG3 cells were serum-starved for 24 hours and pre-treated with physiological concentrations of PAI-1 (5-20 ng/ml) **(A)**, SAA (5-20 µg/ml) (**B),** and CRP (2.5 and 4.5 µg/ml) **(C)** for 24 hours followed by a 30 minute treatment with 100 ng/ml insulin to stimulate the insulin signalling pathway prior to cell lysis. Phosphorylation of the insulin receptor substrate-2 (IRS-2) at Ser731 was measured and quantified relative to the loading control, Hsp90 (**D** shows the representative blot). The APPs used were normalised relative to the insulin control which was set to 1. Data shown represents three to four (for SAA) independent experiments. Statistical analysis comparing the relative APP treatments to the insulin control was performed using a two-tailed unpaired Student's t-test (*$p<0.05$, **$p<0.01$, ***$p<0.001$).

3.3.3 Insulin-induced activation of Akt at both Thr308 and Ser473 is differentially affected by PAI-1, SAA, and CRP

Activation of the central protein of the insulin signalling pathway, Akt, is required for downstream signalling, which regulates energy homeostasis, and more specifically lipid and glucose metabolism in the liver. Phosphorylation of Akt at Thr308 and Ser473 is required for maximum activity (121, 123–125). As mentioned earlier (section 3.2) insulin alone increased phosphorylation of Akt at Thr308 and Ser473 in both the murine (Fig.3.3D and E) and human hepatoma cells (Fig.3.4C and D). Disruption of the insulin-induced phosphorylation at these sites plays an important role in the development of insulin resistance (160, 162). Therefore, the possible effect of the selected APPs on insulin-induced Akt phosphorylation was of interest. Firstly, in BWTG3 cells, treatment with increasing concentrations of PAI-1 (5-20 ng/ml) for 24 hours before insulin exposure significantly ($p<0.001$) reduced insulin-stimulated phosphorylation of Akt at Thr308. The percentage inhibition for 5 ng/ml, 10 ng/ml, and 20 ng/ml was 30%, 41%, and 49% respectively. (Fig.3.9A). In contrast, insulin-induced phosphorylation of Akt at Ser473 was differentially regulated by the concentrations of PAI-1 used (Fig.3.9B). Pre-treatment with 5 ng/ml PAI-1 resulted in a slight but significant ($p<0.05$) decrease in insulin-induced Akt phosphorylation at Ser473, whilst 20 ng/ml PAI-1 significantly ($p<0.001$) increased insulin-induced phosphorylation at this site by 1.4-fold (Fig.3.9B). In contrast, 10 ng/ml PAI-1 had no significant effect on insulin-induced phosphorylation of Akt at Ser473 (Fig.3.9B). SAA, unlike PAI-1, had no significant ($p<0.05$) effect on the insulin-induced phosphorylation of Akt at Thr308 (Fig.3.9C), but significantly ($p<0.01$) attenuated insulin-induced phosphorylation of Akt at Ser473 at all concentrations used (Fig.3.9D). Similar to PAI-1, pre-treatment with CRP, specifically 4.5 µg/ml CRP, significantly ($p<0.01$) reduced insulin-induced Akt phosphorylation at Thr308 by 18% (Fig.3.9E). Both concentrations of CRP used had no significant ($p>0.05$) effect on the insulin-induced phosphorylation of Akt at Ser473 (Fig.3.9F).

Total Akt protein levels were also differentially regulated by the APPs in BWTG3 cells. Firstly, PAI-1 at all the concentrations used had no effect on total Akt protein levels (Fig.3.10A). In contrast, both SAA and CRP affected Akt protein levels albeit dependant on the concentration used. The lowest concentration of SAA (5 µg/ml) used, significantly ($p<0.01$) decreased total Akt levels, whilst 20 µg/ml significantly ($p<0.001$) increased Akt protein levels (Fig.3.10B). Similarly, the lowest concentration of CRP (2.5 µg/ml) used, significantly ($p<0.001$) inhibited total Akt levels, whilst the highest concentration (4.5 µg/ml) used, increased Akt protein levels (Fig.3.10C).

In HepG2 cells, only the highest concentration tested for PAI-1 (20 ng/ml) had a significant effect on insulin-induced phosphorylation of Akt at both Thr308 and Ser473 (Fig.3.11A & B). Treatment with 20 ng/ml PAI-1 resulted in a 20% significant ($p<0.01$) decrease in insulin-induced Akt phosphorylation at Thr308 (Fig.3.11A) Furthermore, it was able to attenuate insulin-stimulated Akt phosphorylation at

Ser473 by 26% ($p<0.05$) (Fig.3.11B). SAA, unlike PAI-1, at all the concentrations tested, significantly ($p<0.001$) reduced insulin-induced Akt phosphorylation at Thr308 (Fig.3.11C). The percentage inhibition for 5, 10, and 20 µg/ml was 49%, 52%, and 61%, respectively. Similarly, SAA at 5 and 10 µg/ml was able to significantly ($p<0.001$ and $p<0.01$ respectively) inhibit insulin-induced phosphorylation at Ser473 by 39% and 34%, respectively (Fig3.11D). Although a slight inhibition was observed for 20 µg/ml SAA no significance could be established ($p>0.05$). Furthermore, pre-treatment with both concentrations used for CRP attenuated insulin-induced activation of Akt at Thr308. CRP was able to significantly ($p<0.01$) reduce insulin-stimulated phosphorylation of Akt at Thr308 by 50% and 59% for at 2.5 and 4.5 µg/ml CRP, respectively (Fig.3.11E). Insulin-induced Akt phosphorylation at Ser473 phosphorylation was also significantly inhibited by 26% ($p<0.05$) and 22% ($p<0.01$) when pre-treated with 2.5 and 4.5 µg/ml CRP, respectively (Fig.3.11F). PAI-1 also had no significant ($p>0.05$) effect on the total Akt levels in HepG2 cells, except at the highest concentration (20 ng/ml), which caused a slight but significant ($p<0.05$) increase of 1.2-fold (Fig3.12A). The lowest concentration of SAA (5 µg/ml) significantly ($p<0.05$) decreased total Akt levels by 36% (Fig.3.12B), while 10 and 20 µg/ml SAA, along with both concentrations of CRP (Fig.3.12C) had no significant ($p>0.05$) effect when compared to insulin alone.

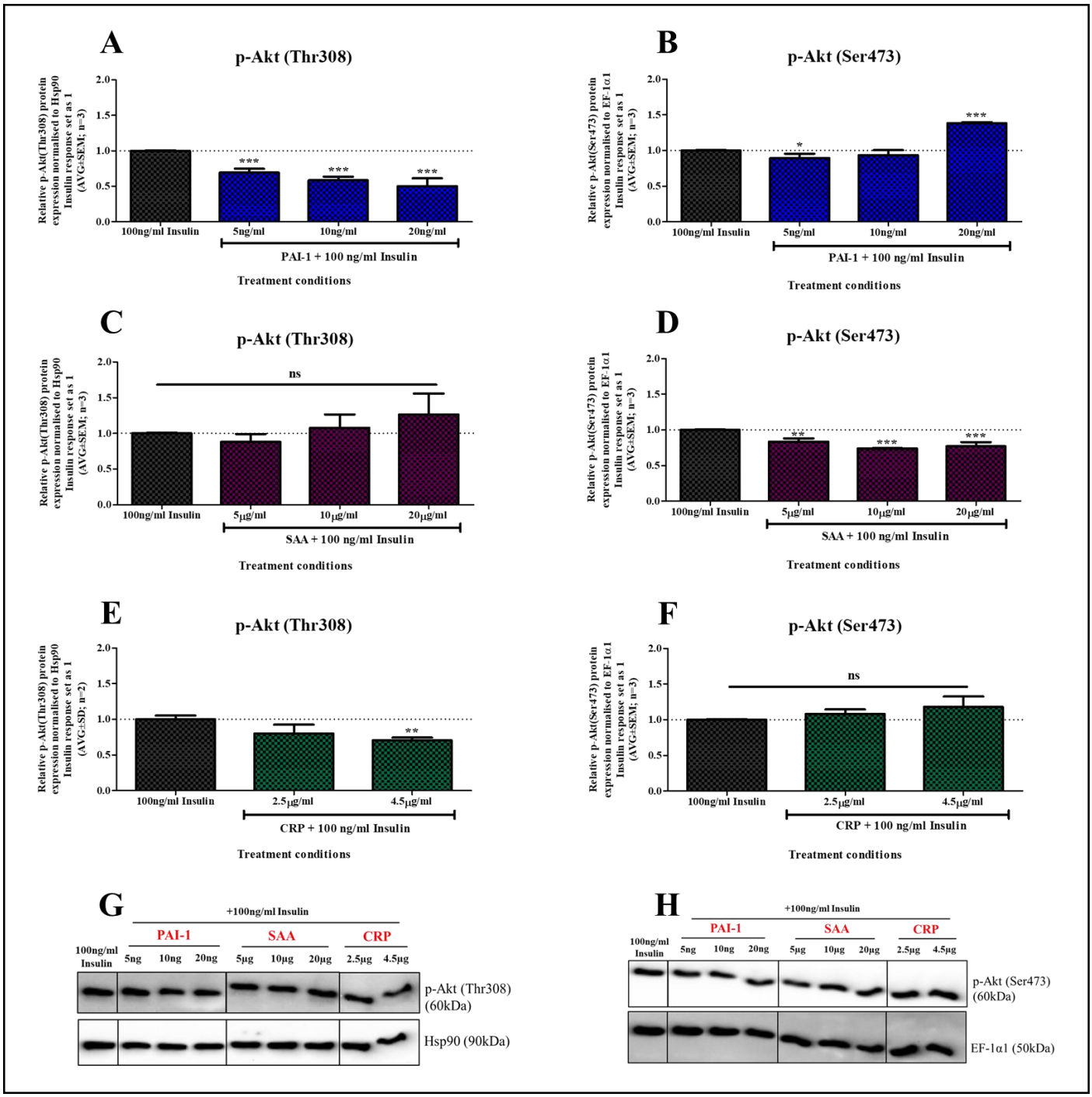

Figure 3.9. The APPs, PAI-1, SAA and CRP regulate the phosphorylation of Akt at Thr308 and Ser473 in the mouse hepatoma cell line, BWTG3. BWTG3 cells were serum-starved for 24 hours and pre-treated with physiological concentrations of PAI-1 (5-20 ng/ml) **(A & B)**, SAA (5-20 μg/ml) **(C & D),** and CRP (2.5 and 4.5 μg/ml) **(E & F)** for 24 hours followed with a 30 minute treatment with 100 ng/ml insulin to stimulate the insulin signalling pathway prior to cell lysis. Phosphorylation of the Akt at Thr308 **(A, C, E)** and Ser473 **(B, D, F)** was measured and quantified relative to the loading control, Hsp90 (for Thr308) and EF-1α1 (for Ser473) (**G & H** show the respective representative blots). The response of the APPs used were normalised relative to the insulin control which was set to 1 and represented by the dotted line. Data shown represents three independent experiments. Statistical analysis comparing the relative APP treatments to the insulin control was performed using a two-tailed unpaired Student's t-test (*p<0.05, **p<0.01, ***p<0.001).

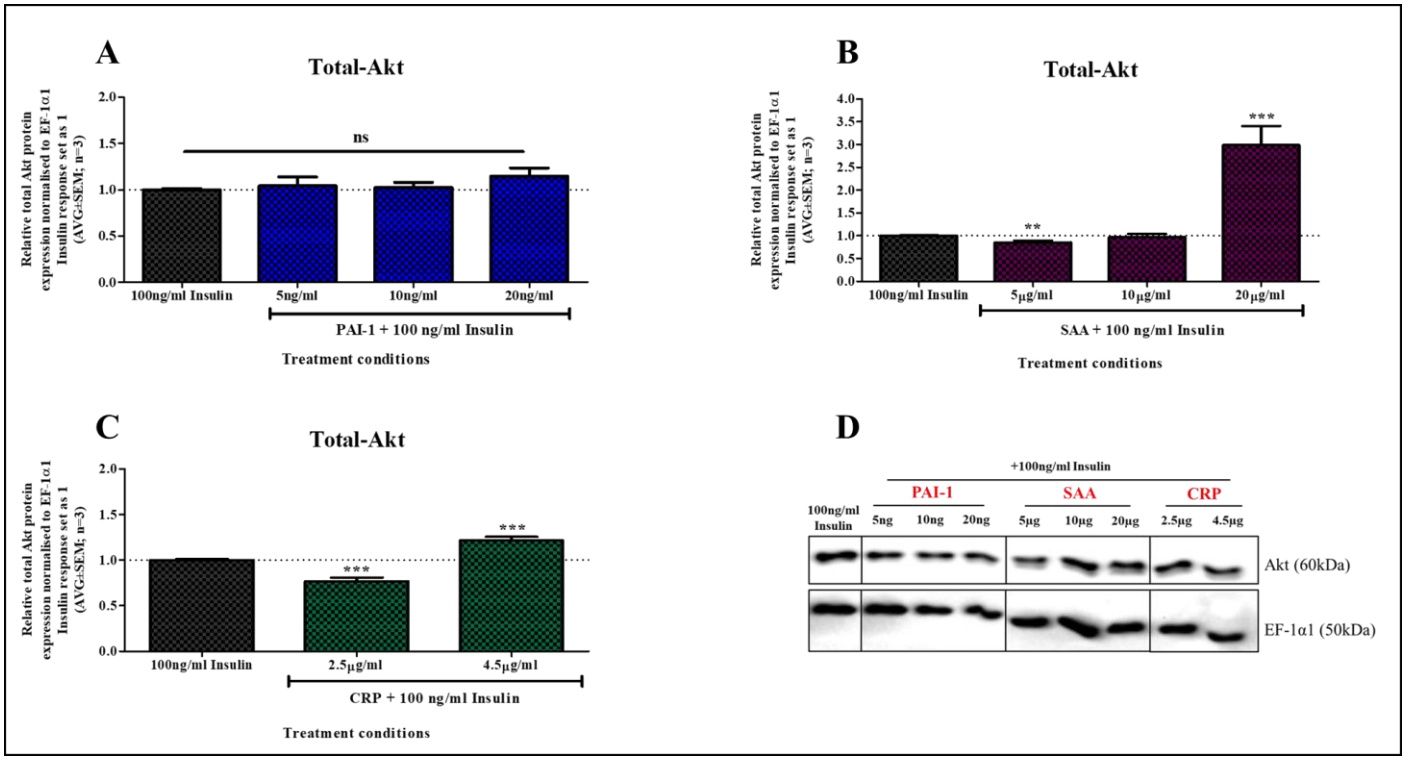

Figure 3.10. The APPs, PAI-1, SAA and CRP differentially regulate Akt in the mouse hepatoma cell line, BWTG3. BWTG3 cells were serum-starved for 24 hours and pre-treated with physiological concentrations of PAI-1 (5-20 ng/ml) **(A)**, SAA (5-20 µg/ml) **(B)** and CRP (2.5 and 4.5 µg/ml) **(C)** for 24 hours followed with a 30 minute treatment with 100 ng/ml insulin to stimulate the insulin signalling pathway prior to cell lysis. Total Akt expression was measured and quantified relative to the loading control, EF-1α1 (**D** shows the representative blot). The response of the APPs used were normalised relative to the insulin control which was set to 1 and represented by the dotted line. Data shown represents three independent experiments. Statistical analysis comparing the relative APP treatments to the insulin control was performed using a two-tailed unpaired Student's t-test (**p<0.01, ***p<0.001).

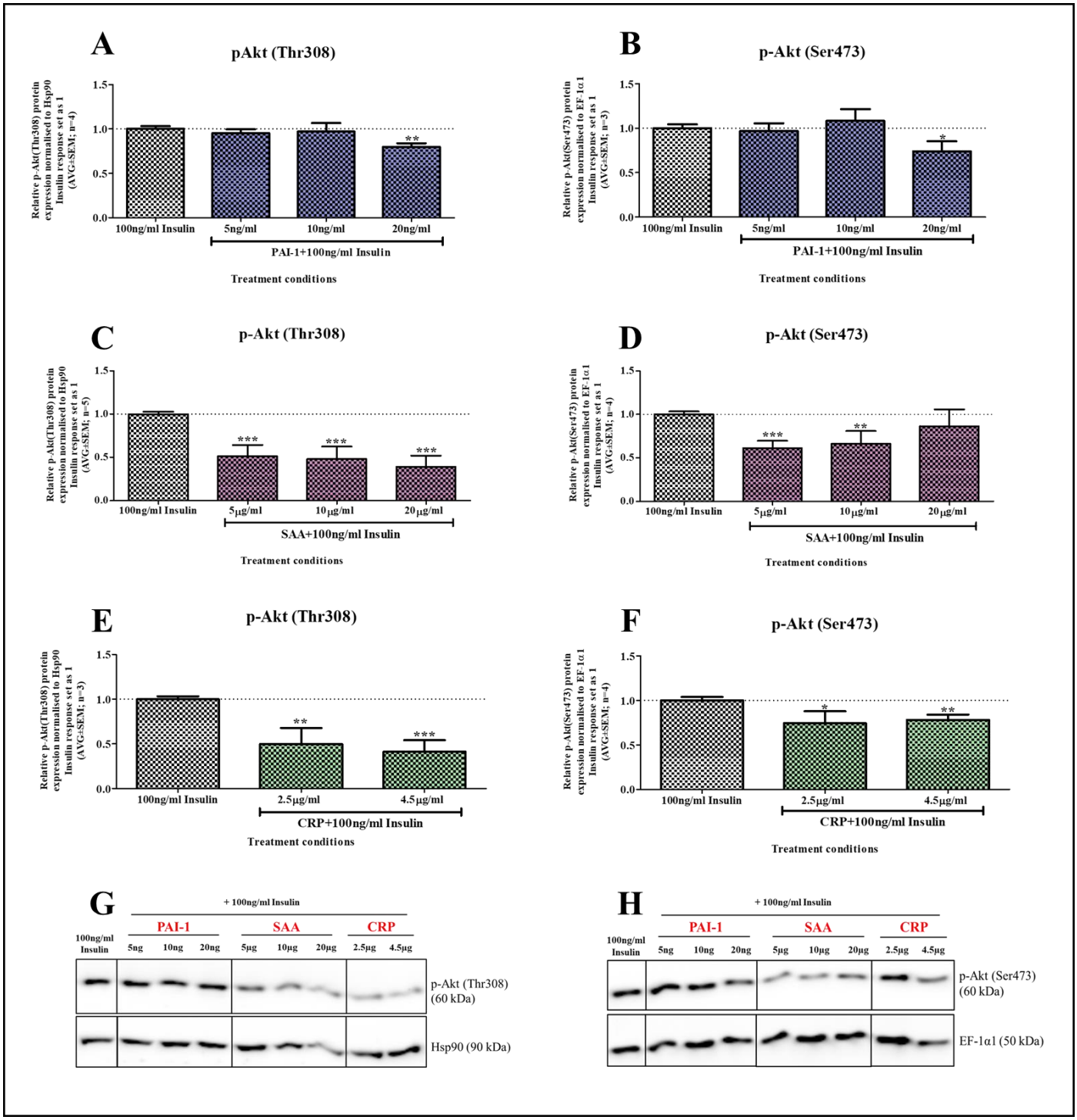

Figure 3.11. The APPs PAI-1, SAA and CRP differentially effect the phosphorylation of Akt at Thr308 and Ser473 in the human hepatoma cell line, HepG2. HepG2 cells were serum-starved for 24 hours and pre-treated with physiological concentrations of PAI-1 (5-20 ng/ml) **(A & B)**, SAA (5-20 μg/ml) **(C & D)** and CRP (2.5 and 4.5 μg/ml) **(E & F)** for 24 hours followed with a 30 minute treatment with 100 ng/ml insulin to stimulate the insulin signalling pathway prior to cell lysis. Phosphorylation of the Akt at Thr308 **(A-E)** and Ser473 **(C-F)** was measured and quantified relative to the loading control, Hsp90 (for Thr308) and EF-1α1 (for Ser473) (**G & H** show the respective representative blot). The response of the APPs used were normalised relative to the insulin control which was set to 1 and represented by the dotted line. Data shown represents three independent experiments. Statistical analysis comparing the relative APP treatments to the insulin control was performed using a two-tailed unpaired Student's t-test (*p<0.05, **p<0.01, ***p<0.001).

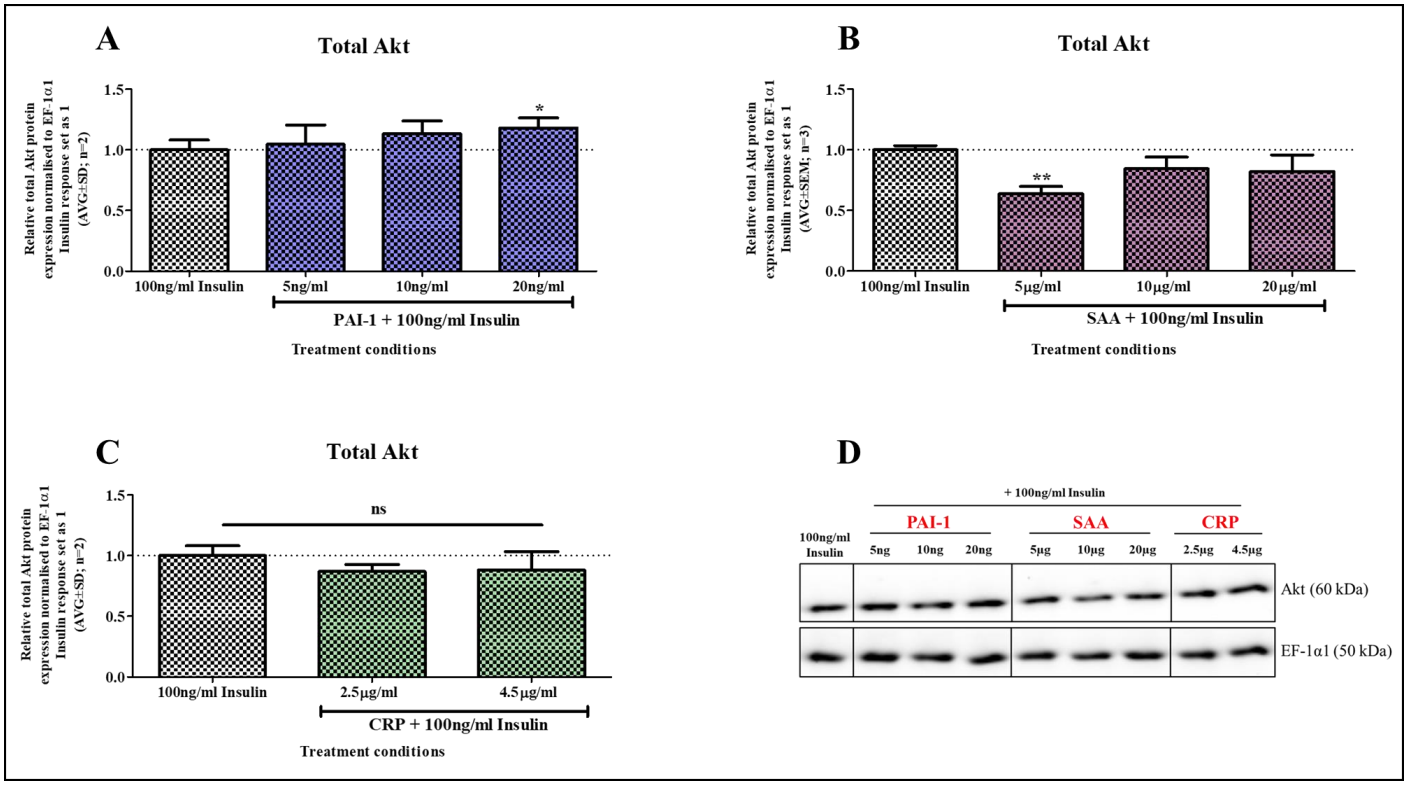

Figure 3.12. The APPs, PAI-1, SAA and CRP differentially effect Akt in the human hepatoma cell line, HepG2. HepG2 cells were serum starved for 24 hours and pre-treated with physiological concentrations of PAI-1 (5-20 ng/ml) **(A)**, SAA (5-20 µg/ml) **(B)** and CRP (2.5 and 4.5 µg/ml) **(C)** for 24 hours followed with a 30 minute treatment with 100 ng/ml insulin to stimulate the insulin signalling pathway prior to cell lysis. Total Akt expression was measured and quantified relative to the loading control, EF-1α1 (**D** shows the representative blot). The response of the APPs used were normalised relative to the insulin control which was set to 1 and represented by the dotted line. Data shown represents two to three independent experiments. Statistical analysis comparing the relative APP treatments to the insulin control was performed using a two-tailed unpaired Student's t-test (*$p<0.05$, **$p<0.01$).

.

3.4 Pro-longed exposure to acute phase proteins, PAI-1, SAA, and CRP increased their inhibitory effect on the insulin signalling pathway

Chronic inflammation is directly, and indirectly, linked to insulin resistance, more specifically obesity-related insulin resistance (20, 166, 183, 202, 203). This is characterized by chronic exposure to pro-inflammatory cytokines, such as interleukin-6 (IL-6) and tumour necrosis factor-α (TNF-α), and inflammatory markers such as SAA and CRP (263, 271, 331). Additionally, PAI-1 is considered an adipokine and marker of obesity (234, 243, 247) as it is increased in response to inflammation in adipocytes. This too is associated with chronic inflammation, which plays a role in the development of insulin resistance (242, 245, 246, 252). Furthermore, the normal acute phase response in the liver is considered rapid and peaks at 24-48 hours (209), but can last up to days (209, 215). Therefore, we decided to investigate whether the length of treatment could play a role in the effect that these APPs, PAI-1, SAA, and CRP, have on the insulin signalling pathway, by looking at what is defined as an "acute" and "chronic" (or pro-longed) exposure. Physiologically relevant concentrations of these APPs were chosen as indicated by the literature (35, 219, 236). Additionally, the dose response results (in section 3.3) were also taken into consideration. Consequently, a concentration of 10 ng/ml PAI-1, 10 µg/ml SAA, and 4.5 µg/ml CRP was chosen, and a time-course was performed by pre-treating murine (BWTG3) and human hepatoma (HepG2) cells with these APPs for 2, 24, and 48 hours followed by 30 minutes insulin exposure. Regulation of the insulin signalling pathway was investigated using western blot analysis.

3.4.1. PAI-1 and CRP similarly affect the activation of the insulin receptor, while SAA has no statistical effect

As shown in section 3.2, in BWTG3 cells, treatment with 100 ng/ml insulin for 30 minute induced the phosphorylation of the IR (Fig.3.3A), while increasing the amount of total receptor (Fig.3.3B), which was subsequently set as 1 as previously mentioned. The time course suggests that PAI-1 and CRP affect insulin-induced phosphorylation of the IR to a similar extent as shown in Fig.3.13A. Pre-treatment for 2 hours caused an initial increase in the insulin-induced phosphorylation, which subsequently decreased significantly ($p<0.05$) at 24 hours, reaching a maximum significant ($p<0.01$) inhibition at 48 hours of 55% and 72% ($p<0.001$) for PAI-1 and CRP, respectively. In contrast to PAI-1 and CRP, SAA potentiated the insulin-induced phosphorylation of the IR over time, reaching a maximum significant ($p<0.05$) increase of 1.5-fold at 24 hours. This effect remained constant at 48 hours. Furthermore, PAI-1 was only able to significantly ($p<0.001$) decrease total IR protein levels (by 71%) at 48 hours, whilst

CRP already at 24 hours significantly ($p<0.05$) decreased total IR protein levels, reaching a maximum significant decrease of 63% at 48 hours ($p<0.001$) (Fig.3.13B). In contrast, SAA, had no significant ($p>0.05$) effect on the total IR levels although a slight but not significant ($p>0.05$) decrease of 18% at 48 hours was observed. This result suggests that pro-longed exposure to PAI-1 and CRP, in BWTG3 cells, is sufficient to attenuate the ability of insulin to increase its cognate receptor levels, which is the initial site of the insulin signalling pathway.

In HepG2 cells, the selected APPs had no significant ($p>0.05$) effect on the total IR levels except for PAI-1 at 24 hours, which caused a significant ($p<0.05$) increase (Fig.3.13D). In contrast, PAI-1 and CRP decreased total IR protein levels to a similar extent at 48 hours by 46 and 57%, respectively, although significance could not be established ($p>0.05$). Furthermore, a two-way ANOVA analysis indicated that the IR phosphorylation in BWTG3 cells and total IR expression in HepG2 cells are significantly ($p<0.001$) dependent on the APP used and the length of exposure (Fig.3.13A & D, respectively). However, this dependence on length of exposure and APP used, with regards to total IR expression in BWTG3 cells was not observed (Fig.3.13B).

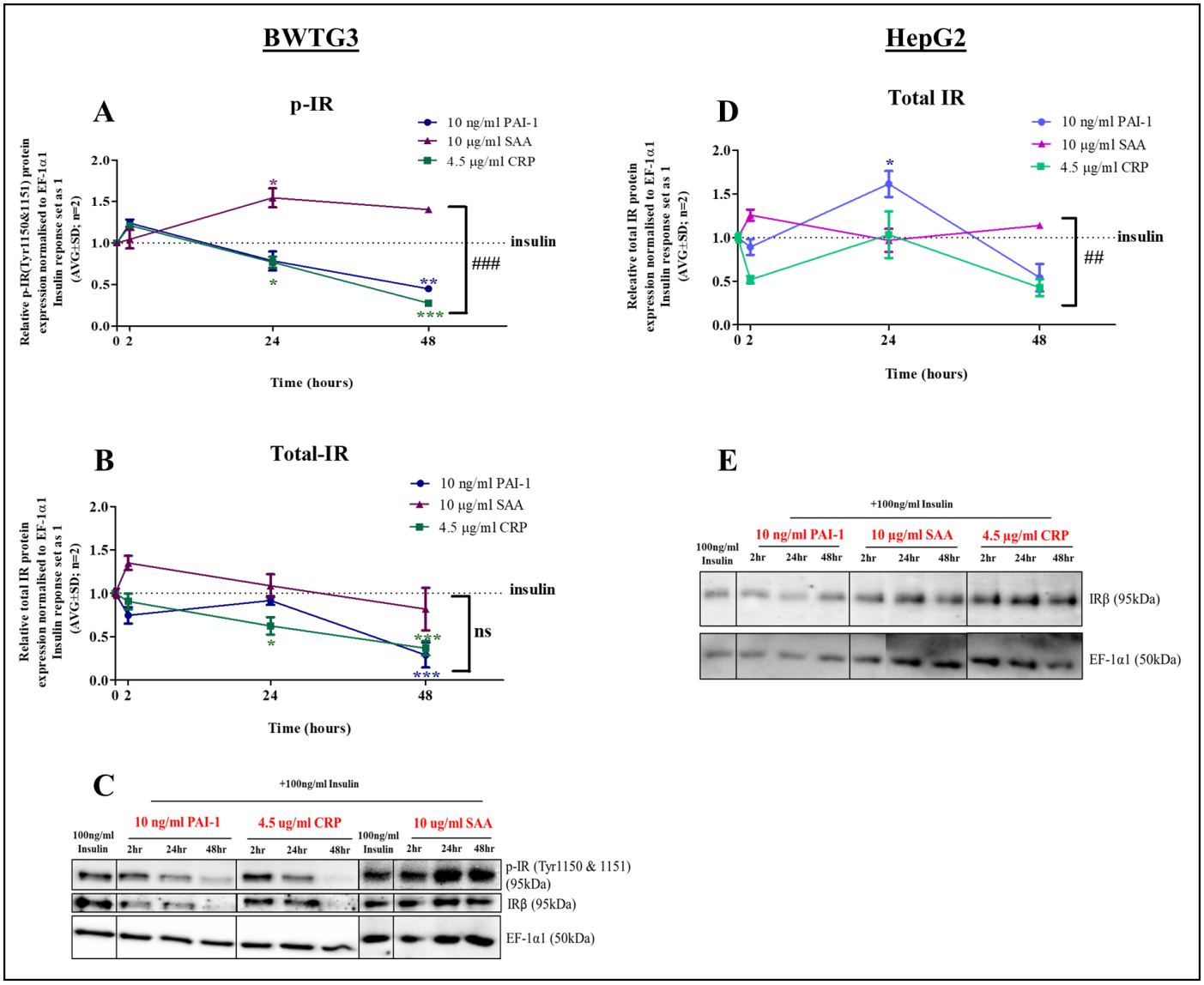

Figure 3.13. The APPs, PAI-1, SAA and CRP decrease the phosphorylation of the insulin receptor as well the total receptor levels over time in both the mouse and human hepatoma cell lines, BWTG3 & HepG2. BWTG3 and HepG2 cells were serum-starved for 24 hours followed with a treatment with 10 ng/ml PAI-1, 10 µg/ml SAA and 4.5 µg/ml CRP for 2, 24 and 48 hours (acute versus chronic exposure). The cells were treated with 100 ng/ml insulin for 30 minutes prior to cell lysis, to activate the insulin signalling pathway. Phosphorylation of the insulin receptor at Tyr1150 & 1511 **(A)** as well as the total receptor expression **(B & D)** was measured and quantified relative to loading control, EF-1α1 (**C & E** show the respective representative blots). The response of the APPs used were normalised relative to the insulin control, which was set to 1, and is represented by the dotted line. Data shown represents two independent experiments. Statistical analysis comparing the time treatments relative to the insulin control was performed using one-way ANOVA with Tukey's Multiple Comparison's Test (*p<0.05, **p<0.01, ***p<0.001). Additionally, the interaction between the time of treatment and the APP on the effect of the insulin receptor was analysed using a two-way ANOVA ($^{\#\#}$p<0.01 and $^{\#\#\#}$p<0.001).

3.4.2. The phosphorylation of IRS-2 at Ser731 is differentially regulated by PAI-1 and CRP with different lengths of exposure

In section 3.3.2 it was shown that, in the BWTG3 cells, the phosphorylation of IRS-2 at Ser731 is differentially affected by the different concentrations of PAI-1, SAA, and CRP used, when treated for 24 hours. In agreement with this, as shown in Fig.3.14A, 10 ng/ml PAI-1, 10 µg/ml SAA, and 4.5 µg/ml CRP affect the phosphorylation of IRS-2 at Ser731 differentially in a time-dependent manner. PAI-1 significantly ($p<0.01$) decreased the phosphorylation of IRS-2 at Ser731 at 2 hours by 25%, which was the maximum observed. This remained unchanged as the time of exposure increased, reaching a similar inhibition of 25% at 48 hours. In contrast, SAA had no significant ($p>0.05$) effect on the phosphorylation of IRS-2 at Ser731, although a 1.6-fold increase was observed at 2 hours, albeit not significant ($p<0.05$), while CRP, although initially increasing the phosphorylation of IRS-2 at Ser731 at 2 hours, it subsequently significantly decreased at 24 and 48 hours ($p<0.01$ and $p<0.001$, respectively), reaching 59% maximal inhibition.

In accordance with the BWTG3 results, the different concentrations of PAI-1, SAA, and CRP differentially affected the phosphorylation of IRS-2 at Ser731 in section 3.3.2. However, when exposed for different time periods, these APPs had no significant ($p>0.05$) effect on the phosphorylation of IRS-2 as shown in Fig.3.14B. Although not significant, pro-longed exposure to SAA and CRP for 48 hours decreased phosphorylation of IRS-2 by 29% and 14%, respectively.

Moreover, a two-way ANOVA analysis indicated that Ser731 phosphorylation of IRS-2 in BWTG3 and HepG2 cells is significantly ($p<0.0001$ and $p<0.05$, respectively) dependent on the two variables i.e. the APP used (PAI-1, SAA, and CRP) and the exposure time (Fig3.14 A & B, respectively).

3.4.3 The activation of Akt at Thr308 is similarly affected by PAI-1 and CRP with different lengths of exposure

As previously shown (Fig.3.3C), in BWTG3 cells, treatment with 100 ng/ml insulin for 30 minutes significantly ($p<0.001$) increased the phosphorylation of Akt at Thr308, which was subsequently set as 1 for further analysis as depicted in Fig.3.15A. Insulin-stimulated phosphorylation of Akt at Thr308 was already inhibited by 10 ng/ml PAI-1 at 2 hours treatment although no significance could be established ($p<0.05$). This inhibition however became more pronounced over time, reaching a maximum inhibition of 41% at 48 hours ($p<0.001$). Like PAI-1, CRP significantly ($p<0.01$) attenuated insulin-stimulated phosphorylation of Akt at Thr308 at 2 hours, which over time gradually reached maximal inhibition of 59% at 48 hours. Thus, indicating that acute as well as chronic exposure to 10 ng/ml PAI-1 and 4.5 µg/ml CRP significantly reduced the ability of insulin to phosphorylate Akt at

the Thr308 site. In contrast, SAA had no significant effect on the insulin-induced Akt phosphorylation at Thr308, although an inhibition of 61% at 2 hours was observed (Fig.3.15A).

In HepG2 cells, as previously shown, insulin treatment resulted in a greater increase in Akt phosphorylation at Thr308 (Fig.3.4C), which was subsequently set as 1. Treatment with SAA and CRP inhibited insulin-induced phosphorylation of Akt at Thr308, with a significant decrease already demonstrated for both at 2 hours (Fig.3.15C). SAA caused a significant ($p<0.01$) decrease of 36% at 2 hours, which was the maximum inhibition observed. CRP however, significantly ($p<0.05$) decreased phosphorylation over the time period investigated, resulting in a 51% decrease at 2 hours which continued to decrease, reaching 58% inhibition at 48 hours. In contrast to SAA and CRP, PAI-1 was unable to significantly affect insulin-induced phosphorylation of Akt at Thr308 ($p>0.05$) in HepG2 cells. Two-way ANOVA analysis indicated that in both BWTG3 (Fig.3.15A) and HepG2 (Fig.3.15D) cells, phosphorylation of Akt at Thr308 is significantly ($p<0.001$ and $p<0.01$, respectively) dependent on both the APP used (PAI-1, SAA, and CRP) and the time of exposure.

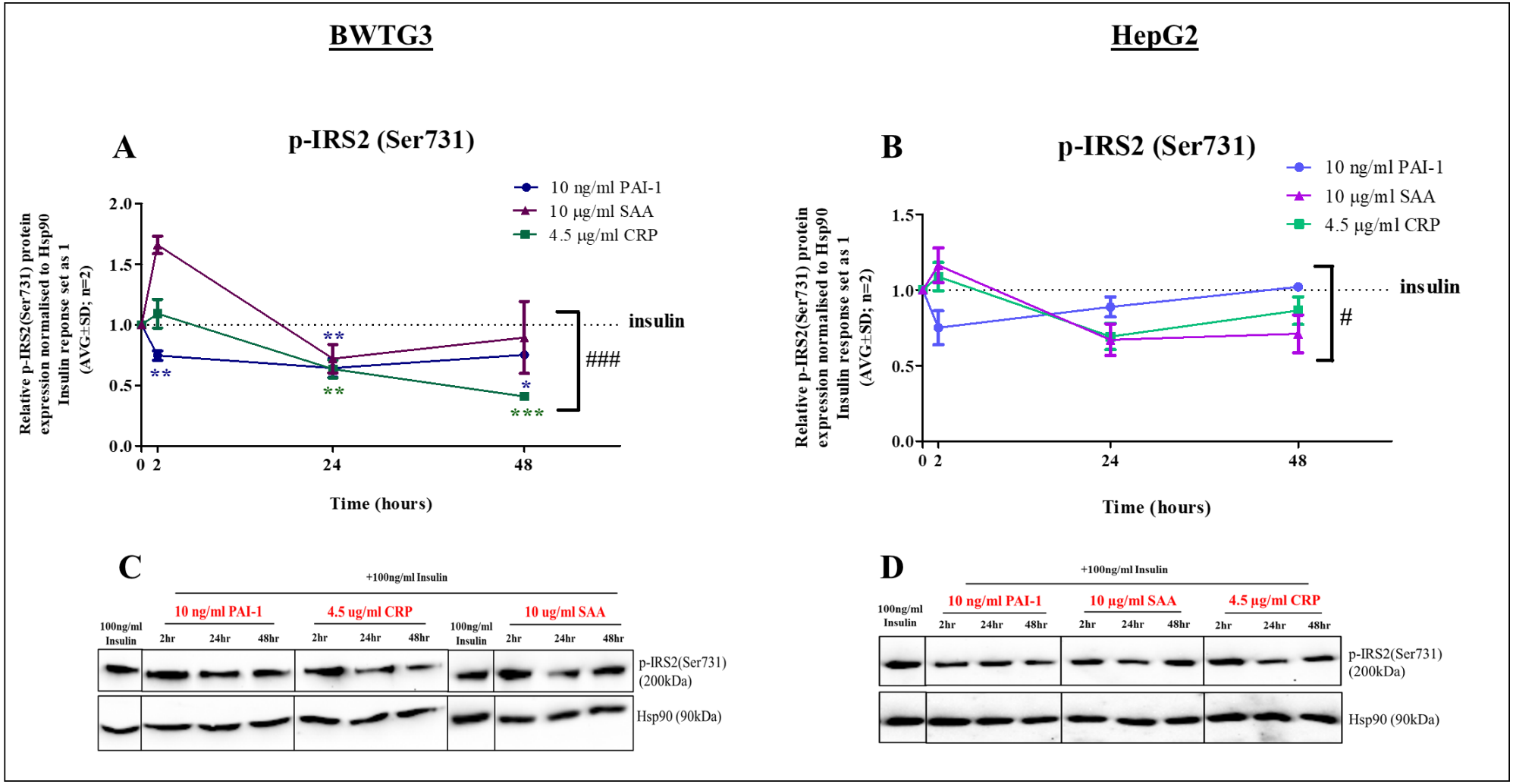

(Figure legend on next page)

Figure 3.14. The APPs, PAI-1, SAA and CRP differentially regulate the phosphorylation of IRS-2 at Ser731 over time in both the mouse and human hepatoma cell lines, BWTG3 & HepG2. BWTG3 (**A & C**) and HepG2 (**B & D**) cells were serum-starved for 24 hours followed by PAI-1, SAA or CRP treatment for 2, 24 and 48 hours (acute versus chronic exposure). The cells were treated with 100 ng/ml insulin for 30 minutes prior to cell lysis, to activate the insulin signalling pathway. Phosphorylation of IRS-2 at Ser731 was measured and quantified relative to the loading control, Hsp90 (**C & D** show the respective representative blots). The response of the APPs used were normalised relative to the insulin control, which was set to 1, and is represented by the dotted line. Data shown represents two independent experiments. Statistical analysis comparing the time treatments relative to the insulin control was performed using one-way ANOVA with Tukey's Multiple Comparison's Test (*p<0.05, **p<0.01, ***p<0.001). Additionally, the interaction between the time of treatment and the APP on the effect of IRS-2 was analysed using a two-way ANOVA ($^{\#}$p<0.05 and $^{\#\#\#}$p<0.001).

3.4.4 PAI-1 and CRP show a similar trend at the Ser473 phosphorylation of Akt and total Akt protein levels

As with prior experiments the insulin-induced effect on both phosphorylation of Akt significantly (p<0.001) Ser473 and total Akt protein levels were set to 1 to evaluate the role of the APPs on insulin-induced signalling.

In BWTG3 cells, pre-treatment with 10 ng/ml PAI-1 for 2 hours reduced the insulin-stimulated phosphorylation of Akt at Ser473 as well as the total Akt levels albeit no significance could be established. This inhibition by PAI-1 remains constant at 24 hours and then decrease at 48 hours. Phosphorylation status of Akt at Ser473 and total Akt protein levels are maximally reduced by 64% (p<0.001) and 53% (p<0.001), respectively at 48 hours by PAI-1 (Fig.3.15B and C). Unlike PAI-1, CRP at the initial time points measured, namely 2- and 24-hours, slightly potentiated insulin-induced phosphorylation of Akt at Ser473 although significance could not be established (Fig.3.15B). Subsequently, at 48 hours, CRP significantly (p<0.001) inhibited insulin-induced phosphorylation of Akt at Ser473 by 54%. Similarly, CRP pre-treatment only had a significant (p<0.001) effect on total Akt protein levels at 48 hours by inhibiting its levels by 53% when compared to insulin treatment alone (Fig.3.15C). Finally, SAA had no significant (p>0.05) effect on Akt phosphorylation at Ser473 (Fig.3.15B). However, the total Akt protein levels were significantly (p<0.05) decreased, by 56%, when BWTG3 cells were pre-treated for 48 hours with SAA before insulin exposure (Fig3.15C).

As shown in Fig.3.15E, HepG2 cells pre-treated with PAI-1 caused a slight (1.3-fold) increase in the insulin-induced phosphorylation of Akt at Ser473 at 24 hours. This modest potentiation of PAI-1 was diminished at 48 hours, resulting in a significant (p<0.05) inhibition of insulin-induced phosphorylation by 25%. Unlike PAI-1, CRP attenuated insulin-induced Ser473 phosphorylation of Akt significantly (p<0.01) by 23% at 24 hours, which reached a maximum inhibition at 48 hours (40%) (p<0.001). In contrast, SAA was unable to affect the ability of insulin to induce Akt phosphorylation at Ser473 (Fig.3.15E). Finally, the selected APPs had no significant (p>0.05) effect on the total Akt levels

(Fig.3.15F), although at 2 hours SAA and CRP did cause a slight increase, which decreased over time resulting in a similar effect in comparison to the insulin control.

Finally, two-way ANOVA indicated that phosphorylation of Akt at Ser473 in BWTG3 ($p<0.01$) and HepG2 ($p<0.001$) cells as well as the total Akt levels in BWTG3 cells ($p<0.05$), but not HepG2 cells, are significantly dependent on both the selected APPs (PAI-1, SAA, and CRP) and the time of treatment.

Taken together, these results indicate that an increase in exposure time to these APPs, especially PAI-1 and CRP, enhances their inhibitory effect on multiple nodes in the insulin signalling pathway.

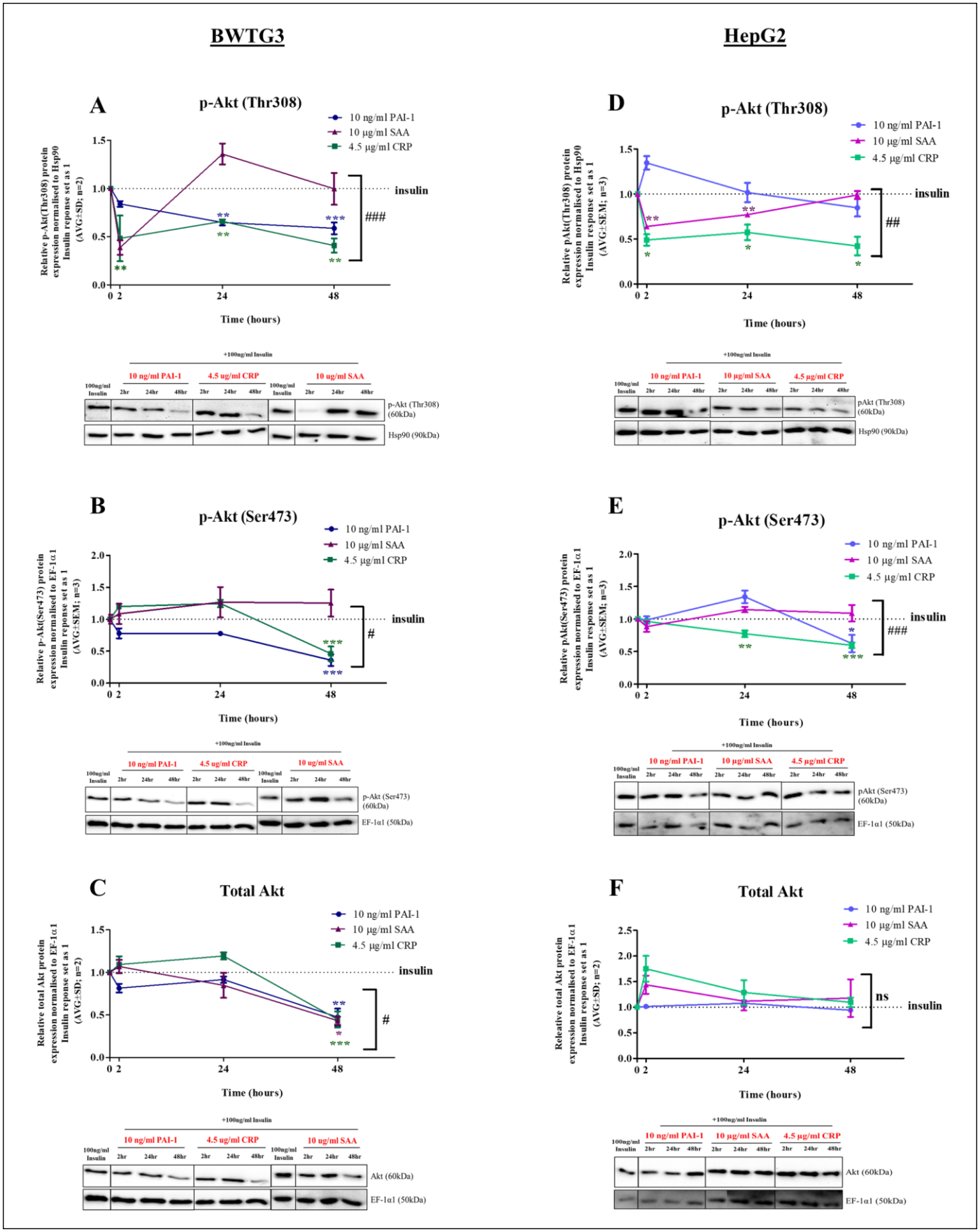

(Figure legend on next page)

Figure 3.15. The APPs, PAI-1, CRP and SAA, decrease the phosphorylation of Akt at both Thr308 and Ser473 as well the total Akt protein levels over time in both the mouse (BWTG3) and human (HepG2) hepatoma cell lines. BWTG3 and HepG2 cells were serum-starved for 24 hours followed by 10 ng/ml PAI-1, 10 µg/ml SAA and 4.5 µg/ml CRP treatment for 2, 24 and 48 hours (acute versus chronic exposure). The cells were treated with 100 ng/ml insulin for 30 minutes prior to cell lysis, to activate the insulin signalling pathway. Phosphorylation of Akt at Thr308 **(A & D)** and Ser473 **(B & E)** as well as total Akt protein expression **(C & F)** was measured and quantified relative to the loading control, EF-1α1 and Hsp90. The response of the APPs used was normalised relative to the insulin control, which was set to 1, and is represented as a dotted line. Data shown represents two independent experiments. Statistical analysis comparing the time treatments relative to the insulin control was performed using one-way ANOVA with Tukey's Multiple Comparison's Test (*p<0.05, **p<0.01, ***p<0.001). Additionally, the interaction between the time of treatment and the APP on the effect of the insulin receptor was analysed using a two-way ANOVA ($^{\#}$p<0.05, $^{\#\#}$p<0.01, $^{\#\#\#}$p<0.001).

3.5 Pro-longed exposure to acute phase proteins, PAI-1, SAA and CRP regulate the mRNA expression of G6Pase and PEPCK

De novo glucose synthesis (also known as gluconeogenesis) is a key process in the liver that is crucial for glucose metabolism. It is known that insulin inhibits this process in response to increased plasma glucose levels, in order to maintain homeostasis. A mechanism through which this occurs is the transcriptional regulation of two key gluconeogenic enzymes, G6Pase and PEPCK. Therefore, real-time PCR (qPCR) was performed to investigate the mRNA expression of the genes encoding these enzymes. In accordance with the previous section, which showed that the effects of the selected APPs, PAI-1, SAA, and CRP, are influenced by the length of exposure, mRNA expression levels were measured over time using the same chosen concentrations: 10 ng/ml PAI-1, 10 µg/ml SAA, and 4.5 µg/ml CRP. The same insulin treatment optimised upstream of the insulin signalling pathway was utilised. It should be noted that the mRNA expression of G6Pase could not be investigated in HepG2 cells due to difficulty experienced with the human G6Pase primers in this investigation, therefore due to limited time, G6Pase mRNA expression could only be investigated in BWTG3 cells.

As expected for such a short treatment time, 100 ng/ml insulin exposure for 30 minutes had no significant ($p>0.05$) effect on G6Pase mRNA expression in BWTG3 cells (Fig3.16). Pre-treatment with PAI-1 significantly ($p<0.05$) increased the mRNA levels of this gene at all the time points investigated (Fig.3.16A). PAI-1 treatment for 2 hours was able to increase G6Pase mRNA levels by 3-fold. This fold increase of mRNA levels was maintained and kept relatively constant over time. In contrast, SAA and CRP was only able to induce G6Pase mRNA expression in BWTG3 cells when treated for 48 hours. SAA and CRP resulted in a 3.5-fold and 4.8-fold increase in G6Pase mRNA expression, respectively, at 48 hours treatment (Fig.3.16B and C).

Although insulin had no effect on G6Pase mRNA expression in BWTG3 cells, 30 minutes exposure to 100 ng/ml insulin was able to significantly ($p<0.001$) inhibit PEPCK mRNA expression (Fig3.17). This

relatively short exposure time to insulin in BWTG3 cells resulted in a 10-fold decrease in PEPCK mRNA levels (Fig.3.17A-C). PAI-1 and CRP could only attenuate the insulin-induced repression of PEPCK mRNA expression when pre-treated for 48 hours in BWTG3 cells (Fig3.17 A & C). The degree of attenuation at 48 hours between the two APPs differ, however. Treatment with PAI-1 for 48 hours resulted in a significant ($p<0.001$) 12.9-fold increase (Fig.3.17A) compared to insulin control, while CRP greatly inhibited insulin-induced repression of PEPCK mRNA expression by up to 225-fold ($p<0.001$) (Fig.3.17C). In contrast to PAI-1 and CRP, SAA at 2 hours already was able to attenuate the ability of insulin to inhibit PEPCK mRNA expression by 14-fold ($p<0.001$). This inhibition of insulin by CRP was, however, short lived as no significant difference ($p>0.05$) was observed between CRP pre-treatment and insulin alone (Fig.3.17B) at later time points.

Furthermore, in HepG2 cells, 100 ng/ml insulin significantly ($p<0.001$) decreased PEPCK mRNA expression by 4-fold and pre-treatment with the selected APPs showed differential effects. Firstly, PAI-1 significantly ($p<0.05$) attenuated insulin-induced inhibition of PEPCK mRNA expression at 24 hours (2.5-fold). Attenuation of insulin by PAI-1 was not observed at the other time points measured (Fig.3.17D). In contrast, SAA was unable to significantly affect insulin-induced inhibition of PEPCK mRNA expression ($p<0.05$) at any of the time points measured (Fig.3.17E). CRP, however, was able to attenuate ($p<0.05$) insulin-induced inhibition of PEPCK mRNA expression at all the time points measured. A maximal response was observed at 24-hours (13-fold), whereas 2 and 48 hours showed a 6.4-fold and 3-fold increase, respectively, when compared to insulin control.

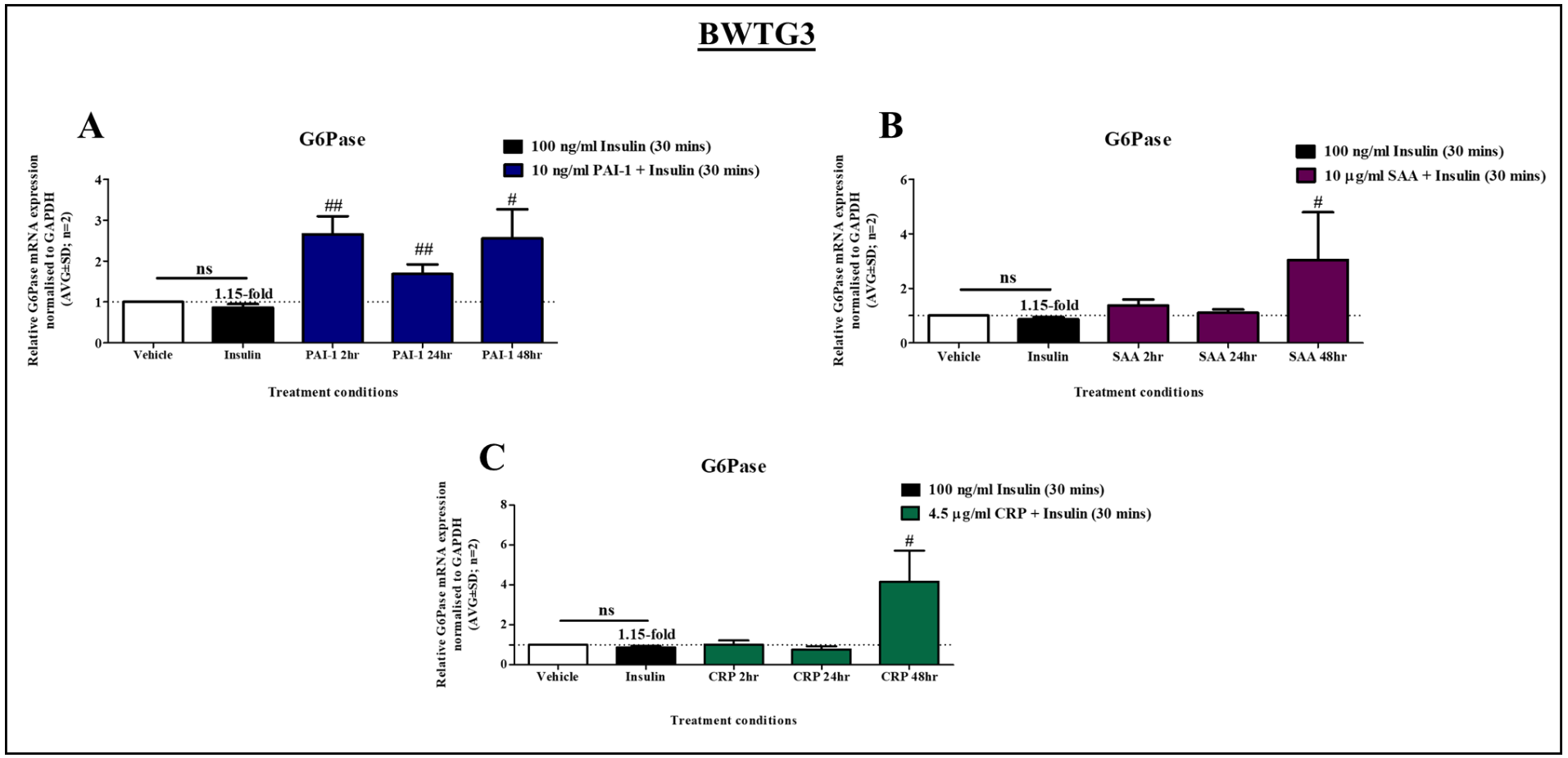

Figure 3.16. The APPs, PAI-1, SAA and CRP, regulate the mRNA expression of the gluconeogenic gene, G6Pase, over time in the mouse hepatoma cell line, BWTG3. BWTG3 cells were serum-starved for 24 hours followed by a treatment with 10 ng/ml PAI-1 **(A)**, 10 µg/ml SAA **(B),** and 4.5 µg/ml CRP **(C)** for 2, 24, and 48 hours (acute versus pro-longed exposure). The cells were treated with 100 ng/ml insulin for 30 minutes prior to cell lysis, to activate the insulin signalling pathway. The mRNA expression of the gluconeogenic gene, G6Pase, was measured using real-time qPCR and quantified relative to the housekeeping gene, GAPDH. The response of insulin was normalized to the vehicle which was set to 1 and is represented as a dotted line. The response of the APPs used was normalized to insulin. Data shown represents two independent experiments. Statistical analysis comparing insulin to the vehicle ($p>0.05$ = not significant) and the time treatments relative to the insulin control was performed using one-way ANOVA with Tukey's Multiple Comparison's Test ($^{\#}p<0.05$, $^{\#}p<0.01$, $^{\#\#\#}p<0.001$).

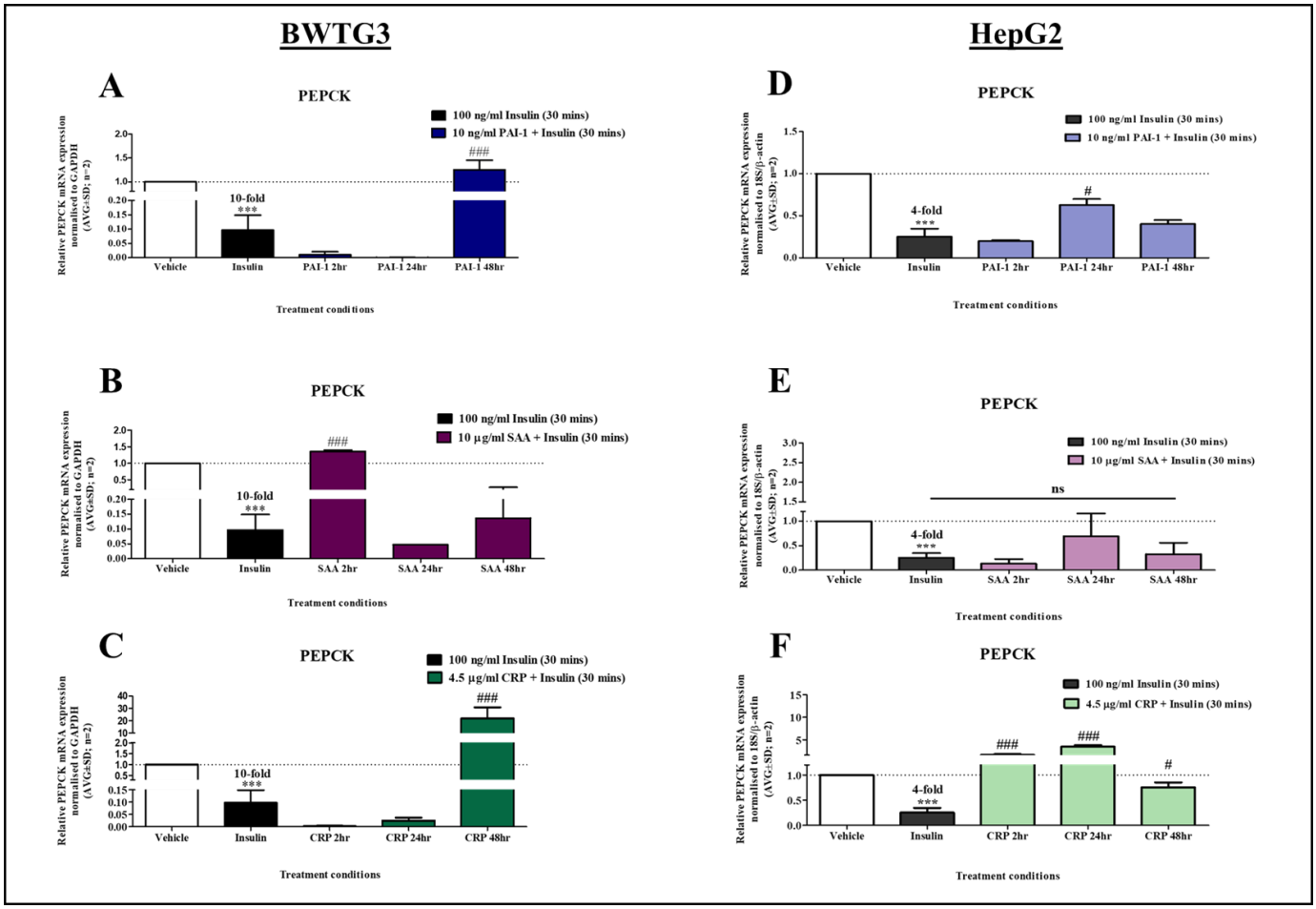

Figure 3.17. The APPs, PAI-1, SAA and CRP, regulate the mRNA expression of the gluconeogenic gene, PEPCK, over time in both the murine and human hepatoma cell lines, BWTG3 and HepG2. BWTG3 and HepG2 cells were serum-starved for 24 hours followed by a treatment with 10 ng/ml PAI-1 **(A & D)**, 10 µg/ml SAA **(B & E)** and 4.5 µg/ml CRP **(C & F)** for 2, 24, and 48 hours (acute versus chronic exposure). The cells were treated with 100 ng/ml insulin for 30 minutes prior to cell lysis, to activate the insulin signalling pathway. mRNA expression of the gluconeogenic gene, PEPCK, was measured using real-time qPCR and quantified relative to the housekeeping gene, GAPDH (for BWTG3) and 18S and β-actin (for HepG2). The response of insulin was normalized to the vehicle which was set to 1 and is represented as a dotted line. The response of the APPs used was normalized to insulin. Data shown represents two independent experiments. Statistical analysis comparing insulin to the vehicle (***$p<0.001$) and the time treatments relative to the insulin control was performed using one-way ANOVA with Tukey's Multiple Comparison's Test ($^{\#}p<0.05$, $^{\#\#}p<0.01$, $^{\#\#\#}p<0.001$).

3.6 Preliminary results show the effect of PAI-1, SAA and CRP on hepatic glucose production in BWTG3 & HepG2 cells

In order to correlate the observed effect of PAI-1, SAA, and CRP on the transcriptional regulation of G6Pase and PEPCK, with hepatic glucose production (HGP), a fluororimetric assay was utilized to measure the extracellular glucose concentrations in the medium of BWTG3 and HepG2 cells, pre-treated with 10ng/ml PAI-1, 10µg/ml SAA, and 4.5 µg/ml CRP for 48 hours. However, this assay needed to be setup and optimized in the research laboratory, which was done by the candidate (see Addendum B). As described in section 2.7, HGP was promoted in BWTG3 and HepG2 cells, by incubating the cells for 6 hours in medium (without glucose) containing gluconeogenic substrates, pyruvate and lactate. Preliminary results show that this 6 hour incubation induced the production of glucose as shown by the increase in extracellular glucose concentrations in the medium of the vehicle, previously lacking glucose, of BWTG3 and HepG2 cells (Table 3.1). Additionally, pre-treatment with the selected APPs had no significant effect on the ability of BWTG3 cells to synthesize *de novo* glucose, in comparison to the control (Table 3.1). In HepG2 cells, however, pre-treatment with 4.5 µg/ml CRP increased the extracellular glucose concentrations by 7.6-fold in comparison to the control (8.4- vs 1.1 µM) although significance could not be established. This was not observed in the presence of 10 ng/ml PAI-1 or 10 µg/ml SAA (Table 3.1).

Table 5.1 Extracellular glucose concentrations measured in the medium of cultured BWTG3 and HepG2 cells pre-treated with PAI-1, SAA and CRP for 48 hours.

Glucose concentrations (µM±SD; n=2)		
	BWTG3	**HepG2**
Vehicle	3.8 ± 1.8 µM	1.1 ± 0.9 µM
10 ng/ml PAI-1	4.0 ± 0.9 µM	1.6 ± 1.2 µM
10 µg/ml SAA*	3.4 µM*	1.2 µM*
4.5 µg/ml CRP	4.5 ± 0.7 µM	8.4 ± 3.2 µM

*SAA represents one biological repeat (n=1)

CHAPTER 4:

DISCUSSION & CONCLUSIONS

4.1 Introduction

T2D affects 451 million people worldwide (2, 4) and is the second most important cause of death in South African adults (8, 9). As insulin resistance is the main risk factor for the development of T2D, it is thus important to investigate the molecular mechanisms that contribute to an insulin-resistant state. Herein, the peripheral target tissues (including the liver, skeletal muscle, and adipose tissue) is unable to respond normally to the physiological concentrations of insulin, leading to deficient insulin action in these tissues (67, 71). Thus, blood glucose concentrations rise, as insulin is unable to inhibit HGP and increase glucose uptake in adipose tissue and skeletal muscle. This leads to the characteristic hyperglycemia observed in T2D, as well as the compensatory hyperinsulinemia (154–156). These aforementioned effects occur as a result of an imbalance between the activation of key proteins or nodes in the insulin signalling pathway, which include the IR, IRS proteins, and Akt, and the negative regulation of the pathway which involves mainly the phosphorylation of the IRS proteins at their Ser/Thr residues (68, 154).

It is well recognized that a chronic inflammatory state plays an important role in the development of insulin resistance (202, 203). Additionally, obesity, which is a known contributor to the development of insulin resistance, is described as a chronic inflammatory condition, therefore it is evident that chronic inflammation plays a role in the development of insulin resistance. A mechanism through which this may occur is *via* APPs, specifically PAI-1, SAA, and CRP as they are associated with chronic inflammation and are additionally used as biological markers for T2D (39, 206, 207). Although many human studies have shown that circulating levels of PAI-1, SAA, and CRP are elevated and also associated with T2D development (34, 35, 273, 36–38, 40, 41, 261, 268, 272), little research is available regarding the mechanism through which these APPs may contribute to the disease state. Additionally, as the liver plays an important role in the development of hyperglycemia and progression to T2D, an understanding of the molecular mechanism of hepatic insulin resistance, and how APPs may play a role in the development thereof, would be beneficial. Therefore, the main focus of this study was to elucidate whether PAI-1, SAA, and CRP could lead to the development of hepatic insulin resistance, specifically by inhibiting the activation of key nodes in the insulin signalling pathway. These include tyrosine phosphorylation and total expression of the IR and phosphorylation of Akt at both Thr308 and Ser473. Additionally, the role of these APPs in the negative regulation of the insulin signalling pathway was also investigated *via* the phosphorylation of IRS-2 at Ser731. The regulation of key gluconeogenic enzymes namely, PECK and G6Pase, responsible for HGP was also investigated to determine if the selected APPs affect further downstream targets of insulin.

4.2 Validating the experimental model of insulin stimulation

The activation of the insulin signalling pathway is initiated when insulin binds to its cognate receptor, the IR, resulting in the autophosphorylation of the receptor at its tyrosine residues (77, 80, 97, 332). An activated IR recruits IRS proteins, which become phosphorylated at their tyrosine residues and subsequently recruits PI3K. This eventually results in the activation of the central protein Akt *via* phosphorylation at both its Thr308 and Ser473 residue, by PDK-1 and mTORC2, respectively (Fig.3.1), resulting in full activation of the protein. Akt regulates glucose metabolism in the liver by regulating downstream targets, which include attenuating the transcription of key gluconeogenic enzymes, G6Pase and PEPCK, *via* the protein FoxO1. In contrast, phosphorylation of the IRS proteins at their serine residues inhibits the ability of the protein to bind to the IR thereby losing its ability to become activated and initiate further downstream signal transduction (149). Perturbations in the activation of IR, IRS, and Akt could lead to cells becoming resistant to insulin, which was of particular interest to this study, especially in regard to hepatic insulin resistance.

HepG2 cells, a well-known cell line, has previously been described as a suitable cell model to investigate hepatic insulin signalling (333). However, to the best of our knowledge, insulin signalling, and its modulation has never been investigated using the BWTG3 cell line. It is for this reason that we had to optimise and validate our experimental model. Firstly, we were able to show that culturing BWTG3 cells in the traditional culture medium, containing 25 mM glucose (6 times higher than what is observed in serum (261) can negatively influence insulin signalling (Fig.3.2) as described by others in the literature (172, 328, 329). Culturing the cells in 5 mM glucose was found to be the most optimal in regard to the insulin sensitivity of the cells (Fig 3.2). Additionally, it was established that using 100 ng/ml (~17 nM) insulin was sufficient for optimal activation of the insulin signalling pathway when compared to 500 ng/ml (~86 nM) insulin, which is similar to the 100 nM more commonly used in the literature (149, 260, 274, 287, 327) (Fig.3.2).

Activation of the insulin signalling pathway was induced in both cell lines albeit to different degrees. For example, phosphorylation of Akt at Thr308 was 7 times less responsive to insulin in BWTG3 cells compared to the HepG2 cell line (Table 4.1), whilst Ser473 phosphorylation of Akt was slightly more pronounced in the BWTG3 cells. This could suggest that PDK1, responsible for Akt phosphorylation at Thr308, is more active in HepG2 cells, whereas mTORC2, which causes phosphorylation of Akt at Ser473 might be more effective in the BWTG3 cell line (Fig.3.1). Furthermore, PEPCK mRNA levels were downregulated to a greater extent in BWTG3 cells compared to the HepG2 cell line upon insulin treatment for 30 minutes, most probably due to the more pronounced Ser473 phosphorylation of Akt in the murine hepatoma cells (Table 4.1). Although, a rapid decline in mRNA transcript levels of PEPCK has been previously documented (129, 334, 335), to the best of our knowledge a 10-fold decrease in PEPCK mRNA has not yet been reported. Surprisingly, insulin was not able to decrease G6Pase mRNA

levels in BWTG3 cells, which suggest that this effect may require a longer insulin treatment in order to observe a significant response, which has been previously shown in rat hepatoma cells treated for 4 hours with insulin (336).

Table 6.1. Summary table of the insulin-stimulated response on key proteins in the insulin signalling pathway observed in BWTG3 and HepG2 cells

Protein	BWTG3	HepG2
p-IR	8.6-fold	ND
Total IR	1.3-fold	1.3-fold
p-IRS-2 (Ser731)	—	—
pAkt (Thr308)	4.2-fold	31-fold
pAkt (Ser473)	81-fold	53-fold
Total Akt	1.7-fold	1.2-fold
G6Pase mRNA	—	ND
PEPCK mRNA	10-fold decrease	4-fold decrease

— No effect ND Not determined

In summary, we could establish an optimal treatment regime allowing us to investigate insulin signalling in liver cell models. Both BWTG3 and HepG2 cells were significantly responsive to insulin and allowed us to examine how APPs would affect insulin signalling.

4.3 Effects of APPs on hepatic insulin signalling

The insulin signalling pathway is a complex signalling cascade consisting of various nodes. These nodes affect each other as well as other signalling proteins and molecules. Disruption of any of these nodes could negatively affect downstream effects induced by insulin. Insulin resistance is defined as the disruption of peripheral insulin signalling (13) and the inhibition of Akt, a central node in the insulin signalling pathway, is described by many researchers as indicative of an insulin resistant state (128, 337), although many other downstream nodes exist, which include GSK, FoxO1, and mTORC1, that could be modulated to induce insulin resistance. Nonetheless, for the purpose of this study and to omit confusion insulin resistance induced by the APPs is presumed when activation of Akt is impaired. Thus, having established the experimental model system for optimal insulin signalling activation in the two liver cell lines: BWTG3 and HepG2, the next step involved investigating how APPs, specifically PAI-1, SAA, and CRP, influence critical nodes in the insulin signalling pathway. As previously mentioned, APPs are routinely used as biological markers for T2D diagnosis. Whether the APPs, of which increased

levels reflect a state of inflammation, play a role in the development of insulin resistance and subsequently T2D is not well defined in the literature, especially in regard to hepatic insulin resistance. Many believe increased APP levels is due to an already established insulin resistance state (67), and thus information on how these APPs affect the progression of insulin resistance is limited. This study aimed to add to the body of knowledge regarding the role that these biological markers of T2D play in establishing an insulin resistant state. In the previous chapter (Chapter 3) we show that the selected APPs differentially regulate various key nodes in the insulin signalling pathway, which correlates with the regulation of important gluconeogenic enzymes that could affect hepatic *de novo* glucose production. Here we will focus on how this conclusion was reached and how these results compare to the literature.

4.3.1 PAI-1 differentially affects hepatic insulin signalling in a dose- and time-dependent manner

PAI-1 is a strong predictor of T2D development as described by Festa and colleagues (34, 35). This APP is increased moderately during the APR, in response to inflammatory stimuli and is known to play a role in tissue remodelling as well as blood clot formation (213, 226). The role of PAI-1 in general biology ties into its association with various disease states, such as obesity and cardiovascular disease (234). For instance, it has been well established that PAI-1 plays a role in the development of obesity by modulating adipocyte differentiation (242–244), which may be facilitated by its ability to inhibit the degradation of extracellular matrix components (an important process during adipocyte differentiation). As obesity is a known contributor to the development of insulin resistance and T2D, it is therefore deemed important to investigate the role of PAI-1 in the development of insulin resistance. It has previously been established that elevated PAI-1 levels is a core feature of insulin resistance and numerous studies have linked PAI-1 to its development, as described in Chapter 1 (Table 1.4). For example, PAI-1 is associated with altered glucose metabolism and hyperglycemia in mice (173, 245, 246, 252, 254). However, little is known about how or if it contributes to the development of the disease state, in addition to the possible molecular mechanism involved.

A wide range of PAI-1 concentrations have been reported in healthy individuals as well as T2D patients. In healthy individuals, PAI-1 levels ranging between 9.4 ng/ml-34 ng/ml (34, 35, 235, 236, 251) have been reported, whilst PAI-1 levels of ±24 ng/ml have been described in T2D patients (34). Furthermore, mice fed a high-fat diet showed elevated PAI-1 levels of up to 6.92 ng/ml (252). Taking into consideration that both a mouse and human liver cell line was utilized in this study, a concentration range of 5, 10, and 20 ng/ml was chosen. In addition, we were also guided by the literature to use10 ng/ml PAI-1 as it has been used previously in an *in vitro* study investigating the effect of PAI-1 on Akt activation in endothelial cells (253). These concentrations may be representative of a typical

range found in circulation and could thus demonstrate the effects of PAI-1 levels in normal circulation on the insulin signalling pathway.

PAI-1 in the current study, was able to induce insulin resistance in both liver cell lines although to different extents. The murine liver cell line was more sensitive to PAI-1-induced inhibition of the insulin signalling pathway (Table 4.2 & 4.3), although the highest concentration used (20 ng/ml) potentiated insulin-induced phosphorylation of Akt at Ser473, probably as a result of the increase in IR phosphorylation observed at this concentration (Fig.3.5A). The HepG2 cell line was less sensitive to PAI-1, with only 20 ng/ml, the highest concentration used, able to attenuate insulin signalling at 24 hours. Similarly, Tamura *et al*., (254) reported decreased phosphorylation of Akt at Ser473 by PAI-1 in HepG2 cells at 24 hours using 860 ng/ml PAI-1, 43 times more concentrated than what was used in the current study, suggesting that this cell line is less responsive to PAI-1. Nonetheless, the degree of Akt attenuation by PAI-1 increased over time (Table 4.4), reaching maximum inhibition at 48 hours in both liver cell lines (Fig.3.15B & E & Table 4.4). Indeed, treatment with 10 ng/ml PAI-1 for 48 hours attenuated all markers investigated, in BWTG3 cells (Table 4.5). However, Akt phosphorylation at Thr308 was not much affected by longer PAI-1 exposure in HepG2 cells (Fig.3.15), suggesting that PAI-1 might target Akt Ser473 specific phosphatases like PHLPP (see Chapter 1), thus preventing Akt from becoming fully activated. Future studies could investigate whether PAI-1 affects the protein levels and activity of Akt Ser473 phosphatases. Nonetheless, the inhibition of Akt by PAI-1 correlates with the increase in mRNA levels of the gluconeogenic enzymes, G6Pase and PEPCK in response to PAI-1 treatment (Table.4.4), as shown by Tamura and colleagues (254). It is therefore surprising that in this study PAI-1 was not able to induce HGP in both liver cell lines used (Table 3.1). However, the increase in glucose production was consistently higher than the control, albeit very small, which might indicate that longer exposure to PAI-1 could significantly affect HGP as suggested by the late attenuation of insulin-induced repression of PEPCK mRNA expression by PAI-1 in both liver cells used (Fig. 3.17). And although PAI-1 could not affect HGP, possibly due to the length of PAI-1 exposure, these results suggest that PAI-1 could influence the development of hepatic insulin resistance by disrupting the insulin signalling pathway.

4.3.2 SAA differentially affects hepatic insulin signalling in a concentration- and cell-line-dependent manner

SAA is a major APP that is increased rapidly in response to inflammation during the APR, and is thus a sensitive marker of inflammation (217, 219). Additionally, this protein is also a biological marker of T2D as well as a marker of obesity, like PAI-1. Indeed, SAA was reported to play a role in the development of obesity by modulating adipocyte differentiation (260, 269). It has also been questioned whether SAA may link the APR to obesity and insulin resistance (269). The role of SAA in the development of insulin resistance in adipocytes has been described, although little is known about the

effect of SAA on the development of hepatic insulin resistance (Chapter 1, Table 1.5). SAA has been shown to decrease GLUT4 mRNA expression in 3T3-L1 adipocytes (263, 274) and chronic exposure to 5-20 µg/ml SAA decreased glucose uptake in these cells (260, 274). Physiological levels as well as the concentrations used in previous *in vitro* studies was considered when choosing the SAA concentrations used in this study. The normal physiological levels of SAA range between 1-5 µg/ml, and elevated levels range between 2.1-24 µg/ml in obese and T2D individuals (37, 38, 263, 267, 268, 272, 273). Additionally, taking into consideration that previous *in vitro* studies utilized SAA concentrations ranging between 1-30 µg/ml (260, 269, 271, 274), concentrations of 5, 10 and 20 µg/ml was decided upon.

The results in this study showed that SAA was able to decrease the activation of the insulin signalling pathway in both murine and human liver cell models, however this effect was variable and dependent on the node investigated in the insulin signalling pathway (Table 4.2 & 4.3). The phosphorylation of Akt at either Thr308 or Ser473 generally coincides with the inhibition of either the IR or IRS, suggesting that the decrease in Akt could be attributed to the modulation of upstream signalling proteins. This modulation entails either decreasing total protein levels or inhibiting its activation. For example, in BWTG3 cells, decreased Akt phosphorylation at Ser473 by 20 µg/ml SAA correlates with increased IRS-2 phosphorylation at Ser731 indicative of its deactivation even though an increase in IR activation (phosphorylation at Tyr1150 &1151) was observed (Table 4.2).

Unfortunately, 10 µg/ml SAA was unable to attenuate insulin signalling over time (Table 4.4) in both cell lines used, in contrast to the dose response experiment in which the cells were exposed to SAA for 24 hours. G6Pase mRNA expression did however increase in response to 48 hours SAA treatment, whilst the repression of PEPCK mRNA levels by insulin was attenuated at 2 hours only. The variability of the SAA time course, however, brings into question its reliability. Because the time course experiments were performed after the dose response studies, we speculate that the stock SAA used might have degraded and became less effective over time, even when kept stored in aliquots at -20°C. The degraded SAA could also have affected HGP as SAA was unable to stimulate *de novo* glucose production (Table 3.1). Further experiments using freshly prepared SAA will be required to validate this hypothesis.

Nonetheless, the dose response experiments did establish that SAA has the ability to induce hepatic insulin resistance (Table 4.2 & 4.3). This is the first study, to the best of our knowledge, to investigate the effect of SAA on hepatic insulin signalling, as well as on the activation of the IR and Akt. Previous studies have shown that SAA decreased the mRNA expression (271) as well as tyrosine phosphorylation of IRS-1 (274) in 3T3-L1 adipocytes. In addition, Ye *et al*., has shown in 3T3-L1 adipocytes that treatment with 20 µg/ml SAA for 48 hours increased the phosphorylation and thus activation of JNK, a protein kinase known to induce serine phosphorylation of IRS-1 (274). JNK activation might explain

the increase in IRS-2 phosphorylation at Ser731 in the BWTG3 cells treated with 20 µg/ml SAA (Fig 3.7B & Table 4.2). Future studies should include the effect of SAA on JNK activation in addition to other MAPKs. We could conclude from these results that SAA modulates insulin signalling in liver cell models, which might influence the development of hepatic insulin resistance and that caution should be exercised when working with SAA as it appears to degrade in solution over time.

Table 4.2. Summary table of the effect of a 24-hour treatment with PAI-1, SAA, CRP on insulin-stimulated activation of key proteins in the pathway in BWTG3 cells (Data from Figs 3.5, 3.7, 3.9 & 3.10).

BWTG3								
	PAI-1			SAA			CRP	
	5 ng/ml	10 ng/ml	20 ng/ml	5 µg/ml	10 µg/ml	20 µg/ml	2.5 µg/ml	4.5 µg/ml
p-IR	↓	—	↑	↓	—	↑	↓	↓
Total IR	—	—	—	↓	↓	↓	—	—
p-IRS2 (Ser731)	↓	—	—	—	—	↑	↓	↓
p-Akt (Thr308)	↓	↓	↓	—	—	—	—	↓
p-Akt (Ser473)	↓	—	↑	↓	↓	↓	—	—
Total Akt	—	—	—	↓	—	↑	↓	↑

↓ Significant decrease ↑ Significant increase — No significant effect

Table 4.3. Summary table of the effect of a 24-hour treatment with PAI-1, SAA, CRP on insulin-stimulated activation of key proteins in the pathway in HepG2 cells (Data from Figs 3.6, 3.8, 3.11 & 3.12).

HepG2								
	PAI-1			SAA			CRP	
	5 ng/ml	10 ng/ml	20 ng/ml	5 µg/ml	10 µg/ml	20 µg/ml	2.5 µg/ml	4.5 µg/ml
Total IR	↑	↑	↑	↑	↓	↓	↓	↓
p-IRS2 (Ser731)	↑	—	—	—	↓	↓	↓	↓
p-Akt (Thr308)	—	—	↓	↓	↓	↓	↓	↓
p-Akt (Ser473)	—	—	↓	↓	↓	—	↓	↓
Total Akt	—	—	↑	↓	—	—	—	—

↓ Significant decrease ↑ Significant increase — No significant effect

4.3.3 CRP is the most effective APP in inhibiting hepatic insulin signalling

CRP, a major APP, is increased rapidly in response to inflammatory stimuli during the APR. It is a sensitive marker of inflammation as well as an indicator for T2D (39, 338) with the progression to T2D connected to increased CRP levels. The increased levels of CRP observed in T2D patients (34, 36, 39–41, 268, 273), played a role in the experimental design of this study. The serum concentrations of CRP reported in patients with T2D varies, with levels ranging from 2.4 µg/ml-6.1 µg/ml (34, 36, 39, 41, 268, 273). CRP levels between 2 and 10 µg/ml are also seen in metabolic inflammatory states (219), thus concentrations in this range was considered suitable for this investigation. It should however be noted, that these concentrations indicate a median range and thus does not reflect true concentrations observed in these disease states. Nonetheless, concentrations of 2.5 and 4.5 µg/ml CRP was chosen in this investigation to determine whether CRP could contribute to the development of insulin resistance in two liver cell lines.

CRP is shown to significantly inhibit the insulin signalling pathway in this study, by mainly affecting both the IR and Akt in both murine and human liver cell models. Generally, CRP acted similarly in both cell lines used with some differences observed. In BWTG3 cells, treatment with both concentrations of CRP for 24 hours, decreased the insulin-induced phosphorylation of the IR at Tyr1150 & 1151, while having no effect on the total IR levels as well as the Ser473 phosphorylation of Akt (Table 4.2). Only, 4.5 µg/ml CRP decreased the Thr308 phosphorylation of Akt, while increasing the total Akt levels (Table 4.2). In HepG2 cells, both concentrations of CRP decreased the insulin-induced activation of all of the nodes investigated which include, total IR expression as well as phosphorylation of Akt at both Thr308 and Ser473, while having no effect on total Akt levels (Table 4.3). The decrease in Akt phosphorylation could be attributed to the decrease in the upstream activation of the IR as observed in BWTG3 cells or the decrease in total IR expression as shown in HepG2 cells (Table 4.2 & 4.3). Although demonstrating slight species specific differences, these results are in agreement with a report by Xi *et al.*, (289) who concluded that CRP plays a significant role in the development of hepatic insulin resistance both *in vivo* (in rats) and *in vitro* (in primary cultured rat hepatocytes). However the authors only observed a decrease in Akt phosphorylation at Ser473 in response to CRP, while Thr308 was unaffected as well as total Akt levels (289), which is in contrast to the results observed in the current study (Table 4.2 and 4.3). These authors did however treat with a higher concentration of CRP (30 µg/ml) for a shorter period (150 minutes), which may explain the differences observed between studies. Furthermore, CRP was also shown to decrease the phosphorylation of Akt at both residues in rat skeletal muscle cells and bovine aortic endothelial cells (287, 288), which is in agreement with the results observed in the current study and suggests that the effect by CRP on the insulin signalling pathway is not tissue specific.

As previously mentioned, IRS phosphorylation at its serine residues is believed to inactivate this adaptor protein, disrupting any further downstream signal including the activation of Akt. And although CRP was able to inhibit insulin-induced phosphorylation of Akt, both concentrations of CRP decreased the phosphorylation of IRS-2 at Ser731 in both liver cell lines, which is surprising as CRP has been shown to induce the phosphorylation and thus activation of, JNK and ERK1/2 (287–289). These kinase proteins are known to induce the serine phosphorylation of the IRS proteins (144, 148). Previous studies have also reported that CRP increased the phosphorylation of IRS-1 at Ser307 and Ser612 in L6 myotubes (rat skeletal muscle) (287), primary cultured rat hepatocytes (289), and bovine aortic endothelial cells (288). However, it could be postulated that the observed decrease in the Ser731 phosphorylation of IRS-2 may be due to a decrease in total IRS-2 expression. This could however not be confirmed at protein level, due to difficulty experienced with the commercially available antibody, but qPCR analysis revealed that, over time, in both BWTG3 and HepG2 cells, IRS-2 mRNA levels increased in response to CRP treatment (Addendum A, Fig.A5). And although CRP was unable to deactivate IRS-2, it appears not to have affected the ability of CRP to inhibit Akt phosphorylation (Table 4.2 & 4.3).

The inflammatory state associated with insulin resistance and T2D is considered to be chronic. For this reason, we wanted to investigate how longer exposure to the APPs affect the ability of the liver cell models to become insulin resistant. “Acute” exposure was considered to be 2 hours treatment, whilst 48 hours were considered “chronic”. The ability of CRP to attenuate the insulin signalling pathway is shown to be time-dependent as pro-longed (chronic) exposure to CRP decreased the insulin-induced activation of all the nodes investigated as well as their total protein levels in both BWTG3 cells, specifically, and Akt in HepG2 cells (Table 4.4 and 4.5). The decrease in insulin-induced phosphorylation of Akt at both residues observed in BWTG3 cells in response to chronic CRP treatment may be due to the 53% decrease in total Akt levels in addition to a significant decrease in total IR (Table 4.5). However, at 2 hours treatment with CRP in HepG2 cells, decreased Akt phosphorylation at Thr308 was already observed, which only became more pronounced over time (Fig.3.15D). The decrease in Akt phosphorylation at Thr308 in HepG2 cells was subsequently followed by a decrease in Ser473 Akt phosphorylation although no significant effect on total IR and Ser731 IRS-2 phosphorylation was observed (Table 4.4). This would suggest that Akt inhibition in the HepG2 cells does not involve these upstream signalling proteins. Directly upstream from Akt is PI3K, which might be inhibited by CRP resulting in decreased Akt activation as total Akt levels were unaffected by CRP in HepG2 cells (Fig.3.15F & Table 4.5). In addition, CRP might affect PTEN or SHIP2, phosphatases responsible for converting PIP_3 to its precursor PIP_2 thereby antagonising PI3K signalling and subsequently Akt activation (64, 82) in HepG2 cells. Furthermore, phosphatases which directly affects Akt phosphorylation, such as PHLPP and PP2A, could be influenced by CRP. Future studies should include PI3K and the phosphatases affecting Akt activation as possible CRP targets.

This attenuation of the insulin signalling pathway culminated in the increase in PEPCK mRNA levels (Fig.3.17E & F). In addition to increasing PEPCK mRNA levels in both BWTG3 and HepG2 cells (Table 4.4 & 4.5), pro-longed exposure to CRP also increased G6Pase mRNA expression in the BWTG3 cell line. Although chronic exposure to CRP increased PEPCK mRNA levels to a greater extent in BWTG3 vs HepG2 cells (Table 4.5), an increase in HGP was only observed in HepG2 cells (Table 3.1). Further HGP experiments, however, need to be conducted due to the assay not being fully optimised due to time constraints. In summary, chronic exposure to CRP induced hepatic insulin resistance in both BWTG3 and HepG2 cells, by causing an overall decrease in the ability of insulin to activate key proteins in the insulin signalling pathway, such as the IR and Akt, which correlates with the ability of CRP to upregulate G6Pase mRNA levels and attenuate insulin induced inhibition of PEPCK (Fig.3.16 & 3.17).

Of all the APPs examined, CRP was the most effective in attenuating insulin signalling over time as summarised in Table 4.5 in the liver cell models. This strengthens the findings by the Women's Healthy Study (40), which associated increased CRP levels in healthy women with the development of future T2D. In addition, this highlights the role of CRP as beyond that of just biological marker for T2D, but also as a possible causative agent of the disease.

Table 4.4. Summary of the overall effects of PAI-1, SAA and CRP over time on insulin-stimulated activation of key proteins in the insulin signalling pathway as well as downstream regulation of G6Pase and PEPCK mRNA, in BWTG3 and HepG2 cells (Data from Figs 3.13, 3.14 & 3.15).

	BWTG3									HepG2								
	10 ng/ml PAI-1			10 µg/ml SAA			4.5 µg/ml CRP			10 ng/ml PAI-1			10 µg/ml SAA			4.5 µg/ml CRP		
	2hr	24hr	48hr	2hr	24hr	48hr	2hr	24hr	48hr	2hr	24hr	48hr	2hr	24hr	48hr	2hr	24hr	48hr
p-IR	—	—	↓	—	↑	—	—	↓	↓	ND	ND	ND	ND	ND	ND	ND	ND	ND
Total IR	—	—	↓	—	—	—	—	↓	↓	—	↑	—	—	—	—	—	—	—
p-IRS2 (Ser731)	↓	↓	↓	—	—	—	—	↓	↓	—	—	—	—	—	—	—	—	—
p-Akt (Thr308)	—	↓	↓	—	—	—	↓	↓	↓	—	—	—	↓	↓	—	↓	↓	↓
p-Akt (Ser473)	—	—	↓	—	—	—	—	—	↓	—	—	↓	—	—	—	—	↓	↓
Total Akt	—	—	↓	—	—	↓	—	—	↓	—	—	—	—	—	—	—	—	—
G6Pase mRNA	↑	↑	↑	—	—	↑	—	—	↑	ND	ND	ND	ND	ND	ND	ND	ND	ND
PEPCK mRNA	—	—	↑	↑	—	—	—	—	↑	—	↑	—	—	—	—	↑	↑	↑

↓ Significant decrease ↑ Significant increase — No significant effect ND Not determined

Table 4.7. Maximal percentage inhibition or fold-increase observed at 48 hours in BWTG3 and HepG2 cells

	10 ng/ml PAI-1		10 µg/ml SAA		4.5 µg/ml CRP	
	BWTG3	HepG2	BWTG3	HepG2	BWTG3	HepG2
p-IR	55%	ND	1.4-fold	ND	72%	ND
Total IR	71%	46%	18%	—	63%	57%
p-IRS2 (Ser731)	25%	—	—	29%	59%	14%
p-Akt (Thr308)	41%	—	—	—	59%	58%
p-Akt (Ser473)	64%	25%	—	—	54%	40%
Total Akt	53%	—	56%	—	53%	—
G6Pase mRNA	3-fold	ND	3.5-fold	ND	4.8-fold	ND
PEPCK mRNA	12.8-fold	1.6-fold	—	—	225-fold	3-fold

— No effect ND Not determined

4.4 Conclusions and Future work

To conclude, all three APPs investigated affected insulin signalling albeit to different degrees depending on the dose and length of exposure (Tables 4.2, 4.3 & 4.4) in the liver cell models. Generally longer exposure to the APPs appeared to be most effective in establishing hepatic insulin resistance except for SAA (Table 4.4). The modulating effect of the APPs on critical nodes of the insulin signalling pathway corresponds to the ability of the APPs to increase G6Pase mRNA levels and inhibit insulin-induced repression of PEPCK mRNA. These results imply that PAI-1, SAA, and CRP are capable of establishing an insulin resistant state affecting HGP that could result in hyperglycaemia, a characteristic of T2D. Thus, our hypothesis that PAI-1, SAA and CRP negatively affect the insulin signalling pathway, leading to deficient insulin action is accepted. To the best of our knowledge, this study is the first to show the direct effects of PAI-1, SAA and CRP on the activation of the insulin signalling pathway in hepatoma cell lines, thus establishing their role in the development of hepatic insulin resistance. Additionally, this study highlights the differences between these APPs in terms of their inhibitory effects on hepatic insulin signalling.

In order to improve our understanding of the role of PAI-1, SAA and CRP in the development of hepatic insulin resistance, this study can be extended to investigating the possible mechanisms of the observed effects of these APPs on the insulin signalling pathway. This includes components of the MAPK

pathway, such as JNK and ERK1/2, which is known to induce the serine phosphorylation of the IRS proteins (64, 82, 118, 144, 148). As well as tyrosine phosphatases such as PTP1B, which is an essential component inhibiting the insulin receptor (82, 131). Furthermore, investigating the effects of PAI-1, SAA and CRP on PDK-1 and mTORC2 can provide insight into the regulation of Akt activation at Thr308 and Ser473 by these APPs as observed in Chapter 3. Finally, as the insulin-induced suppression of gluconeogenesis is mediated by the transcription factor FoxO1, future studies could aim to investigate the effect of PAI-1, SAA and CRP on the phosphorylation, and thus inhibition, of FoxO1, which could provide context to the observed attenuation of insulin's inhibition of G6Pase and PEPCK.

Factors influencing APP levels such as obesity, inflammation, and stress are known to cause insulin resistance and the development of T2D (22, 23, 179, 180, 185, 186, 194, 204, 205, 24, 25, 167, 170–172, 175, 176). This study raises the question of whether these physiological conditions affect insulin signalling *via* the production of APPs such as PAI-1, SAA, and CRP. It would explain why pro-inflammatory cytokines and GCs, known antagonists of each other's activity, are associated with insulin resistance as they have been reported to co-operatively upregulate APP expression (26, 28–33). Future work should thus entail linking pro-inflammatory cytokines- and GC-induced insulin resistance to the APPs, providing insight into a possible novel mechanism explaining the development of this disease in response to obesity, inflammation, and stress.

REFERENCES

1. Alberti KGM., Zimmet P. 1998. Definition, diagnosis and classification of diabetes mellitus and its complications. Part 1: Diagnosis and classification of diabetes mellitus. Provisional report of a WHO consultation. Diabet Med 15:539–553.

2. Chatterjee S, Khunti K, Davies MJ. 2017. Type 2 diabetes. Lancet.

3. Guthrie RA, Guthrie DW. 2004. Pathophysiology of diabetes mellitus. Crit Care Nurs Q 27:113-125.

4. Zheng Y, Ley SH, Hu FB. 2018. Global aetiology and epidemiology of type 2 diabetes mellitus and its complications. Nat Rev Endocrinol 14:88–98.

5. Abdul-Ghani MA, DeFronzo RA. 2009. Plasma glucose concentration and prediction of future risk of type 2 diabetes. Diabetes Care 32:S194–S198.

6. Chein L, Magliano DJ, Zimmet P. 2012. The worldwide epidemiology of type 2 diabetes mellitus - present and future perspectives. Nature 8:228–236.

7. IDF Diabetes AtlasIDF Diabetes Atlas, 2017, 8th edition.

8. Mayosi BM, Flisher AJ, Lalloo UG, Sitas F, Tollman SM, Bradshaw D. 2009. The burden of non-communicable diseases in South Africa. Lancet 374:934–947.

9. Pheiffer C, Pillay-Van Wyk V, Joubert JD, Levitt N, Nglazi MD, Bradshaw D. 2018. The prevalence of type 2 diabetes in South Africa: A systematic review protocol. BMJ Open 8:1–4.

10. Lingala SM, Ghany MGMMhs. 2016. Molecular phathophysiology of hepatic glucose production. Mol Asp Med 25:289–313.

11. Rines AK, Sharabi K, Tavares CDJ, Puigserver P. 2016. Targeting hepatic glucose metabolism in the treatment of type 2 diabetes. Nat Rev Drug Discov 15:786–804.

12. Wilcox G. 2005. Insulin and Insulin Resistance. Clin Biochem 26:19–39.

13. Hunter SJ, Garvey WT. 1998. Insulin Action and Insulin Resistance: Diseases Involving Defects in Insulin Receptors, Signal Transduction, and the Glucose Transport Effector System. Am J Med 105:331–345.

14. Bazotte RB, Silva LG, Schiavon FPM. 2014. Insulin resistance in the liver: Deficiency or excess of insulin? Cell Cycle 13:2494–2500.

15. Kraegen EW, Clark PW, Jenkins AB, Daley EA, Chisholm DJ, Storlien LH. 1991. Development of muscle insulin resistance after liver insulin resistance in high-fat-fed rats. Diabetes 40:1397–1403.

16. Patel BM, Goyal RK. 2019. Liver and insulin resistance: New wine in old bottle!!! Eur J Pharmacol 862:1–14.

17. Miranda PJ, DeFronzo RA, Califf RM, Guyton JR. 2005. Metabolic syndrome: Definition, pathophysiology, and mechanisms. Am Heart J 149:33–45.

18. Bandt C. 2005. Inflammation, stress and diabetes. J Clin Invest 115:1111–1119.

19. Qatanani M, A. Lazar M. 2010. Mechansims of obesity-associated insulin resistance: many choice on the menu. Genes Dev 36:490–499.

20. Greevenbroek MMJ Van, Schalkwijk CG, Stehouwer CDA. 2013. Obesity-associated low-grade inflammation. J Med 71:174–187.

21. Tanti JF, Ceppo F, Jager J, Berthou F. 2013. Implication of inflammatory signaling pathways in obesity-induced insulin resistance. Front Endocrinol (Lausanne) 3:1–15.

22. Senn JJ, Klover PJ, Nowak IA, Mooney RA. 2002. Interleukin-6 induces cellular insulin resistance in hepatocytes. Diabetes 51:3391–3399.

23. Kanety H, Feinstein R, Papa MZ, Hemi R, Karasik A. 1995. Tumor Necrosis Factor α-induced Phosphorylation of Insulin Receptor Substrate-1 (IRS-1). J Biol Chem 270:23780–23784.

24. Feinstein R, Kanety H, Papa MZ, Lunenfeld B, Karasik A. 1993. Tumor necrosis factor-α suppresses insulin-induced tyrosine phosphorylation of insulin receptor and its substrates. J Biol Chem 268:26055–26058.

25. Hotamisligil GS, Peraldi P, Budavari A, Ellis R, Morris F, Hotamisligil GS, Peraldi P, Budavari A, Ellis R, White MF, Spiegelmant BM. 1996. IRS-1-Mediated Inhibition of Insulin Receptor Tyrosine Kinase Activity in TNF-α-and Obesity-Induced Insulin Resistance. Science 271:665–668.

26. Ganapathi MK, Rzewnicki D, Samols D, Jiang SL, Kushner I. 1991. Effect of combinations of cytokines and hormones on synthesis of serum amyloid A and C-reactive protein in Hep 3B cells. J Immunol 147:1261–5.

27. Thorn CF, Whitehead AS. 2002. Differential Glucocorticoid Enhancement of the Cytokine-Driven Transcriptional Activation of the Human Acute Phase Serum Amyloid A Genes, SAA1 and SAA2. J Immunol 169:399–406.

28. Thorn CF, Lu ZY, Whitehead AS. 2004. Regulation of the Human Acute Phase Serum Amyloid A Genes by Tumour Necrosis Factor-α, Interleukin-6 and Glucocorticoids in Hepatic and Epithelial Cell Lines. Scand J Immunol 59:152–158.

29. Depraetere S, Willems J, Joniau M. 1991. Stimulation of CRP secretion in HepG2 cells: Cooperative effect of dexamethasone and interleukin 6. Agents Actions 34:369–375.

30. Sommer G, Weise S, Kralisch S, Scherer PE, Lössner U, Blüher M, Stumvoll M, Fasshauer M. 2008. The adipokine SAA3 is induced by interleukin-1β in mouse adipocytes. J Cell Biochem 104:2241–2247.

31. Thorn CF, Lu ZY, Whitehead AS. 2003. Tissue-specific regulation of the human acute-phase serum amyloid A genes, SAA1 and SAA2, by glucocorticoids in hepatic and epithelial cells. Eur J Immunol 33:2630–2639.

32. Smith JW, McDonald TL. 2008. Production of serum amyloid A and C-reactive protein by HepG2 cells stimulated with combinations of cytokines or monocyte conditioned media: the effects of prednisolone. Clin Exp Immunol 90:293–299.

33. Kimura H, Li X, Torii K, Okada T, Kamiyama K, Mikami D, Takahashi N, Yoshida H. 2009. Dexamethasone enhances basal and TNF-α-stimulated production of PAI-1 via the glucocorticoid receptor regardless of 11β-hydroxysteroid dehydrogenase 2 status in human proximal renal tubular cells. Nephrol Dial Transplant 24:1759–1765.

34. Festa A, Agostino RD, Tracy RP, Haffner SM. 2002. Elevated Levels of Acute-Phase Proteins and Plasminogen Activator Inhibitor-1 Predict the Development of Type-2 Diabetes: The Insulin Resistance Atherosclerosis Study. Diabetes 51:1131–7.

35. Festa A, Williams K, Tracy RP, Wagenknecht LE, Haffner SM. 2006. Progression of

Plasminogen Activator Inhibitor-1 and Fibrinogen Levels in Relation to Incident Type 2 Diabetes. Circulation 113:1753–1759.

36. Müller S, Martin S, Koenig W, Hanifi-Moghaddam P, Rathmann W, Haastert B, Giani G, Illig T, Thorand B, Kolb H. 2002. Impaired glucose tolerance is associated with increased serum concentrations of interleukin 6 and co-regulated acute-phase proteins but not TNF-alpha or its receptors. Diabetologia 45:805–812.

37. Marzi C, Huth C, Herder C, Baumert J, Thorand B, Rathmann W, Meisigner C, Wichmann H, Roden M, Peters M, Grallert H, Koenig W, Illig T. 2013. Acute-Phase Serum Amyloid A Protein and Its Implication in the Development of Type-2 Diabetes in the KORA S4/F4 Study. Diabetes Care 36:1321–1326.

38. Leinonen E, Hurt-Camejo E, Wiklund O, Hultén LM, Hiukka A, Taskinen MR. 2003. Insulin resistance and adiposity correlate with acute-phase reaction and soluble cell adhesion molecules in type 2 diabetes. Atherosclerosis 166:387–394.

39. Festa A, D'Agostino R, Howard G, Mykkänen L, Tracy RP, Haffner SM. 2000. Chronic subclinical inflammation as part of the insulin resistance syndrome: The insulin resistance atherosclerosis study (IRAS). Circulation 102:42–47.

40. Pradhan AD, Manson JE, Rifai N, Buring JE, Ridker PM. 2001. C-reactive protein, interleukin 6, and risk of developing type 2 diabetes mellitus. JAMA 286:327–34.

41. Barzilay JI, Abraham L, Heckbert SR, Cushman M, Kuller LH, Resnick HE, Tracy RP. 2001. The Relation of Markers of Inflammation to the Development of Glucose Disorders in the Elderly. Diabetes 50:2384–9.

42. Titchenell PM, Chu Q, Monks BR, Birnbaum MJ. 2015. Hepatic insulin signalling is dispensable for suppression of glucose output by insulin in vivo. Nat Commun 6:1–9.

43. Liangyou R. 2016. Energy metabolism in the liver. Compr Physiol 25:289–313.

44. Hatting M, Tavares CDJ, Sharabi K, Rines AK, Puigserver P. 2018. Insulin regulation of gluconeogenesis. Ann N Y Acad Sci 1411:21–35.

45. Zhang X, Yang S, Chen J, Su Z. 2019. Unraveling the regulation of hepatic gluconeogenesis. Front Endocrinol (Lausanne) 10:1–17.

46. Jitrapakdee S. 2012. Transcription factors and coactivators controlling nutrient and hormonal regulation of hepatic gluconeogenesis. Int J Biochem Cell Biol 44(1): 33-45

47. Lin H V., Accili D. 2011. Hormonal regulation of hepatic glucose production in health and disease. Cell Metab 14:9–19.

48. Beck-Nielsen H, Hother-Nielsen O, Staehr P. 2002. Is hepatic glucose production increased in type 2 diabetes mellitus? Curr Diab Rep 2:231–236.

49. Barthel A, Schmoll D. 2003. Novel concepts in insulin regulation of hepatic gluconeogenesis. Am J Physiol Metab 285:E685–E692.

50. Rines AK, Sharabi K, Tavares CDJ, Puigserver P, Medical H. 2016. Targeting hepatic glucose output in the treatment of type 2 diabetes. Nat Rev Drug Discov 15:786–804.

51. Valenti L, Rametta R, Dongiovanni P, Maggioni M, Fracanzani AL, Zappa M, Lattuada E, Roviaro G, Fargion S. 2008. Increased expression and activity of the transcription factor FOXO1 in nonalcoholic steatohepatitis. Diabetes 57:1355–1362.

52. Schmoll D, Walker KS, Alessi DR, Grempler R, Burchell A, Guo S, Walther R, Unterman TG. 2000. Regulation of glucose-6-phosphatase gene expression by protein kinase Bα and the Forkhead transcription factor FKHR: Evidence for insulin response unit-dependent and -independent effects of insulin on promoter activity. J Biol Chem 275:36324–36333.

53. Titchenell PM, Lazar MA, Birnbaum MJ. 2017. Unraveling the Regulation of Hepatic Metabolism by Insulin. Trends Endocrinol Metab 28:497–505.

54. O-sullivan I, Zhang W, Wasserman DH, Liew CW, Liu J, Paik J, Depinho RA, Stolz DB, Kahn CR, Schwartz MW, Unterman TG. 2015. FoxO1 integrates direct and indirect effects of insulin on hepatic glucose production and glucose utilization. Nat Commun 6:1–12.

55. Edgerton DS, Chu CA, Cherrington AD, Edgerton DS, Lautz M, Scott M, Everett CA, Stettler KM, Neal DW, Chu CA, Cherrington AD. 2006. Insulin's direct effects on the liver dominate the control of hepatic glucose production. J Clin Invest 116:521–527.

56. Edgerton DS, Ramnanan CJ, Grueter CA, Johnson KMS, Lautz M, Neal DW, Williams PE, Cherrington AD. 2009. Effects of insulin on the metabolic control of hepatic gluconeogenesis in vivo. Diabetes 58:2766–2775.

57. Girard J. 2006. Insulin's effect on the liver: "Direct or indirect?" continues to be the question. J Clin Invest 116:302–304.

58. Girard J. 2006. The inhibitory effects of insulin on hepatic glucose production are both direct and indirect. Diabetes 55:23–25.

59. Adkins A, Basu R, Persson M, Dicke B, Shah P, Vella A, Schwenk WF, Rizza RA. 2003. Higher insulin concentrations are required to suppress gluconeogenesis than glycogenolysis in nondiabetic humans. Diabetes 52:2213–2220.

60. Gastaldelli A, Toschi E, Pettiti M, Frascerra S, Quin A, Sironi AM, Natali A, Ferrannini E. 2001. Effect of Physiological Hyperinsulinemia on Gluconeogenesis in Nondiabetic Subjects and in Type 2 Diabetic Patients. Diabetes 50:1807–1812.

61. Magnusson I, Rothman DL, Katz LD, Shulman RG, I GS. 1992. Increased Rate of Gluconeogenesis in Type 11 Diabetes Mellitus: A 13C Nuclear Magnetic Resonance Study. J Clin Invest 90:1323–1327.

62. Gerich JE, Nurjhan N. 1993. Gluconeogenesis in Type-2 diabetes. New concepts in Pathogenesis of NIDDM 253–258.

63. Banting, F. G & Best CH. 1922. Pancreatic Extracts in the Treatment of Diabetes Mellitus. Can Med Assoc J. 141-146

64. Haeusler RA, McGraw TE, Accili D. 2018. Metabolic Signalling: Biochemical and cellular properties of insulin receptor signalling. Nat Rev Mol Cell Biol 19:31–44.

65. Meyts P De. 2004. Insulin and its receptor : structure , function and evolution. BioEssays 26:1351–1362.

66. Fu, Z., Gilbert, E. R., Liu D. 2014. Regulation of insulin synthesis and secretion and pancreatic beta-cell dysfunction in diabetes. Curr Diab Rep 9:25–53.

67. Meshkani R, Adeli K. 2009. Mechanisms linking the metabolic syndrome and cardiovascular disease: Role of hepatic insulin resistance. J Tehran Univ Hear Cent 4:77–84.

68. Petersen MC, Shulman GI. 2018. Mechanisms of Insulin Action and Insulin Resistance. Physiol Rev 98:2133–2223.

69. Bozza EA. 1976. Insulin signalling and the regulation of glucose transport. Mol Med 104:497–502.

70. Di Camillo B, Carlon A, Eduati F, Toffolo GM. 2016. A rule-based model of insulin signalling pathway. BMC Syst Biol 10:1–13.

71. Saltiel AR, Kahn CR. 2001. Insulin signalling and the regulation of glucose and lipid metabolism. Nature 414:799–806.

72. Ormazabal V, Nair S, Elfeky O, Aguayo C, Salomon C, Zuñiga FA. 2018. Association between insulin resistance and the development of cardiovascular disease. Cardiovasc Diabetol 17:1–14.

73. DeFronzo RA, Tripathy D. 2009. Skeletal muscle insulin resistance is the primary defect in type 2 diabetes. Diabetes Care 32: 157-163

74. Choi SM, Tucker DF, Gross DN, Easton RM, DiPilato LM, Dean AS, Monks BR, Birnbaum MJ. 2010. Insulin Regulates Adipocyte Lipolysis via an Akt-Independent Signaling Pathway. Mol Cell Biol 30:5009–5020.

75. Freychet P, Roth J, Neville DM. 1971. Insulin receptors in the liver: specific binding of (^{125}I) insulin to the plasma membrane and its relation to insulin bioactivity. Proc Natl Acad Sci US 68:1833–1837.

76. Kasuga M, Karlsson FA, Kahn CR. 1982. Insulin Stimulates the Phosphorylation of the 95,000-Dalton Subunit of its Own Receptor. Science 215:185–187.

77. Kahn, C. R., White MF. 1988. The insulin receptor and the molecular mechanism of insulin action. J Clin Invest 82:1151–1156.

78. Kasuga M, Zick Y, Blithe DL, Crettaz M, Kahn CR. 1982. Insulin stimulates tyrosine phosphorylation of the insulin receptor in a cell-free system. Nature 298: 667-669

79. Obberghen E Van. 1984. The insulin receptor: Its structure and function. Biochem Pharmacol 33:889–896.

80. Lee J, Pilch PF. 1994. The insulin receptor: structure, function, and signaling. Am J Physiol 266:C319–C334.

81. Hubbard SR. 2010. Structure and mechanism of the insulin receptor tyrosine kinase. Handbook of Cell Signaling, 2/eSecond Edi. Elsevier Inc.

82. Boucher J, Kleinridders A, Kahn CR. 2014. Insulin Receptor Signaling in Normal and Insulin-Resistant States. Cold Spring Harb Perspect Biol 6:a009191.

83. De Meyts P. 2008. The insulin receptor: a prototype for dimeric, allosteric membrane receptors? Trends Biochem Sci 33:376–384.

84. Patti ME, Kahn CR. 1999. The Insulin Receptor - A Critical Link In Glucose Homeostasis And Insulin Action. J Basic Clin Physiol Pharmacol 10:1–14.

85. Cheatham B, Kahn CR. 1995. Insulin Action and the Insulin Signaling Network. Endocr Rev 16(2):117-142.

86. Siddle K. 2011. Signalling by insulin and IGF receptors: Supporting acts and new players. J Mol Endocrinol 47:1-10.

87. Mosthaf L, Grako K, Dull TJ, Coussens L, Ullricho A, Mcclain DA. 1990. Functionally

distinct insulin receptors generated tissue-specific alternative splicing. EMBO 9:2409–2413.

88. Ward CW, Menting JG, Lawrence MC. 2013. The insulin receptor changes conformation in unforseen ways on ligand binding: Sharpening the picture of insulin receptor activation. Bioessays 35:945–954.

89. Ward CW, Garrett TPJ. 2001. The relationship between the L1 and L2 domains of the insulin and epidermal growth factor receptors and leucine-rich repeat modules. BMC Bioinformatics 2:1-10.

90. Lee J, Miyazaki M, Romeo GR, Shoelson SE. 2014. Insulin receptor activation with transmembrane domain ligands. J Biol Chem 289:19769–19777.

91. Kavran JM, Mccabe JM, Byrne PO, Katherine M, Wang Z, Ramek A, Sarabipour S, Shaw DE, Hristova K, Cole PA, Leahy DJ. 2015. How IGF-1 activates its receptor. Elife 1:1–28.

92. Maruyama IN. 2015. Activation of transmembrane cell-surface receptors via a common mechanism? The “rotation model.” BioEssays 37:959–967.

93. Tavaré JM, Siddle K. 1993. Mutational analysis of insulin receptor function. Consensus and controversy. BBA - Mol Cell Res 1178:21–39.

94. Catalano KJ, Maddux BA, Szary J, Youngren JF, Goldfine ID, Schaufele F. 2014. Insulin resistance induced by hyperinsulinemia coincides with a persistent alteration at the insulin receptor tyrosine kinase domain. PLoS One 9:1–11.

95. Dickens M, Tavaré JM. 1992. Analysis of the order of autophosphorylation of human insulin receptor tyrosines 1158, 1162 and 1163. Biochem Biophys Res Commun 186:244–250.

96. Tornqvist HE, Pierce MW, Frackelton AR, Nemenoff RA, Avruch J. 1987. Identification of insulin receptor tyrosine residues autophosphorylated in vitro. J Biol Chem 262:10212–10219.

97. White MF, Shoelson SE, Keutmann H, Kahn CR. 1988. A cascade of tyrosine autophosphorylation in the β-subunit activates the phosphotransferase of the insulin receptor. J Biol Chem 263:2969–2980.

98. Feener EP, Backer JM, King GL, Wilden PA, Xiao Jian Sun, Kahn CR, White MF. 1993. Insulin stimulates serine and tyrosine phosphorylation in the juxtamembrane region of the insulin receptor. J Biol Chem 268:11256–11264.

99. White MF. 1997. The insulin signalling system and the IRS proteins. Diabetologia 40:2–17.

100. Kitamura T, Kahn CR, Accili D. 2003. Insulin receptor knockout mice. Annu Rev Physiol 65:313–331.

101. Kulkarni RN, Bru JC, Winnay JN, Postic C, Magnuson MA, Kahn CR. 1999. Tissue-specific knockout of the insulin receptor in pancreatic beta cells creates insulin secretory defect similar to that in type-2 diabetes 96:329–339.

102. Michael MD, Kulkarni RN, Postic C, Previs SF, Shulman GI, Magnuson MA, Kahn CR. 2000. Loss of Insulin Signaling in Hepatocytes Leads to Severe Insulin Resistance and Progressive Hepatic Dysfunction. Mol Cell 6:87–97.

103. Okamoto H, Obici S, Accili D, Rossetti L. 2005. Restoration of liver insulin signaling in Insr knockout mice fails to normalize hepatic insulin action. J Clin Invest 115:1314–1322.

104. Bruning JC, Michael MD. 1998. A Muscle-Specific Insuin Receptor Knockout Exhibits Features of Metabolic Syndrome. Mol Cell 2:559–569.

105. O'Neill BT, Lauritzen HPMM, Hirshman MF, Smyth G, Goodyear LJ, Kahn CR. 2015. Differential Role of Insulin/IGF-1 Receptor Signaling in Muscle Growth and Glucose Homeostasis. Cell Rep 11:1220–1235.

106. Blüher M, Blu M, Kahn BB, Kahn CR. 2013. Extended Longevity in Mice Lacking the Insulin Receptor in Adipose Tissue. Science 572:572–574.

107. De Craene J-O, Bertazzi D, Bär S, Friant S, Grainger DL, Tavelis C, Ryan AJ, Hinchliffe K a, Vicinanza M, Gratian MJ, Bowen M, Rubinsztein DC, Hasegawa J, Strunk BS, Weisman LS, Viaud J, Mansour R, Antkowiak A, Mujalli A, Valet C, Chicanne G, Xuereb JM, Terrisse AD, Séverin S, Gratacap MP, Gaits-Iacovoni FF, Payrastre B, Picas L, Gaits-Iacovoni FF, Goud B, Viaud J, Boal F, Tronchère H, Gaits-Iacovoni FF, Payrastre B, Lemmon M a, Takasuga S, Sasaki T. 2017. Domains and Phosphoinositides. J Mol Sci 93:81–93.

108. White MF. 1997. The insulin signalling system and the IRS proteins. Diabetologia 40:2–17.

109. Wu J, Tseng YD, Xu CF, Neubert TA, White MF, Hubbard SR. 2008. Structural and biochemical characterization of the KRLB region in insulin receptor substrate-2. Nat Struct Mol Biol 15:251–258.

110. Kido Y, White MF, Accili D, Kido Y, Burks DJ, Withers D, Bruning JC, Kahn CR, White MF, Accili D. 2000. Tissue-specific insulin resistance in mice with mutations in the insulin receptor, IRS-1 and IRS-2. J Clin Invest 105:199–205.

111. Tamemoto H, Kadowaki T, Tobe K, Yagi T, Sakura H, Hayakawa T, Terauchi Y, Ueki K, Kaburagi Y, Satoh S, Sekihara H, Yoshioka S, Horikoshi H, Furuta Y, Ikawa Y, Kasuga M, Yazaki Y, Aizawa S. 1994. Insulin resistance and growth retardation in mice lacking insulin receptor substrate-1. Nature 372:182–186.

112. Araki E, Llpes M, Patti M-E. 1994. Alternative pathway of insulin signalling in mice with targeted disruption of the IRS-1 gene. Nature 372:186-190.

113. Miki H, Yamauchi T, Suzuki R, Komeda K, Tsuchida A, Kubota N, Terauchi Y, Kamon J, Kaburagi Y, Matsui J, Akanuma Y, Nagai R, Kimura S, Tobe K, Kadowaki T. 2001. Essential Role of Insulin Receptor Substrate 1 (IRS-1) and IRS-2 in Adipocyte Differentiation. Mol Cell Biol 21:2521–2532.

114. Kubota N, Tobe K, Terauchi Y, Eto K, Yamauchi T, Suzuki R, Tsubamoto Y, Komeda K, Nakano R, Miki H, Satoh S, Sekihara H, Sciacchitano S, Lesniak M, Aizawa S, Nagai R, Kimura S, Akanuma Y, Taylor SI, Kadowaki T. 2000. Disruption of Insulin Receptor Substrate 2 Causes Type 2 Diabetes Because of Liver Insulin Resistance and Lack of Compensatory Beta-cell Hyperplasia. Diabetes 49:1880–1889.

115. Withers, D. J., Gutierrez, J. S., Towery, H., Burks, D., Ren, JM., Previs, S., Zhang, Y., Bernal, D., Pons, S., Shulman, G. I., Bonner-Weir, S., White MF. 1998. Disruption of IRS-2 causes type-2 diabetes in mice. J Pharmacol Exp Ther 391:1303–1315.

116. Kubota N, Kubota T, Itoh S, Kumagai H, Kozono H, Takamoto I, Mineyama T, Ogata H, Tokuyama K, Ohsugi M, Sasako T, Moroi M, Sugi K, Kakuta S, Iwakura Y, Noda T, Ohnishi S, Nagai R, Tobe K, Terauchi Y, Ueki K, Kadowaki T. 2008. Dynamic Functional Relay between Insulin Receptor Substrate 1 and 2 in Hepatic Insulin Signaling during Fasting and Feeding. Cell Metab 8:49–64.

117. Rother KI, Imai Y, Caruso M, Beguinot F, Formisano P, Accili D. 1998. Evidence that IRS-2 phosphorylation is required for insulin action in hepatocytes. J Biol Chem 273:17491–17497.

118. Copps KD, White MF. 2012. Regulation of insulin sensitivity by serine/threonine

phosphorylation of insulin receptor substrate proteins IRS1 and IRS2. Diabetologia 55:2565–2582.

119. Myers MG, Backer JM, Xiao Jian Sun, Shoelson S, Hu P, Schlessinger J, Yoakim M, Schaffhausen B, White MF. 1992. IRS-1 activates phosphatidylinositol 3'-kinase by associating with src homology 2 domains of p85. Proc Natl Acad Sci U S A 89:10350–10354.

120. Shaw LM. 2011. The insulin receptor substrate (IRS) proteins: At the intersection of metabolism and cancer. Cell Cycle 10:1750–1756.

121. Alessi, D. R., James, S.R., Downes, C. P., Holmes, A. B., Gaffney, P.R.J., Reese, C. B., Cohen P. 1993. Characterization of a 3-phosphoinositide-dependent protein kinase which phosphorylates and activates protein kinase B-alpha. J Pharmacol Exp Ther 267:1484–1492.

122. Stephens L, Anderson K, Stokoe D, Erdjument-Bromage H, Painter GF, Holmes AB, Gaffney PRJ, Reese CB, McCormick F, Tempst P, Coadwell J, Hawkins PT. 1998. Prohtein kinase B kinases that mediate phosphatidylinositol 3,4,5- trisphosphate-dependent activation of protein kinase B. Science 279:710–714.

123. DD S, DA G, SM A, DM S. 2005. Phosphorylation and regulation of Akt//PKB by the rictor-mTOR complex. Science 307:1098–1101.

124. Alessi DR, Downes CP. 1998. The role of PI 3-kinase in insulin action. Biochim Biophys Acta 1436:151–164.

125. Bayascas JR, Alessi DR. 2005. Regulation of Akt/PKB Ser473 phosphorylation. Mol Cell 18:143–145.

126. Alessi DR, Andjelkovic M, Caudwell B, Cron P, Morrice N, Cohen P, Hemmings BA. 1996. Mechanism of activation of protein kinase B by insulin and IGF-1. EMBO J 15:6541–6551.

127. Persad S, Attwell S, Gray V, Mawji N, Deng JT, Leung D, Yan J, Sanghera J, Walsh MP, Dedhar S. 2001. Regulation of protein kinase B/Akt-serine 473 phosphorylation by integrin-linked kinase: Critical roles for kinase activity and amino acids arginine 211 and serine 343. J Biol Chem 276:27462–27469.

128. Mariniello K, Min Y, Ghebremeskel K. 2019. Phosphorylation of protein kinase B, the key enzyme in insulin-signaling cascade, is enhanced in linoleic and arachidonic acid–treated HT29 and HepG2 cells. Nutrition 57:52–58.

129. Sutherland C, O'Brien RM, Granner DK. 2007. Insulin action gene regulation. Mech Insul Action Med Intell Unit 110–132.

130. Manning BD, Toker A. 2017. AKT/PKB Signaling: Navigating the Network. Cell 169(3):381-405.

131. Valverde ÁM, González-Rodríguez Á. 2011. IRS2 and PTP1B: Two opposite modulators of hepatic insulin signalling. Arch Physiol Biochem 117:105–115.

132. Elchebly M, Payette P, Michaliszyn E, Cromlish W, Collins S, Loy AL, Normandin D, Cheng A, Himms-Hagen J, Chan CC, Ramachandran C, Gresser MJ, Tremblay ML, Kennedy BP. 1999. Increased insulin sensitivity and obesity resistance in mice lacking the protein tyrosine phosphatase-1B gene. Science 283:1544–1548.

133. Klaman LD, Boss O, Peroni OD, Kim JK, Martino JL, Zabolotny JM, Moghal N, Lubkin M, Kim Y-B, Sharpe AH, Stricker-Krongrad A, Shulman GI, Neel BG, Kahn BB. 2000. Increased Energy Expenditure, Decreased Adiposity, and Tissue-Specific Insulin Sensitivity in Protein-Tyrosine Phosphatase 1B-Deficient Mice. Mol Cell Biol 20:5479–5489.

134. Clampit JE, Meuth JL, Smith HT, Reilly RM, Jirousek MR, Trevillyan JM, Rondinone CM. 2003. Reduction of protein-tyrosine phosphatase-1B increases insulin signaling in FAO hepatoma cells. Biochem Biophys Res Commun 300:261–267.

135. Gonzalez-Rodriguez A, Clampit JE, Escribano O, Benito M, Rondinone CM, Valverde AM. 2007. Developmental switch from prolonged insulin action to increased insulin sensitivity in protein tyrosine phosphatase 1B-deficient hepatocytes. Endocrinology 148:594–608.

136. González-Rodríguez Á, Mas Gutierrez JA, Sanz-González S, Ros M, Burks DJ, Valverde ÁM. 2010. Inhibition of PTP1B restores IRS1-mediated hepatic insulin signaling in IRS2-deficient mice. Diabetes 59:588–599.

137. Egawa K, Maegawa H, Shimizu S, Morino K, Nishio Y, Bryer-Ash M, Cheung AT, Kolls JK, Kikkawa R, Kashiwagi A. 2001. Protein-tyrosine Phosphatase-1B Negatively Regulates Insulin Signaling in L6 Myocytes and Fao Hepatoma Cells. J Biol Chem 276:10207–10211.

138. Gum RJ, Gaede LL, Koterski SL, Heindel M, Clampit JE, Zinker BA, Trevillyan JM, Ulrich RG, Jirousek MR, Rondinone CM. 2003. Reduction of protein tyrosine phosphatase 1B increases insulin-dependent signaling in ob/ob mice. Diabetes 52:21–28.

139. Paz K, Hemi R, Leroith D, Karasik A, Elhanany E, Kanety H, Zick Y. 1997. A Molecular Basis for Insulin Resistance: Elevated Serine/Threonine Phosphorylation of IRS-1 and IRS-2 Inhibits Their Binding To The Juxtamembrane Region of The Insulin Receptor And Impairs Their Ability To Undergo Insulin-Induced Tyrosine Phosphorylation. J Biol Chem 272:29911–29918.

140. Karasik A, Rothenberg PL, Yamada K, White MF, Kahn CR. 1990. Increased protein kinase C activity is linked to reduced insulin receptor autophosphorylation in liver of starved rats. J Biol Chem 265:10226–10231.

141. Shao J, Catalano PM, Yamashita H, Ruyter I, Smith S, Youngren J, Friedman J E. 2000. Decreased Insulin Receptor Tyrosine Kinase Activity and Plasma Cell Membrane Glycoprotein-1 Overexpression in Skeletal Muscle from Obese Women With Gestational Diabetes Mellitus (GDM). Evidence for Increased Serine/Threonine Phosphorylation in Pregnancy and GDM. Diabetes 49:603–610.

142. Petersen MC, Rinehart J, Shulman GI, Petersen MC, Madiraju AK, Gassaway BM, Marcel M, Nasiri AR, Butrico G, Marcucci MJ, Zhang D, Abulizi A, Zhang X, Philbrick W, Hubbard SR. 2016. Insulin receptor Thr 1160 phosphorylation mediates lipid-induced hepatic insulin resistance Find the latest version : Insulin receptor Thr 1160 phosphorylation mediates lipid-induced hepatic insulin resistance. J Clin Invest 126:4361–4371.

143. Aguirre V, Werner ED, Giraud J, Lee YH, Shoelson SE, White MF. 2002. Phosphorylation of Ser307 in insulin receptor substrate-1 blocks interactions with the insulin receptor and inhibits insulin action. J Biol Chem 277:1531–1537.

144. Yenush L, Aguirre V, Uchida T, Yenush L, Davis R, White MF. 2016. The c-Jun NH2-terminal Kinase Promotes Insulin Resistance during Association with Insulin Receptor Substrate-1 and Phosphorylation of Ser307 The c-Jun NH 2 -terminal Kinase Promotes Insulin Resistance Phosphorylation of Ser 307 *. J Biol Chem 275:9407–9054.

145. Pederson TM, Kramer DL, Rondinone CM. 2001. Serine/threonine phosphorylation of IRS-1 triggers its degradation: Possible regulation by tyrosine phosphorylation. Diabetes 50:24–31.

146. Ueno M, Carvalheira JBC, Tambascia RC, Bezerra RMN, Amaral ME, Carneiro EM, Folli F, Franchini KG, Saad MJA. 2005. Regulation of insulin signalling by hyperinsulinaemia: Role of IRS-1/2 serine phosphorylation and the mTOR/p70 S6K pathway. Diabetologia 48:506–

518.

147. Gao Z, Hwang D, Bataille F, Lefevre M, York D, Quon MJ, Ye J. 2002. Serine phosphorylation of insulin receptor substrate 1 by inhibitor κB kinase complex. J Biol Chem 277:48115–48121.

148. Bloch-Damti A, Potashnik R, Gual P, Le Marchand-Brustel Y, Tanti JF, Rudich A, Bashan N. 2006. Differential effects of IRS1 phosphorylated on Ser307 or Ser632 in the induction of insulin resistance by oxidative stress. Diabetologia 49:2463–2473.

149. Park K, Li Q, Rask-Madsen C, Mima A, Mizutani K, Winnay J, Maeda Y, D'Aquino K, White MF, Feener EP, King GL. 2013. Serine Phosphorylation Sites on IRS2 Activated by Angiotensin II and Protein Kinase C To Induce Selective Insulin Resistance in Endothelial Cells. Mol Cell Biol 33:3227–3241.

150. Fritsche L, Neukamm SS, Lehmann R, Kremmer E, Hennige AM, Hunder-Gugel A, Schenk M, Häring H-U, Schleicher ED, Weigert C. 2011. Insulin-induced serine phosphorylation of IRS-2 via ERK1/2 and mTOR: studies on the function of Ser ^{675} and Ser ^{907}. Am J Physiol Metab 300:E824–E836.

151. Stiles B, Wang Y, Stahl A, Bassilian S, Lee WP, Kim YJ, Sherwin R, Devaskar S, Lesche R, Magnuson MA, Wu H. 2004. Live-specific deletion of negative regulator Pten results in fatty liver and insulin hypersensitivity. Proc Natl Acad Sci USA 101:2082–2087.

152. Kagawa S, Soeda Y, Ishihara H, Oya T, Sasahara M, Yaguchi S, Oshita R, Wada T, Tsuneki H, Sasaoka T. 2008. Impact of transgenic overexpression of SH2-containing inositol 5′-phosphatase 2 on glucose metabolism and insulin signaling in mice. Endocrinology 149:642–650.

153. Clément S, Krause U, Desmedt F, Tanti JF, Behrends J, Pesesse X, Sasaki T, Penninger J, Doherty M, Malaisse W, Dumont JE, Le Marchand-Brustel Y, Erneux C, Hue L, Schurmans S. 2001. The lipid phosphatase SHIP2 controls insulin sensitivity. Nature 409:92–97.

154. Guo S. 2014. Insulin Signaling, Resistance, adn the Metabolic Syndrome: Insights from Mouse Models to Disease Mechanisms. J Endocrinol 220:1–36.

155. Qi Y, Xu Z, Zhu Q, Thomas C, Kumar R, Feng H, Dostal DE, White MF, Baker KM, Guo S. 2013. Myocardial loss of IRS1 and IRS2 causes heart failure and is controlled by p38α MAPK during insulin resistance. Diabetes 62:3887–3900.

156. Gonzalez E, Flier E, Molle D, Accili D, McGraw TE. 2011. Hyperinsulinemia leads to uncoupled insulin regulation of the GLUT4 glucose transporter and the FoxO1 transcription factor. Proc Natl Acad Sci USA 108:10162–10167.

157. Mlinar B, Marc J, Janež A, Pfeifer M. 2007. Molecular mechanisms of insulin resistance and associated diseases. Clin Chim Acta 375:20–35.

158. Pratipanawatr W, Pratipanawatr T, Cusi K, Berria R, Adams JM, Jenkinson CP, Maezono K, Defronzo RA, Mandarino LJ. 2001. Skeletal Muscle Insulin Resistance in Normoglycemic Subjects With a Strong Family History of Type 2 Diabetes is Associated With Decreased Insulin-Stimulated Insulin Receptor Substrate-1 Tyrosine Phosphorylation. Diabetes 50:2572–2578.

159. Uysal KT, Wiesbrock SM, Marino MW, Hotamisligil GS. 1997. Protection from obesity-induced insulin resistance in mice lacking TNF-alpha function. Nature 389:610–613.

160. Hagiwara A, Cornu M, Cybulski N, Polak P, Betz C, Trapani F, Terracciano L, Heim MH, Rüegg MA, Hall MN. 2012. Hepatic mTORC2 activates glycolysis and lipogenesis through

Akt, glucokinase, and SREBP1c. Cell Metab 15:725–738.

161. Miyake K, Ogawa W, Matsumoto M, Nakamura T, Sakaue H, Kasuga M. 2002. Hyperinsulinemia, glucose intolerance, and dyslipidemia induced by acute inhibition of phosphoinositide 3-kinase signaling in the liver. J Clin Invest 110:1483–1491.

162. Mora A, Lipina C, Tronche F, Sutherland C, Alessi DR. 2005. Deficiency of PDK1 in liver results in glucose intolerance, impairment of insulin-regulated gene expression and liver failure. Biochem J 385:639–648.

163. Guo S, Copps KD, Dong X, Park S, Cheng Z, Pocai A, Rossetti L, Sajan M, Farese R V., White MF. 2009. The Irs1 Branch of the Insulin Signaling Cascade Plays a Dominant Role in Hepatic Nutrient Homeostasis. Mol Cell Biol 29:5070–5083.

164. Ye J. 2013. Mechanisms of insulin resistance in obesity. Front Med 7:14–24.

165. Stienstra R, Duval C, Müller M, Kersten S. 2007. PPARs, obesity, and inflammation. PPAR Research 1–10.

166. Xu, H., Tartaglia, L.A., Chen H. 2003. Chronic inflammation plays a crucial role in the development of obesity-related insulin resistance. J Clin Invest 112:1821–1830.

167. Saad MJA, Folli F, Kahn J., Kahn CR. 1993. Modulation of Insulin Receptor, Insulin Receptor Substrate-1, and Phosphatidylinositol 3-kinase in liver and muscle of Dexamethasone-treated rats. J Clin Immunol 92:2065–2072.

168. Burén J, Lai YC, Lundgren M, Eriksson JW, Jensen J. 2008. Insulin action and signalling in fat and muscle from dexamethasone-treated rats. Arch Biochem Biophys 474:91–101.

169. Bazuine M, Carlotti F, Jahangir Tafrechi RS, Hoeben RC, Maassen JA. 2004. Mitogen-Activated Protein Kinase (MAPK) phosphatase-1 and -4 attenuate p38 MAPK during dexamethasone-induced insulin resistance in 3T3-L1 adipocytes. Mol Endocrinol 18:1697–1707.

170. Ruzzin J, Wagman AS, Jensen J. 2005. Glucocorticoid-induced insulin resistance in skeletal muscles: Defects in insulin signalling and the effects of a selective glycogen synthase kinase-3 inhibitor. Diabetologia 48:2119–2130.

171. Sakoda H, Ogihara T, Anai M, Funaki M, Inukai K, Katagiri H, Fukushima Y, Onishi Y, Ono H, Fujishiro M, Kikuchi M, Oka Y, Asano T. 2000. Dexamethasone-induced insulin resistance in 3T3-L1 adipocytes is due to inhibition of glucose transport rather than insulin signal transduction. Diabetes 49:1700–1708.

172. Kroder G, Bossenmaier B, Kellerer M, Capp E, Stoyanov B, Mühlhöfer A, Berti L, Horikoshi H, Ullrich A, Häring H. 1996. Tumor necrosis factor-α- and hyperglycemia-induced insulin resistance: Evidence for different mechanisms and different effects on insulin signaling. J Clin Invest 97:1471–1477.

173. Kohler HP. 2002. Insulin resistance syndrome: Interaction with coagulation and fibrinolysis. Swiss Med Wkly 132:241–252.

174. Rosmond R. 2003. Stress induced disturbances of the HPA axis: a pathway to Type 2 diabetes? Med Sci Monit 9:35–39.

175. Pasieka AM, Rafacho A. 2016. Impact of glucocorticoid excess on glucose tolerance: Clinical and preclinical evidence. Metabolites 6(3):1-21.

176. Qi D, Rodrigues B. 2007. Glucocorticoids produce whole body insulin resistance with changes

in cardiac metabolism. Am J Physiol Metab 292:E654–E667.

177. Reynolds RM, Walker BR. 2003. Human insulin resistance: The role of glucocorticoids. Diabetes, Obes Metab 5:5–12.

178. Mazziotti G, Gazzaruso C, Giustina A. 2011. Diabetes in Cushing syndrome: Basic and clinical aspects. Trends Endocrinol Metab 22:499–506.

179. Ferris HA, Kahn CR. 2012. New mechanisms of glucocorticoid-induced insulin resistance: make no bones about it. J Clin Invest 122:3854–3857.

180. Severino C, Brizzi P, Solinas A, Secchi G, Maioli M, Tonolo G. 2002. Low-dose dexamethasone in the rat: a model to study insulin resistance. Am J Physiol Metab 283:E367–E373.

181. Almon RR, Dubois DC, Jusko WJ. 2007. A microarray analysis of the temporal response of liver to methylprednisolone: A comparative analysis of two dosing regimens. Endocrinology 148:2209–2225.

182. Almon R., DuBois DC, Jin Y., Jusko W. 2005. Temporal profiling of the transcriptional basis for the development of corticosteroid-induced insulin resistance in rat muscle. J Endocrinol 184:219–232.

183. Cooke AA, Connaughton RM, Lyons CL, McMorrow AM, Roche HM. 2016. Fatty acids and chronic low grade inflammation associated with obesity and the metabolic syndrome. Eur J Pharmacol 785:207–214.

184. Lijnen HR, Maquoi E, Morange P, Voros G, Van Hoef B, Kopp F, Collen D, Juhan-Vague I, Alessi MC. 2003. Nutritionally induced obesity is attenuated in transgenic mice overexpressing plasminogen activator inhibitor-1. Arterioscler Thromb Vasc Biol 23:78–84.

185. Freidenberg GR, Reichart D, Olefsky JM, Henry RR. 1988. Reversibility of defective adipocyte insulin receptor kinase activity in non-insulin-dependent diabetes mellitus. Effect of weight loss. J Clin Invest 82:1398–1406.

186. Bak JF, Møller N, Schmitz O, Saaek A, Pedersen O. 1992. In vivo insulin action and muscle glycogen synthase activity in Type 2 (non-insulin-dependent) diabetes mellitus: effects of diet treatment. Diabetologia 35:777–784.

187. Jensen MD, Haymond MW, Rizza RA, Cryer PE, Miles JM. 1989. Influence of body fat distribution on free fatty acid metabolism in obesity. J Clin Invest 83:1168–1173.

188. Shulman GI. 2000. Cellular mechanisms of insulin resistance. J Clin Invest 106:171–176.

189. Yu C, Chen Y, Cline GW, Zhang D, Zong H, Wang Y, Bergeron R, Kim JK, Cushman SW, Cooney GJ, Atcheson B, White MF, Kraegen EW, Shulman GI. 2002. Mechanism by which fatty acids inhibit insulin activation of insulin receptor substrate-1 (IRS-1)-associated phosphatidylinositol 3-kinase activity in muscle. J Biol Chem 277:50230–50236.

190. Hotamisligil GS, Shargill NS, Spiegelman BM. 1993. Adipose expression of tumor necrosis factor-α: Direct role in obesity-linked insulin resistance. Science 259:87–91.

191. Sethi JK, Hotamisligil GS. 1999. The role of TNFα in adipocyte metabolism. Semin Cell Dev Biol 10:19–29.

192. Hotamisligil GS. 2000. Molecular mechanisms of insulin resistance and the role of the adipocyte. Int J Obes 24:S23–S27.

193. Hotamisligil GS, Arner P, Caro JF, Atkinson RL, Spiegelman BM. 1995. Increased adipose tissue expression of tumor necrosis factor-α in human obesity and insulin resistance. J Clin Invest 95:2409–2415.

194. Hotamisligil GS, Murray DL, Choy LN, Spiegelman BM. 1994. Tumor necrosis factor α inhibits signaling from the insulin receptor. Proc Natl Acad Sci USA 91:4854–4858.

195. Rangwala SM, Rich AS, Rhoades B, Shapiro JS, Obici S, Rossetti L, Lazar MA. 2004. Abnormal glucose homeostasis due to chronic hyperresistinemia. Diabetes 53:1937–1941.

196. Muse ED, Obici S, Bhanot S, Monia BP, McKay RA, Rajala MW, Scherer PE, Rossetti L. 2004. Role of resistin in diet-induced hepatic insulin resistance. J Clin Invest 114:232–239.

197. Rajala MW, Obici S, Scherer PE, Rossetti L. 2003. Adipose-derived resistin and gut-derived resistin-like molecule–β selectively impair insulin action on glucose production. J Clin Invest 111:225–230.

198. Kern PA, Ranganathan S, Li C, Wood L, Ranganathan G. 2001. Adipose tissue tumor necrosis factor and interleukin-6 expression in human obesity and insulin resistance. Am J Physiol - Endocrinol Metab 280:745–751.

199. Banerjee RR, Rangwala SM, Shapiro JS, Rich AS, Rhoades B, Qi Y, Wang J, Rajala MW, Pocai A, Scherer PE, Steppan CM, Ahima RS, Obici S, Rossetti L, Lazar MA. 2004. Regulation of Fasted Blood Glucose by Resistin. Science 303:1195–1198.

200. Combs TP, Pajvani UB, Berg AH, Lin Y, Jelicks LA, Laplante M, Nawrocki AR, Rajala MW, Parlow AF, Cheeseboro L, Ding YY, Russell RG, Lindemann D, Hartley A, Baker GRC, Obici S, Deshaies Y, Ludgate M, Rossetti L, Scherer PE. 2004. A Transgenic Mouse with a Deletion in the Collagenous Domain of Adiponectin Displays Elevated Circulating Adiponectin and Improved Insulin Sensitivity. Endocrinology 145:367–383.

201. Kubota N, Terauchi Y, Yamauchi T, Kubota T, Moroi M, Matsui J, Eto K, Yamashita T, Kamon J, Satoh H, Yano W, Froguel P, Nagai R, Kimura S, Kadowaki T, Noda T. 2002. Disruption of adiponectin causes insulin resistance and neointimal formation. J Biol Chem 277:25863–25866.

202. Rehman K, Akash MSH. 2016. Mechanisms of inflammatory responses and development of insulin resistance: How are they interlinked? J Biomed Sci 23:1–18.

203. Wu Y, Wu T, Wu J, Zhao L, Li Q, Varghese Z, Moorhead JF, Powis SH, Chen Y, Ruan XZ. 2013. Chronic inflammation exacerbates glucose metabolism disorders in C57BL/6J mice fed with high-fat diet. J Endocrinol 219:195–204.

204. Jager J, Grémeaux T, Cormont M, Le Marchand-Brustel Y, Tanti JF. 2007. Interleukin-1β-induced insulin resistance in adipocytes through down-regulation of insulin receptor substrate-1 expression. Endocrinology 148:241–251.

205. Kanemaki T, Kitade H, Kaibori M, Sakitani K, Hiramatsu Y, Kamiyama Y, Ito S, Okumura T. 1998. Interleukin 1β and interleukin 6, but not tumor necrosis factor α, inhibit insulin-stimulated glycogen synthesis in rat hepatocytes. Hepatology 27:1296–1303.

206. Pickup JC, Crook MA. 1998. Is type 2 DM a disease of the innate immune system? Diabetologia 41:1241–1248.

207. Pickup JC, Mattock MB, Chusney GD, Butt D. 1997. NIDDM as a disease of the innate immune system: association of acute-phase reactants and interleukin-6 with metabolic syndrome X. Diabetologia 40:1286–1292.

208. Janciauskiene, S., Welte, T., Mahadeva R. 2011. Acute Phase Proteins: Regulation and Functions of Acute Phase Proteins. Intech 25-60.

209. Gruys E, Toussaint MJM, Niewold TA, Koopmans SJ. 2005. Acute phase reaction and acute phase proteins. J Zhejiang Univ Sci 6B:1045–1056.

210. Cray C, Zaias J, Altman NH. 2009. Acute phase response in animals: A review. Comp Med 59:517–526.

211. Kushner I. 1982. The Phenomenon of the Acute Phase Response. Ann NY Acad Sci 389:39–48.

212. Moshage H. 1997. Article Cytokines and the Hepatic Acute Phase. J Pathol 181:257–266.

213. Suffredini AF, Fantuzzi G, Badolato R, Oppenheim JJ, O'Grady NP. 1999. New insights into the biology of the acute phase response. J Clin Immunol 19:203–214.

214. Heinrich PC, Castell J V, Andus T. 1990. Interleukin-6 and the acute phase response. Biochem J 265:621–636.

215. Sipe JD. 1995. The Acute Phase Response in the Pathogenesis of Inflammatory Disease. Clin Immunother 3:297–307.

216. Castell J V., Gómez-lechón MJ, David M, Fabra R, Trullenque R, Heinrich PC. 1990. Acute-phase response of human hepatocytes: Regulation of acute-phase protein synthesis by interleukin-6. Hepatology 12:1179–1186.

217. Gabay, C & Kushner I. 1999. Acute-phase proteins and other systemic responses to inflammation. N Engl J Med 448–454.

218. Baumann H. 1989. Hepatic acute phase reaction in vivo and in vitro. Vitr Cell Dev Biol - Anim 25:115–126.

219. Markanday A. 2015. Acute Phase Reactants in Infections: Evidence-Based Review and a Guide for Clinicians. OFID 1–8.

220. Hill LA, Bodnar TS, Weinberg J, Hammond GL, Sciences P. 2016. Corticosteroid-Binding Globulin is a biomarker of inflammation onset and severity in female rats. J Endocrinol 230:215–225.

221. Black PH. 2003. The inflammatory response is an integral part of the stress response: Implications for atherosclerosis, insulin resistance, type II diabetes and metabolic syndrome X. Brain Behav Immun 17:350–364.

222. McMillan DE. 1989. Increased levels of acute-phase serum proteins in diabetes. Metabolism 38:1042–1046.

223. Jonsson A, Wales JK. 1976. Blood Glycoprotein Levels in Diabetes Mellitus. Diabetologia 12:245–250.

224. Horrevoets, A. J. G. 2004. Plasminogen activator inhibitor 1 (PAI-1): in vitro activities and clinical relevance. Br J Haemotology 125:12–23.

225. Lijnen HR. 2005. Pleiotropic functions of plasminogen activator inhibitor-1. J of Thromb Haemost 3:35–45.

226. Yildiz SY, Kuru P, Oner ET, Agirbasli M. 2014. Functional Stability of Plasminogen Activator Inhibitor-1. Sci World J: 1-11.

227. Binder BR, Christ G, Gruber F, Grubic N, Hufnagl P, Krebs M, Mihaly J, Prager GW. 2002. Plasminogen activator inhibitor 1: physiological and pathophysiological roles. News Physiol Sci 17:56–61.

228. Lyon CJ, Hsueh WA. 2003. Effect of plasminogen activator inhibitor-1 in diabetes mellitus and cardiovascular disease. Am J Med 115:62–68.

229. Jiang Q, Gingles NA, Olivier MA, Miles LA, Parmer RJ. 2011. The anti-fibrinolytic SERPIN , plasminogen activator inhibitor 1 (PAI-1), is targeted to and released from catecholamine storage vesicles. Blood 117:7155–7164.

230. Dewilde M, Van De Craen B, Compernolle G, Madsen JB, Strelkov S, Gils A, Declerck PJ. 2010. Subtle structural differences between human and mouse PAI-1 reveal the basis for biochemical differences. J Struct Biol 171:95–101.

231. Kooistra T, Sprengers ED, Hinsbergh VWMVAN. 1986. Rapid inactivation of the plasminogen-activator inhibitor upon secretion from cultured human endothelial cells. Biochem J 239:497–503.

232. Cesari, M., Pahor, M. and Incalzi, R A. 2010. Plasminogen activator inhibitor-1 (PAI-1): A key factor linking fibrinolysis and age-related subclinical and clinical conditions. Cardiovasc Ther 28:1–28.

233. Alessi MC, Juhan-Vague I. 2006. PAI-1 and the metabolic syndrome: Links, causes, and consequences. Arterioscler Thromb Vasc Biol 26:2200–2207.

234. Taeye B De, Smith LH, Vaughan DE. 2005. Plasminogen activator inhibitor-1: a common denominator in obesity, diabetes and cardiovascular disease. Curr Opin Pharmocology 5:149–154.

235. Pottern val Loon BJ, Kluft C, Radder JK, Meinders AE. 1993. The Cardiovascular Risk Factor Plasminogen Activator Is Related to Insulin Resistance. Metabolism 42:945–949.

236. Martinez-eyarre C, Segarra A, On PC, Argelaguer X, Vila J, Ruiz P, Fort J, Camps J, Moliner E, E JB, Pelegr A, Marco F, Olmos A, Piera L. 2001. Circulating Levels of Plasminogen Activator Inhibitor Type-1 , Tissue Plasminogen Activator , and Thrombomodulin in Hemodialysis Patients : Biochemical Correlations and Role as Independent Predictors of Coronary Artery Stenosis. J Am Soc Nephrol 12:1255–1263.

237. Juhan-Vague I, Alessi MC, Mavri A, Morange PE. 2003. Plasminogen activator inhibitor-1, inflammation, obesity, insulin resistance and vascular risk. J Thromb Haemost 1:1575–1579.

238. Morange PE, Bastelica D, Bonzi MF, Van Hoef B, Collen D, Juhan-Vague I, Lijnen HR. 2002. Influence of PAI-1 on adipose tissue development in a murine model of diet-induced obesity. Thromb Haemost 87:306–310.

239. Samad F, Loskutoff DJ. 1996. Tissue distribution and insulin regulation of plasminogen activator inhibitor-1 in obese mice. Fibrinolysis 10:75.

240. Sawdey MS, Loskutoff DJ. 1991. Regulation of murine type 1 plasminogen activator inhibitor gene expression in vivo. Tissue specificity and induction by lipopolysaccharide, tumor necrosis factor-α, and transforming growth factor-β. J Clin Invest 88:1346–1353.

241. Alessi MC, Peiretti F, Morange P, Henry M, Nalbone G, Juhan-Vague I. 1997. Production of plasminogen activator inhibitor 1 by human adipose tissue: Possible link between visceral fat accumulation and vascular disease. Diabetes 46:860–867.

242. Liang X, Kanjanabuch T, Mao S-L, Hao C-M, Tang Y-W, Declerck PJ, Hasty AH,

Wasserman DH, Fogo AB, Ma L-J. 2006. Plasminogen activator inhibitor-1 modulates adipocyte differentiation. Am J Physiol Metab 290:E103–E113.

243. Lijnen HR, Alessi MC, Van Hoef B, Collen D, Juhan-Vague I. 2005. On the role of plasminogen activator inhibitor-1 in adipose tissue development and insulin resistance in mice. J Thromb Haemost 3:1174–1179.

244. Crandall DL, Quinet EM, El Ayachi S, Hreha AL, Leik CE, Savio DA, Juhan-Vague I, Alessi MC. 2006. Modulation of adipose tissue development by pharmacological inhibition of PAI-1. Arterioscler Thromb Vasc Biol 26:2209–2215.

245. Schäfer K, Fujisawa K, Konstantinides S, Loskutoff DJ. 2001. Disruption of the plasminogen activator inhibitor 1 gene reduces the adiposity and improves the metabolic profile of genetically obese and diabetic ob/ob mice. FASEB J 15:1840–1842.

246. Ma L, Mao S, Taylor KL, Kanjanabuch T, Guan Y, Zhang Y, Brown NJ, Swift LL, Mcguinness OP, Wasserman DH, Vaughan DE, Fogo AB. 2004. Prevention of obesity and IR in mice lacking plasminogen activator inhibitor-1. Diabetes 53:336–346.

247. Correia MLG, Haynes WG. 2006. A Role for Plasminogen Activator Inhibitor-1 in Obesity : From Pie to PAI ? Arterioscler Thromb Vasc Biol 26:2183–2185.

248. Juhan-Vague I, Alessi MC, Vague P. 1991. Increased plasma plasminogen activator inhibitor-1 levels. A possible link between insulin resistance and atherothrombosis. Diabetologia 34:891–898.

249. Alessi M-C, Poggi M, Juhan-Vague I. 2007. Plasminogen activator inhibitor-1, adipose tissue and insulin resistance. Curr Opin Lipidol 18:240–5.

250. Bastard JP, Piéroni L, Hainque B. 2000. Relationship between plasma plasminogen activator inhibitor 1 and insulin resistance. Diabetes Metab Res Rev 16:192–201.

251. Kruszynska YT, Yu JG, Olefsky JM, Sobel BE. 2000. Effects of triglitazone on blood concentrations of plasminogen activator inhibitor-1 in patients with type-2 diabetes and in lean and obese normal subjects. Diabetes 49:633–639.

252. Tamura Y, Kawao N, Yano M, Okada K, Matsuo O, Kaji H. 2014. Plasminogen activator inhibitor-1 deficiency ameliorates insulin resistance and hyperlipidemia but not bone loss in obese female mice. Endocrinology 155:1708–1717.

253. Balsara RD, Castellino FJ, Ploplis VA. 2006. A novel function of plasminogen activator inhibitor-1 in modulation of the AKT pathway in wild-type and plasminogen activator inhibitor-1-deficient endothelial cells. J Biol Chem 281:22527–22536.

254. Tamura Y, Kawao N, Yano M, Okada K, Okumoto K, Chiba Y, Matsuo O, Kaji H. 2015. Role of plasminogen activator inhibitor-1 in glucocorticoid-induced diabetes and osteopenia in mice. Diabetes 64:2194–2206.

255. Eklund KK, Niemi K, Kovanen PT. 2012. Immune functions of serum amyloid A. Crit Rev Immunol 32:335–348.

256. Malle E, De Beer F. 1996. Human serum amyloid A (SAA) protein : a prominent acute-phase reactant for clinical practice. Eur J Clin Invest 26:427–435.

257. Uhlar CM, Whitehead AS. 1999. Serum amyloid A, the major vertebrate acute-phase reactant. Eur J Biochem 265:501–523.

258. Getz GS, Krishack PA, Reardon CA. 2016. Serum amyloid A and atherosclerosis. Curr Opin

Lipidol 27:531–535.

259. Buck M, Gouwy M, Wang J, Snick J, Opdenakker G, Struyf S, Damme J. 2016. Structure and Expression of Different Serum Amyloid A (SAA) Variants and their Concentration-Dependent Functions During Host Insults. Curr Med Chem 23:1725–1755.

260. Filippin-Monteiro FB, De Oliveira EM, Sandri S, Knebel FH, Albuquerque RC, Campa A. 2012. Serum amyloid A is a growth factor for 3T3-L1 adipocytes, inhibits differentiation and promotes insulin resistance. Int J Obes 36:1032–1039.

261. Lin Y, Rajala MW, Berger JP, Moller DE, Barzilai N, Scherer PE. 2001. Hyperglycemia-induced Production of Acute Phase Reactants in Adipose Tissue. J Biol Chem 276:42077–42083.

262. Sjöholm K, Palming J, Olofsson LE, Gummesson A, Svensson PA, Lystig TC, Jennische E, Brandberg J, Torgerson JS, Carlsson B, Carlsson LMS. 2005. A microarray search for genes predominantly expressed in human omental adipocytes: Adipose tissue as a major production site of serum amyloid A. J Clin Endocrinol Metab 90:2233–2239.

263. Yang R, Lee M, Hu H, Pollin TI, Ryan AS, Nicklas BJ, Snitker S, Horenstein RB, Hull K, Goldberg NH, Goldberg AP, Shuldiner AR, Fried SK. 2006. Acute-Phase Serum Amyloid A : An Inflammatory Adipokine and Potential Link between Obesity and Its Metabolic Complications. PLoS Med 3(6):0884-0894.

264. Kisilevsky R, Manley PN. 2012. Acute-phase serum amyloid A: Perspectives on its physiological and pathological roles. Amyloid 19:5–14.

265. Hua S, Song C, Geczy CL, Freedman S Ben, Witting PK. 2009. A role for acute-phase serum amyloid A and high-density lipoprotein in oxidative stress, endothelial dysfunction and atherosclerosis. Redox Rep 14:187–196.

266. Jijon HB, Madsen KL, Walker JW, Allard B, Jobin C. 2005. Serum amyloid A activates NF-κB and proinflammatory gene expression in human and murine intestinal epithelial cells. Eur J Immunol 35:718–726.

267. Poitou C, Viguerie N, Cancello R, De Matteis R, Cinti S, Stich V, Coussieu C, Gauthier E, Courtine M, Zucker JD, Barsh GS, Saris W, Bruneval P, Basdevant A, Langin D, Clément K. 2005. Serum amyloid A: Production by human white adipocyte and regulation by obesity and nutrition. Diabetologia 48:519–528.

268. Sjöholm K, Lundgren M, Olsson M, Eriksson JW. 2009. Association of serum amyloid A levels with adipocyte size and serum levels of adipokines: Differences between men and women. Cytokine 48:260–266.

269. Faty A, Ferre P, Commans S. 2012. The Acute Phase Protein Serum Amyloid A Induces Lipolysis and Inflammation in Human Adipocytes through Distinct Pathways. PLoS One 7:1–10.

270. de Oliveira EM, Ascar TP, Silva JC, Sandri S, Migliorini S, Fock RA, Campa A. 2016. Serum amyloid A links endotoxaemia to weight gain and insulin resistance in mice. Diabetologia 59:1760–1768.

271. Scheja L, Heese B, Zitzer H, Michael MD, Siesky AM, Pospisil H, Beisiegel U, Seedorf K. 2008. Acute-Phase Serum Amyloid A as a Marker of Insulin Resistance in Mice. Exp Diabetes Res 2008:1–11.

272. Kumon Y, Suehiro T, Itahara T, Ikeda Y, Hashimoto K. 1994. Serum amyloid A protein in patients with non-insulin-dependent diabetes mellitus. Clin Biochem 27:469–473.

273. Ebeling P, Teppo AM, Koistinen HA, Viikari J, Rönnemaa T, Nissén M, Bergkulla S, Salmela P, Saltevo J, Koivisto VA. 1999. Troglitazone reduces hyperglycaemia and selectively acute-phase serum proteins in patients with Type II diabetes. Diabetologia 42:1433–1438.

274. Ye XY, Xue YM, Sha JP, Li CZ, Zhen ZJ. 2009. Serum amyloid A attenuates cellular insulin sensitivity by increasing JNK activity in 3T3-L1 adipocytes. J Endocrinol Invest 32:568–575.

275. Tillett WS, Francis T. 1930. Serological reactions in pneumonia with a nonprotein somatic fraction of pneumococcus. J Exp Med 52:561–571.

276. Pepys MB, Hirschfield GM. 2003. C-reactive protein: a critical update. J Clin Invest 111:1805–1812.

277. Li JJ, Fang CH. 2004. C-reactive protein is not only an inflammatory marker but also a direct cause of cardiovascular diseases. Med Hypotheses 62:499–506.

278. Kramer F, Torzewski J, Kamenz J, Veit K, Hombach V, Dedio J, Ivashchenko Y. 2008. Interleukin-1β stimulates acute phase response and C-reactive protein synthesis by inducing an NFκB- and C/EBPβ-dependent autocrine interleukin-6 loop. Mol Immunol 45:2678–2689.

279. Calabro P, Chang DW, Willerson JT, Yeh ETH. 2005. Release of C-reactive protein in response to inflammatory cytokines by human adipocytes: Linking obesity to vascular inflammation. J Am Coll Cardiol 46:1112–1113.

280. Sproston NR, Ashworth JJ. 2018. Role of C-reactive protein at sites of inflammation and infection. Front Immunol 9:1–11.

281. Fonseca LAM, Sumita NM, Duarte NJC, Lichtenstein A, Duarte AJS. 2013. Review article C-reactive protein: clinical applications and proposals for a rational use. Rev Assoc Med Bras 59:85–92.

282. Kuller LH, Tracy RP, Shaten J, Meilahn EN. 1996. Relation of C-reactive protein and coronary heart disease in the MRFIT nested case-control study. Am J Epidemiol 144:537–547.

283. Mendall MA, Patel P, Ballam L, Strachan D, Northfield TC. 1996. C Reactive protein and its relation to cardiovascular risk factors: A population based cross sectional study. Br Med J 312:1061–1065.

284. Yudkin JS, Stehouwer CDA, Emeis JJ, Coppack SW. 1999. Obesity, Insulin Resistance, and Endothelial Dysfunction. Arteriosclerosis 19:972–978.

285. Hak AE, Stehouwer CDA, Bots ML, Polderman KH, Schalkwijk CG, Westendorp ICD, Hofman A, Witteman JCM. 1999. Associations of C-Reactive Protein With Measures of Obesity, Insulin Resistance, and Subclinical Atherosclerosis in Healthy, Middle-Aged Women. Arterioscler Thromb Vasc Biol 19:1986–1991.

286. Ndumele CE, Pradhan AD, Ridker PM. 2006. Interrelationships Between Inflammation, C-Reactive Protein, and Insulin Resistance. J Cardiometab Syndr 1:107–196.

287. Alessandris CD, Lauro R, Presta I, Sesti G. 2007. C-reactive protein induces phosphorylation of insulin receptor substrate-1 on Ser307 and Ser612 in L6 myocytes, thereby impairing the insulin signalling pathway that promotes glucose transport. Diabetologia 50:840–849.

288. Xu J, Morita I, Ikeda K, Miki T, Yamori Y. 2007. C-Reactive Protein Suppresses Insulin Signaling in Endothelial Cells: Role of Spleen Tyrosine Kinase. Mol Endocrinol 21:564–573.

289. Xi L, Xiao C, Bandsma RHJ, Naples M, Adeli K, Lewis GF. 2011. C-Reactive Protein Impairs Hepatic Insulin Sensitivity and Insulin Signaling in Rats: Role of Mitogen-Activated Protein

Kinases. Hepatology 53:127–135.

290. Muhammad IF, Borné Y, Hedblad B, Nilsson PM, Persson M, Engström G. 2016. Acute-phase proteins and incidence of diabetes: a population-based cohort study. Acta Diabetol 53:981–989.

291. Pradhan AD, Manson JE, Buring JE, Ridker PM. 2019. C-Reactive Protein, Interleukin 6, and Risk of Developing Type 2 Diabetes Mellitus 286:327–334.

292. Xi L, Xiao C, Bandsma RHJ, Naples M, Adeli K, Lewis GF. 2011. C-Reactive Protein Impairs Hepatic Insulin Sensitivity and Insulin Signaling in Rats: Role of Mitogen- Activated Protein Kinases. Hepatology 53:127–135.

293. Alessi MC, Juhan-Vague I, Kooistra T, Declerck PJ, Collen D. 1988. Insulin stimulates the synthesis of plasminogen activator inhibitor-1 by the human hepatocellular cell line HepG2. Thromb Haemost 60:491–494.

294. Banfi C, Eriksson P, Giandomenico G, Mussoni L, Sironi L, Hamsten A, Tremoli E. 2001. Transcriptional Regulation of Plasminogen Activator Inhibitor Type 1 Gene by Insulin. Diabetes 50:1522–1530.

295. Nordt TK, Schneider DJ, Sobel BE. 1994. Augmentation of the Synthesis of Plasminogen Activator Inhibitor Type-1 by Precursors of Insulin A Potential Risk Factor for Vascular Disease. Ciculation 89:321–330.

296. Schneider DJ, Nordt TK, Sobel BE. 1992. Stimulation by proinsulin of expression of plasminogen activator inhibitor type-l in endothelial cells. Diabetes 41:890–895.

297. Samad F, Pandey M, Bell PA, Loskutoff DJ. 2000. Insulin continues to induce plasminogen activator inhibitor 1 gene expression in insulin-resistant mice and adipocytes. Mol Med 6:680–692.

298. Sakamoto T, Woodcock-mitchell J, Marutsuka K, Mitchell JJ, Sobel BE, Fujii S. 1999. TNF-a and insulin, alone and synergistically, induce plasminogen activator inhibitor-1 expression in adipocytes. Am Physiol Soc 276:85–90.

299. Mukai Y, Wang C, Rikitake Y, Liao J. 2007. Phosphatidylinositol 3-kinase/protein kinase Akt negatively regulates the plasminogen activitor inhibitor type-1 expression in vascular endothelial cells. Am J Physiol Hear Circ Physiol 292:1–15.

300. Allison BA, Nilsson L, Karpe F, Hamsten A, Eriksson P. 1999. Effects of Native, Triglyceride-Enriched, and Oxidatively Modified LDL on Plasminogen Activator Inhibitor-1. Arterioscler Thromb Vasc Biol 19:1354–1360.

301. Sironi L, Mussoni L, Prati L, Baldassarre D, Camera M, Banfi C, Tremoli E. 1996. Plasminogen activator inhibitor type-1 synthesis and mRNA expression in HepG2 cells are regulated by VLDL. Arterioscler Thromb Vasc Biol 16:89–96.

302. Nordt TK, Klassen KJ, Schneider DJ, Sobel BE. 1993. Augmentation of synthesis of plasminogen activator inhibitor type-1 in arterial endothelial cells by glucose and its implications for local fibrinolysis. Arterioscler Thromb Vasc Biol 13:1822–1828.

303. Seki T, Gelehrter TD. 1996. Interleukin-1 induction of type-1 plasminogen activator inhibitor (PAI-1) gene expression in the mouse hepatocyte line, AML 12. J Cell Physiol 168:648–656.

304. Healy AM, Gelehrter TD. 1994. Induction of plasminogen activator inhibitor-1 in HepG2 human hepatoma cells by mediators of the acute phase response. J Biol Chem 269:19095–19100.

305. Samad F, Yamamoto K, Loskutoff DJ. 1996. Distribution and regulation of plasminogen activator inhibitor-1 in murine adipose tissue in vivo: Induction by tumor necrosis factor-α and lipopolysaccharide. J Clin Invest 97:37–46.

306. Pandey M, Loskutoff DJ, Samad F. 2005. Molecular mechanisms of tumor necrosis factor-α-mediated plasminogen activator inhibitor-1 expression in adipocytes. FASEB J 19:1317–1319.

307. Swiatkowskia M, Szemraj J, Al-nedawi K, Pawlowska Z. 2002. Reactive oxygen species upregulate expression of PAI-1 in endothelial cells. Cell Mol Biol Lett 7:1065–1071.

308. Halleux CM, Declerck PJ, Tran SL, Detry R, Brichard SM. 1999. Hormonal control of plasminogen activator inhibitor-1 gene expression and production in human adipose tissue: Stimulation by glucocorticoids and inhibition by catecholamines. J Clin Endocrinol Metab 84:4097–4105.

309. Wickert L, Chatain N, Kruschinsky K, Gressner AM. 2007. Glucocorticoids activate TGF-β induced PAI-1 and CTGF expression in rat hepatocytes. Comp Hepatol 6:1–9.

310. Lucore CL, Fujii S, Wun TC, Sobel BE, Billadello JJ. 1988. Regulation of the expression of type 1 plasminogen activator inhibitor in Hep G2 cells by epidermal growth factor. J Biol Chem 263:15845–15848.

311. Hozumi A, Osaki M, Sakamoto K, Goto H, Fukushima T, Baba H, Shindo H. 2010. Dexamethasone-induced plasminogen activator inhibitor-1 expression in human primary bone marrow adipocytes. Biomed Res 31:281–286.

312. Reilly CF, McFall RC. 1991. Platelet-derived growth factor and transforming growth factor-β regulate plasminogen activator inhibitor-1 synthesis in vascular smooth muscle cells. J Biol Chem 266:9419–9427.

313. Ganapathi MK, May LT, Schultz D, Brabenec A, Weinstein J, Sehgal PB, Kushner I. 1988. Role of interleukin-6 in regulating synthesis of C-reactive protein and serum amyloid A in human hepatoma cell lines. Biochem Biophys Res Commun 157:271–277.

314. Raynes JG, Eagling S, J MKPW. 1991. Acute-phase protein synthesis in human hepatoma cells: differential regulation of serum amyloid A (SAA) and haptoglobin by interleukin-1 and interleukin-6. Clin Exp Immunol 83:448–491.

315. Steel DM, Whitehead AS. 1991. Heterogeneous modulation of acute-phase-reactant mRNA levels by interleukin-lβ and interleukin-6 in the human hepatoma cell line PLC/PRF/5. Biochem J 277:477–482.

316. Uhlar CM, Grehan S, Steel DM, Steinkasserer A, Whitehead AS. 1997. Use of the acute phase serum amyloid A2 (SAA2) gene promoter in the analysis of pro- and anti-inflammatory mediators: Differential kinetics of SAA2 promoter induction by IL-1β and TNF-α compared to IL-6. J Immunol Methods 203:123–130.

317. Frasshauer M, Klein J, Kralisch S, Klier M, Lossner U, Bluher M, Paschke R. 2004. Serum amyloid A3 expression is stimulated by dexamethasone and interleukin-6 in 3T3-L1 adipocytes. J Endocrinol 183:561–567.

318. Mahajan V V., Apte IC, Shende SS. 2012. Acute phase reactants in type 2 diabetes mellitus and their correlation with the duration of diabetes mellitus. J Clin Diagnostic Res 5:1165–1168.

319. Tan KCB, Chow WS, Tam S, Bucala R, Betteridge J. 2004. Association between Acute-Phase Reactants and Advanced Glycation End Products in Type 2 Diabetes. Diabetes Care 27:223–228.

320. Grundy SM, Brewer HB, Cleeman JI, Smith SC, Lenfant C. 2004. Definition of Metabolic Syndrome: Report of the National Heart, Lung, and Blood Institute/American Heart Association Conference on Scientific Issues Related to Definition. Circulation 109:433–438.

321. Chen TR. 1977. In situ detection of mycoplasma contamination in cell cultures by fluorescent Hoechst 33258 stain. Exp Cell Res 104:255–262.

322. Aranda PS, LaJoie DM, Jorcyk CL. 2012. Bleach Gel: A Simple Agarose Gel for Analyzing RNA Quality. Electrophoresis 33:366–369.

323. Matsumoto M, Sakai M. 2012. Glucose Production Assay in Primary Mouse Hepatocytes. Bio-protocol 2:1–4.

324. Zhou M, Diwu Z, Panchuk-voloshina N, Haugland RP. 1997. A Stable Nonfluorescent Derivative of Resorufin for the Fluorometric Determination of Trace Hydrogen Peroxide : Applications in Detecting the Activity of Phagocyte NADPH Oxidase and Other Oxidases. Anal Biochem 253:162–168.

325. Zhao B, Summers FA, Mason RP. 2012. Photooxidation of Amplex Red to resorufin: implications of exposing the Amplex Red assay to light. Free Radic Biol Med 53:1080–1087.

326. Smith PK, Krohn RI, Hermanson GT, Mallia AK, Gartner FH, Provenzano MD, Fujimoto EK, Goeke NM, Olson BJ, Klenk DC. 1985. Measurement of protein using bicinchoninic acid. Anal Biochem 150:76–85.

327. Zhang H, Ge Z, Ang S, Meng R, Bi Y, Zhu D. 2017. Erythropoietin ameliorates PA-induced insulin resistance through the IRS/AKT/FOXO1 and GSK-3β signaling pathway, and inhibits the inflammatory response in HepG2 cells. Mol Med Rep 16:2295–2301.

328. Buren J, Liu H, Lauritz J, Eriksson JW. 2003. High Glucose and Insulin in combination cause IRS1 and PKB desensitisation in primary culture rat adipocytes, possible implications for insulin resistance in type 2 diabetes. Eur J Endocrinol 148:157–167.

329. De Nigris V, Pujadas G, La Sala L, Testa R, Genovese S, Ceriello A. 2015. Short-term high glucose exposure impairs insulin signaling in endothelial cells. Cardiovasc Diabetol 14:1–7.

330. Sun XJ, Wang LM, Zhang Y, Yenush L, Myers MG, Glasheen E, Lane WS, Pierce JH, White MF. 1995. Role of IRS-2 in insulin and cytokine signalling. Nature 337(6545):173-177.

331. Chen L, Chen R, Wang H, Liang F. 2015. Mechanisms Linking Inflammation to Insulin Resistance. Int J Endocrinol:1-9.

332. Schmelzle K, Kane S, Gridley S, Lienhard GE, White FM. 2006. Temporal dynamics of tyrosine phosphorylation in insulin signaling. Diabetes 55:2171–2179.

333. Sefried S, Häring HU, Weigert C, Eckstein SS. 2018. Suitability of hepatocyte cell lines HepG2, AML12 and THLE-2 for investigation of insulin signalling and hepatokine gene expression. Open Biol 8:1–11.

334. Granner D, Andreone T, Sasaki K, Beale E. 1983. Inhibition of transcription of the phosphoenolpyruvate carboxykinase gene by insulin. Nature 305(5934):549-551.

335. O'Brien RM, Granner DK. 1990. PEPCK Gene as Model of Inhibitory Effects of Insulin on Gene Transcription. Diabetes Care 13:327–339.

336. Barthel A, Schmoll D, Krüger KD, Bahrenberg G, Walther R, Roth RA, Joost HG. 2001. Differential regulation of endogenous glucose-6-phosphatase and phosphoenolpyruvate carboxykinase gene expression by the forkhead transcription factor FKHR in H4IIE-hepatoma

cells. Biochem Biophys Res Commun 285:897–902.

337. Huang X, Liu G, Guo J, Su ZQ. 2018. The PI3K/AKT pathway in obesity and type 2 diabetes. Int J Biol Sci 14:1483–1496.

338. Valiollah S, Mojtaba E, Vahid I, Ali SM. 2011. Association of C Reactive Protein with Insulin Resistance in Type 2 Diabetic. Int Conf Biosci Biochem Bioinforma IPCBEE 5:407–409.

339. Csepregi R, Temesfői V, Sali N, Poór M, Needs PW, Kroon PA, Kőszegi T. 2018. A one-step extraction and luminescence assay for quantifying glucose and ATP levels in cultured HepG2 cells. Int J Mol Sci 19(9):1-18.

ADDENDUM A:
ADDITIONAL DATA

A1. BWTG3 and HepG2 cells used in this study were mycoplasma negative.

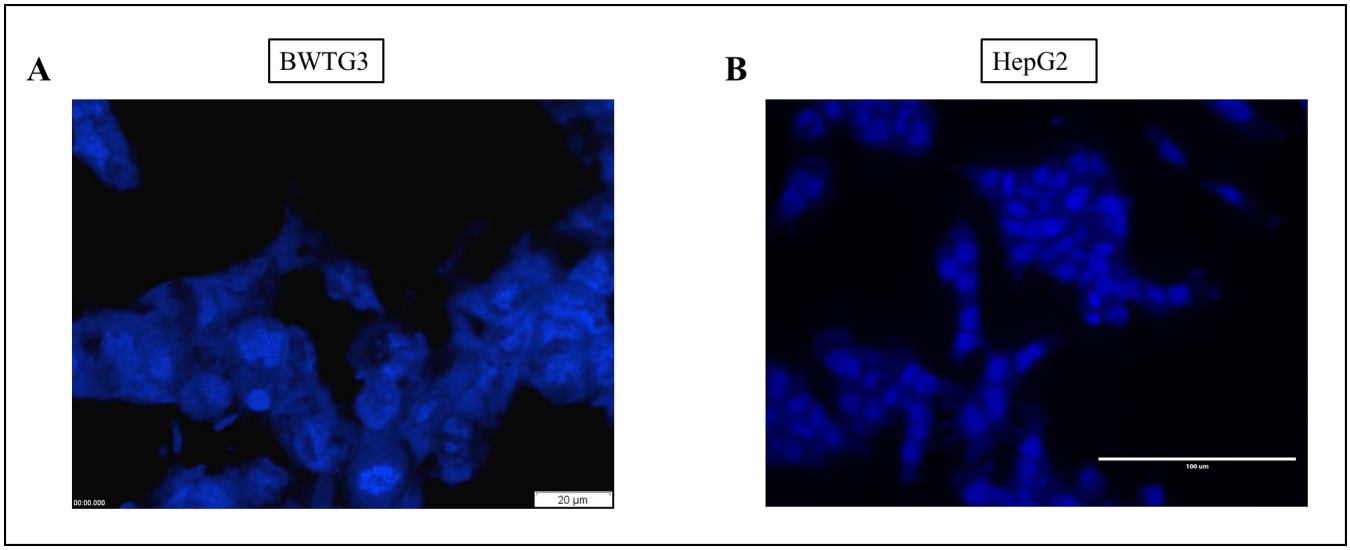

Figure A1. Mycoplasma negative BWTG3 (A) and HepG2 (B) cells. Cells were fixed with methanol and glacial acetic acid in a 3:1 ratio before staining with the DNA Hoechst 33258 dye (Sigma-Aldrich, SA). The Hoechst-dye only stain DNA-containing nuclei. Fluorescent images were obtained using the Olympus XI81 inverted fluorescent microscope.

A2. RNA isolated from BWTG3 and HepG2 cells were intact.

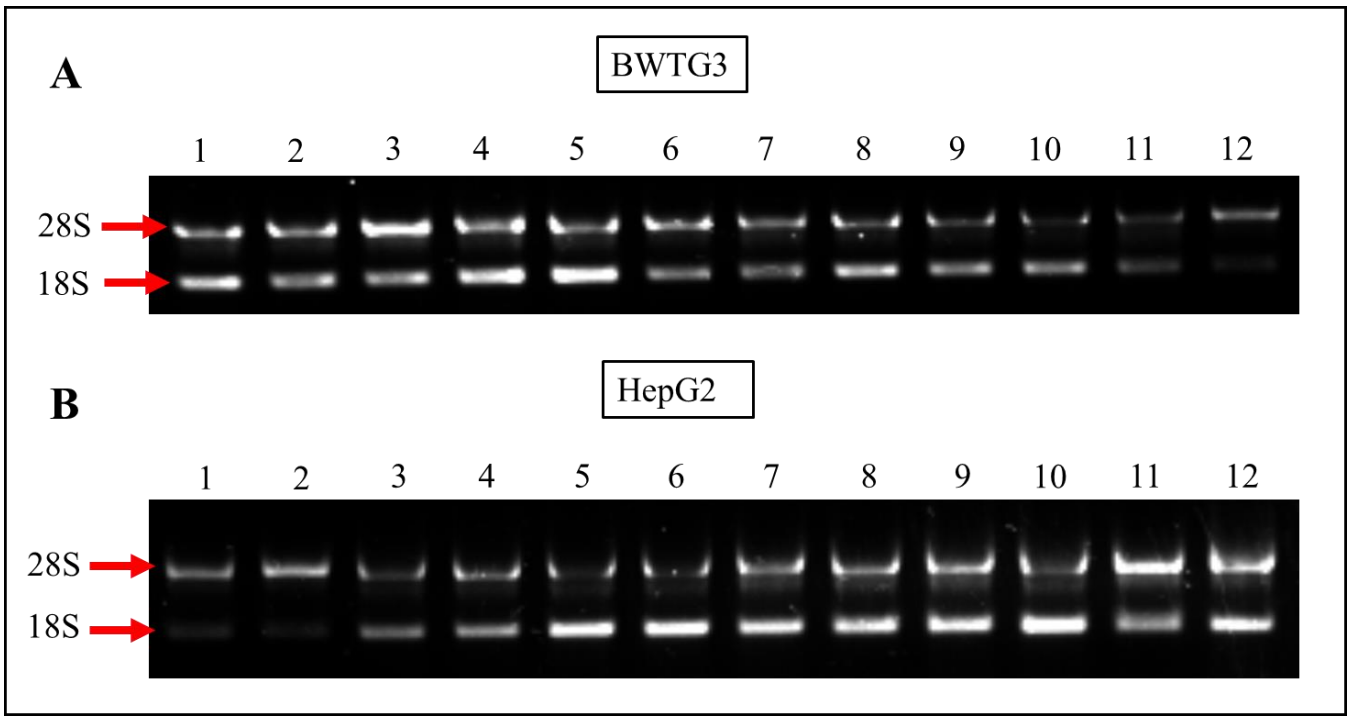

Figure A2. Representative 1% denaturing agarose gel indicating intact RNA isolated from BWTG3 and HepG2 cells. Total RNA was isolated from BWTG3 (A) and HepG2 (B) cells treated with either vehicle (DMEM-full) (Lane 1), 100 ng/ml insulin (Lanes 2 & 3), 10 ng/ml PAI-1 (Lanes 4-6), 10 µg/ml SAA (Lanes 7-9) and 4.5 µg/ml CRP (Lanes 10-12) for 2, 24 and 48 hours. RNA was isolated using Tri-reagent as described in Chapter 2, section 2.3. A total of 1 µg RNA was loaded onto the agarose gel and visualised with Nancy-520 nucleic acid stain.

A3. The correct qPCR products were confirmed with agarose gel electrophoresis.

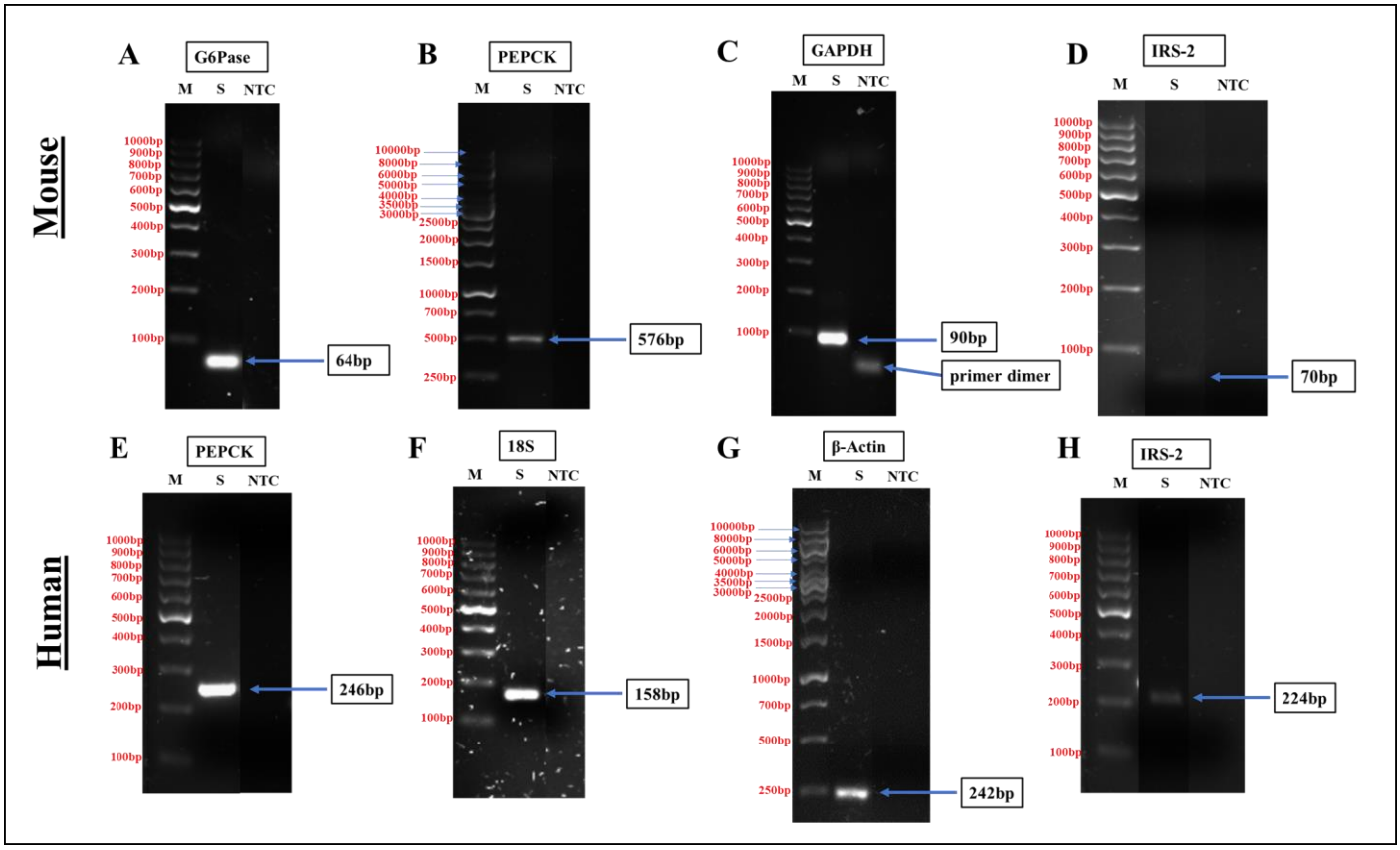

Figure A3. Representative agarose gels indicating qPCR products of mouse (A-D) and human genes (E-H) used in this study. PCR products were subjected to agarose (2% w/v) gel electrophoresis and visualised with Nancy-520 nucleic acid stain. M: O'GeneRuler 1kB (B & G) or 100bp (A, C-F, H) DNA ladder (ThermoFisher Scientific, USA); S: sample treated with vehicle (DMEM-full), NTC: non-template control.

A4. Fluorescence measured of the fluorescent product, resorufin, in the medium of the BWTG3 and HepG2 cells pre-treated with PAI-1, SAA and CRP for 48 hours.

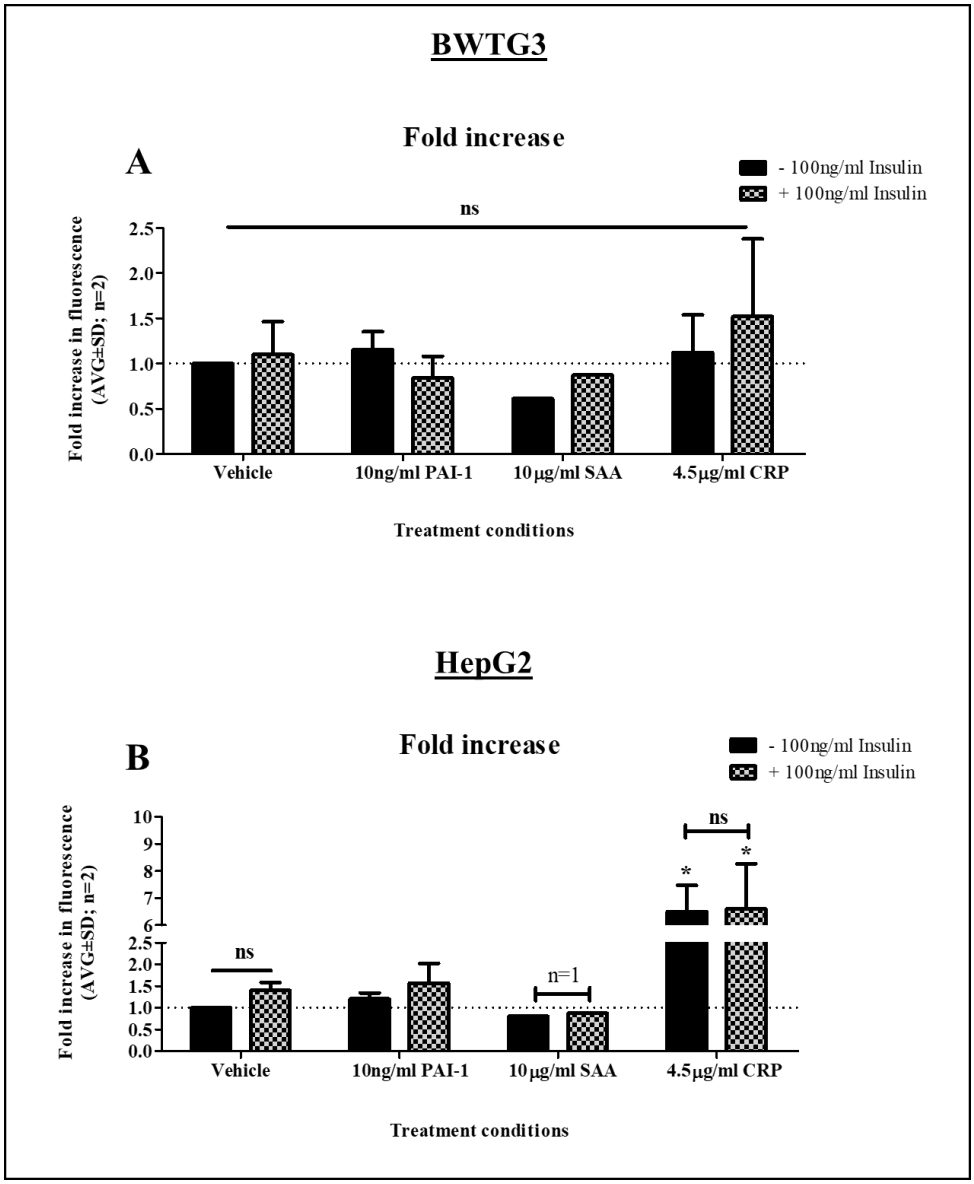

Figure A4. Fold increase in fluorescence measured of the fluorescent product, resorufin, in the medium of BWTG3 and HepG2 cells. BWTG3 and HepG2 cells were serum-starved for 24 hours, followed with a pre-treatment with 10 ng/ml, 10 µg/ml SAA and 4.5 µg/ml CRP for 48 hours. In the final hour of the APP pre-treatment, the cells were treated with 100 ng/ml insulin for 1 hour. The cells were washed twice with 1X pre-warmed PBS and incubated with glucose production buffer (containing 20 mM sodium lactate and 2 mM sodium pyruvate as substrates for gluconeogenesis) for 6 hours, in the presence of the test compounds (10 ng/ml, 10 µg/ml SAA and 4.5 µg/ml CRP) as well as 100 ng/ml insulin. The medium was collected, and glucose content was measured using the optimised detection method.

A5. IRS-2 mRNA expression in BWTG3 and HepG2 cells showing effects of selected APPs, PAI-1, SAA and CRP at different lengths of exposure.

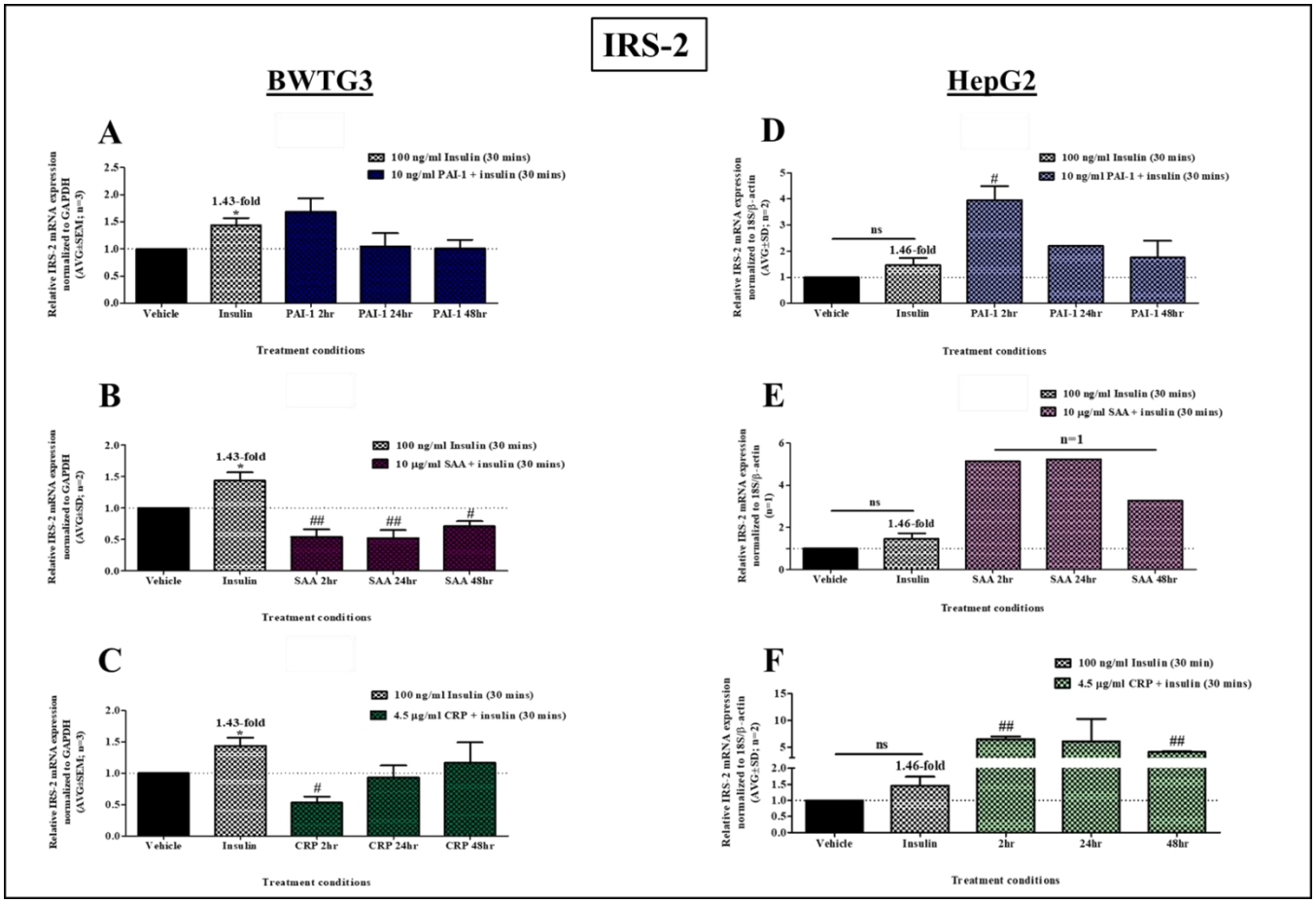

Figure A5. IRS-2 mRNA expression measured in BWTG3 and HepG2 cells using qPCR analysis, showing effects of selected APPs at different treatment times. BWTG3 and HepG2 cells were serum-starved for 24 hours followed with a treatment with 10 ng/ml PAI-1, 10 µg/ml SAA and 4.5 µg/ml for 2, 24 and 48 hours (acute versus chronic exposure). The cells were treated with 100 ng/ml insulin for 30 minutes prior to cell lysis, to activate the insulin signalling pathway. mRNA expression of the IRS-2 gene was measured using real-time qPCR and quantified relative to the housekeeping gene, GAPDH (for BWTG3) and 18S and β-actin (for HepG2). Data shown represents two to three independent experiments, except (E) which shows one independent experiment. Statistical analysis comparing insulin to the vehicle (*$p<0.05$) and the time treatments relative to the insulin control was performed using one-way ANOVA with Tukey's Multiple Comparison's Test ($^{\#}p<0.05$, $^{\#\#}p<0.01$, $^{\#\#\#}p<0.001$).

ADDENDUM B:

OPTIMISING A TECHNIQUE TO MEASURE EXTRACELLULAR GLUCOSE CONTENT OF BWTG3 AND HEPG2 CELLS

Glucose detection method: AmpliFlu/Glucose oxidase assay

In order to measure and quantify the extracellular glucose content in the medium of BWTG3 and HepG2 cells, the principles of the Amplex Red/Glucose oxidase kit (ThermoFisher Scientific) was followed. This kit makes use of two enzymes: glucose oxidase (GOD) and peroxidase (POD) to convert the available glucose in the medium to a detectable product. For this, two reactions occurs: firstly, glucose oxidase catalyzes the conversion of glucose to D-gluconolactone and H_2O_2. Secondly, the oxidation of the substrate Amplex Red, by H_2O_2 to the fluorescent product resorufin, is catalyzed by horse radish peroxidase (HRP) (324, 325). Resorufin has a fluorescence excitation and emission maxima at 571 nm and 585 nm, respectively, which is measured with a fluorescence microplate reader.

In order to optimize a method in the research laboratory that is based on these principles, the limitations of this reaction had to be considered. For instance, the absorption and fluorescence of resorufin is pH-dependant, and a pH of 7.4 is recommended. As the Amplex/Red Glucose oxidase kit made use of a 50 mM sodium phosphate buffer (pH 7.4), we decided to test using PBS (pH 7.34) and the glucose production buffer (pH 7.3) as diluents. The background fluorescence of these solutions was additionally monitored. The glucose production buffer produced a consistent background whereas the background fluorescence of the PBS was variable between experiments. Therefore, the glucose production buffer was used as a diluent for the preparation of the working reagent which contains the AmpliFlu, GOD and HRP, in subsequent experiments. Additionally, although the difference between AmpliFlu and Amplex Red was not defined in literature, a paper by Csepregi *et al.* (339) optimized a method of detecting resorufin, following the principles of the Amplex Red/Glucose oxidase kit using AmpliFlu. In this paper, the authors prepared a working reagent with 16 µM AmpliFlu, 4.5 µU/ml GOD and 0.13 µU/ml POD. Herein, they measured the intracellular glucose content of HepG2 cells, in which glucose uptake was inhibited. However, when we tested these concentrations of the reagents to measure the extracellular glucose content of BWTG3 and HepG2 cells, inconsistent results were produced with no change between the no-glucose control and the glucose containing medium/samples. Therefore, we decided to test the concentrations used in the Amplex Red/Glucose oxidase kit. A working reagent was prepared in glucose production buffer containing: 10 µM AmpliFlu, 2U/ml GOD and 0.2 U/ml HRP. Prior to testing the BWTG3 and HepG2 samples, we prepared glucose standards in a concentration range of 4-40 µM, in glucose production buffer. 50 µl of these standards were added to a 96-well microplate with 50 µl of the aforementioned working reagent (1:1 ratio), which produced a glucose concentration range between 2-20 µM. These concentrations of D-glucose were chosen as the GOD-POD reaction can detect as little as 3 µM glucose as described in the Amplex Red/Glucose oxidase kit and by Csepregi *et al.* (339). A glucose standard curve was produced (Fig.B1), with glucose concentrations ranging between 2-20 µM, and showed a linear increase in the detection of the fluorescent product, resorufin.

B1. Standard curve of D-glucose in a concentration range of 2-20 µM.

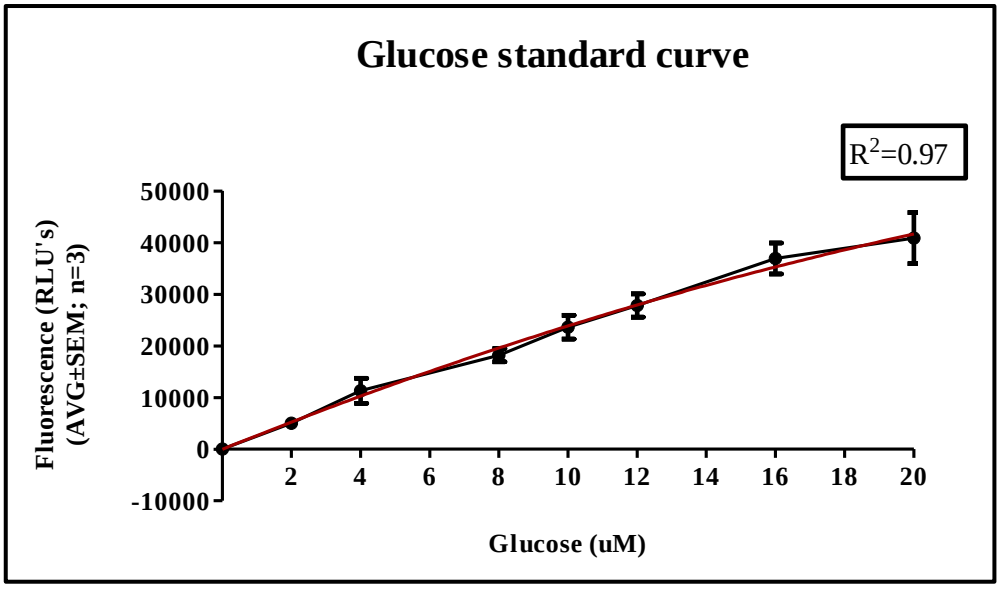

Figure B1. Standard curve produced using glucose concentrations ranging from 2-20 µM. D-Glucose in concentrations 4-40 µM was incubated with 10 µM AmpliFlu, 2 U/ml GOD and 0.2 U/ml HRP, in glucose production buffer, in a 1:1 ratio, at room temperature for 30 minutes. Fluorescence of the reaction product, resorufin, was measured at an excitation of 571 nm and emission of 585 nm Background fluorescence, determined for a no-glucose control reaction, was subtracted from each value. The black line represents the standard curve produced and the red line represents the non-linear fit of the curve.

The standard curve produced indicated that concentrations of the reagents, used in the Amplex Red/Glucose oxidase kit, was conducive to detect glucose concentrations in this range. Therefore, 10 µM AmpliFlu, 2 U/ml GOD and 0.2 U/ml HRP was used to detect the glucose content in the medium of BWTG3 and HepG2 in following experiments (Fig.A4). The glucose concentrations in each BWTG3 and HepG2 sample was measured by interpolating the fluorescence readings of each sample (Fig.A4) in to the standard curve produced (Fig.B1), using the GraphPad Prism® version 5 software.